WELUT-85/W02
DECEMBER 1984

A WORKSHOP MODEL SIMULATING FATE AND EFFECT OF DRILLING MUDS AND CUTTINGS ON BENTHIC COMMUNITIES

Fish and Wildlife Service

U.S. Department of the Interior

WELUT-85/W02
December 1984

A WORKSHOP MODEL SIMULATING FATE AND EFFECT OF DRILLING MUDS AND CUTTINGS ON BENTHIC COMMUNITIES

by

Gregor T. Auble
Austin K. Andrews
David B. Hamilton
James E. Roelle
Western Energy and Land Use Team
U.S. Fish and Wildlife Service
2627 Redwing Road
Fort Collins, CO 80526-2899

and

Thomas G. Shoemaker
Colorado State University
Fort Collins, CO 80523

Performed for
Office of Research and Development
U.S. Environmental Protection Agency

Western Energy and Land Use Team
Division of Biological Services
Research and Development
Fish and Wildlife Service
U.S. Department of the Interior
Washington, DC 20240

DISCLAIMER

This report describes a model developed from the input of a number of participants at a workshop. The contents do not necessarily reflect positions of the U.S. Fish and Wildlife Service, the U.S. Environmental Protection Agency, or specific workshop participants.

This report should be cited as:

Auble, G. T., A. K. Andrews, D. B. Hamilton, J. E. Roelle, and T. G. Shoemaker. 1984. A workshop model simulating fate and effect of drilling muds and cuttings on benthic communities. U.S. Fish Wildl. Serv. Western Energy and Land Use Team, Ft. Collins, CO. WELUT-85/W02. 189 pp.

SUMMARY

Oil and gas exploration and production at marine sites has generated concern over potential environmental impacts resulting from the discharge of spent drilling muds and cuttings. This concern has led to a broad array of publicly and privately sponsored research. This report describes a cooperative modeling effort designed to focus information resulting from this research through construction of explicit equations that simulate the potential impacts of discharged drilling fluids (muds) and cuttings on marine communities. The model is the result of collaboration among more than 30 scientists. The principal cooperating organizations were the U.S. Environmental Protection Agency, the U.S. Minerals Management Service, the Offshore Operators Committee, and the Alaska Oil and Gas Association.

The overall simulation model can be conceptualized as three connected submodels: Discharge and Plume Fate, Sediment Redistribution, and Benthic Community Effects. On each day of simulation, these submodels are executed in sequence, with flows of information between submodels. The Benthic Community Effects submodel can be further divided into sections that calculate mortality due to burial, mortality due to toxicity, mortality due to resuspension disturbance, and growth of the community.

The model represents a series of seven discrete 1-m^2 plots at specified distances along a transect in one direction away from a discharge point. It consists of coupled difference equations for which parameter values can easily be set to evaluate different conditions or to examine the sensitivity of

output to various assumptions. Sets of parameter values were developed to represent four general cases or scenarios: (1) a shallow (5 m), cold environment with ice cover during a substantial fraction of the year, such as might be encountered in the Beaufort Sea, Alaska; (2) a shallow (20 m), temperate environment, such as might be encountered in the Gulf of Mexico; (3) a deeper (80 m), temperate environment, such as might be encountered in the Gulf of Mexico; and (4) a very deep (1,000 m) environment, such as might be encountered on the Atlantic slope.

The focus of the modeling effort was on the connection of a reasonable representation of physical fate to the biological responses of populations, rather than on highly detailed representations of individual processes. For example, the calculations of physical fate are not as detailed as those in the recently published model of Brandsma et al. (1983). The value of the model described herein is in the broad scope of processes that are explicitly represented and linked together. The model cannot be considered to produce reliable predictions of the quantitative impacts of discharged drilling fluids and cuttings on biological populations at a particular site. Limitations of the model in predicting integrated fate and effects can be traced to three general areas: level of refinement of the algorithms used in the model; lack of understanding of the processes determining fate and effects; and parameter and data values.

Despite the limitations, several qualitative conclusions concerning both potential impacts and the importance of various remaining data gaps can be drawn from the modeling effort. These include:

(1) Simple, unequivocal conclusions about fate and effects across geographical regions and drilling operations are difficult, if not misleading, due to the large amount of variability in characteristics of discharged materials (e.g., oil content and toxicity), discharge conditions (e.g., duration of drilling operations), physical environments (e.g., water depth, current direction, and sediment disturbance regimes), and biological communities (e.g., intrinsic growth rates). Different combinations of these characteristics can result in substantial differences in simulated environmental fate and biological effects. For example, simulated recovery in some high-energy environments occurs within months after the cessation of discharge operations, even at heavily impacted sites, whereas simulated recovery in some low-energy environments takes years at heavily impacted sites.

(2) Considerable difficulties remain in the reliable extrapolation of results from laboratory toxicity experiments to predictions of population effects in the field.

(3) The volume of material discharged and duration of operations in the production drilling operations simulated by the model are sufficient to produce substantial simulated biological impacts at some plots, both in terms of differences from a control plot during the period of discharge operations, and in terms of the recovery period following the perturbations.

(4) Evaluation of the significance of potential effects involves the following factors:

- Definition of a specific spatial and temporal reference frame (e.g., What is the natural variation? Is 1 year to be considered a "long" or "short" time? Is 50 m to be considered a "large" or "trivial" distance?).

- Consideration of rare or unique resources and particularly sensitive biotic assemblages.

- Consideration of the potential for long term, cumulative effects.

Some of these aspects are clearly beyond the scope of this modeling effort (e.g., the model does not simulate the long term fate of resuspended material). The model does, however, contain an internal "reference frame" by comparison to simulated behavior at a control plot. The model, in general, simulates substantial "natural" variation at the reference or control plots, both over time, due to sediment disturbance events in medium to high energy environments, and over space, due to geographically varying conditions, such as water depth and current regime.

CONTENTS

	Page
SUMMARY	iii
FIGURES	viii
TABLES	xiv
ACKNOWLEDGMENTS	xvi
INTRODUCTION	1
Adaptive Environmental Assessment Workshops	1
Objectives	2
Relationship to Previous Work	3
Scope of Report	5
MODEL DESCRIPTION	7
Model Bounds	7
Summary of Calculations	7
MODEL BEHAVIOR	24
Workshop Scenarios	24
Sensitivity	82
Summary	89
DISCUSSION	94
Limits to Predictive Capability	94
Qualitative Results	96
REFERENCES	98
APPENDICES	
A. Model Structure	102
B. Formulation of Discharge and Plume Fate Submodel	103
C. Formulation of Sediment Redistribution Submodel	130
D. Formulation of Benthic Community Effects Submodel	150

FIGURES

Number		Page
1	Diagrammatic top view of a deposition pattern and the location of simulated plots	8
2	Information exchanges between submodels	9
3	General sequence of calculations concerning discharge and fate	10
4	Diagrammatic cross section of deposition of material from cuttings discharge	12
5	Diagrammatic cross section of mud plume dynamics for case 1: mud plume impacts bottom and collapses	13
6	Diagrammatic cross section of mud plume dynamics for case 2: dynamic collapse of mud plume at a trap depth above the bottom	13
7	Conceptualization of sediment dynamics at a plot	15
8	General sequence of calculations concerning sediment redistribution	16
9	General sequence of calculations concerning benthic community effects	19
10	Mortality rates for late successional macrofaunal assemblage as a function of depth of burial	20
11	Scenario 1: cumulative deposition of discharged material at 5-m plot, 1-yr run	27
12	Scenario 1: cumulative deposition of discharged material at 50-m plot, 1-yr run	28
13	Scenario 1: cumulative deposition of discharged material at 500-m plot, 1-yr run	29
14	Scenario 1: sediment disturbance regime, 1-yr run	31

FIGURES (continued)

Number		Page
15	Scenario 1: net accumulation of sediment at 5, 50, and 500-m plots, 1-yr run	31
16	Scenario 1: fraction of sediment from bulk mud discharge in top 5-cm layer at 5 and 50-m plots, 1-yr run	32
17	Scenario 1: fraction of sediment from bulk mud discharge in top 5-cm layer at 500 and 1,500-m plots, 1-yr run	33
18	Scenario 1: macrofaunal assemblages at control plot, 1-yr run	35
19	Scenario 1: macrofaunal assemblages at 50-m plot, 1-yr run	36
20	Scenario 1: macrofaunal assemblages at 500-m plot, 1-yr run	37
21	Scenario 1: macrofaunal assemblages at 1,500-m plot, 1-yr run	38
22	Scenario 1: cumulative deposition of total discharged material at 50-m plot, 10-yr run	41
23	Scenario 1: net accumulation of sediment at 50-m and control plots, 10-yr run	41
24	Scenario 1: fraction of sediment from bulk mud discharge in top 5-cm layer at 500 and 1,500-m plots, 10-yr run	42
25	Scenario 1: fraction of sediment from bulk mud discharge in top 5-cm layer at 5 and 50-m plots, 10-yr run	43
26	Scenario 1: macrofaunal assemblages at control plot, 10-yr run	45
27	Scenario 1: macrofaunal assemblages at 1,500-m plot, 10-yr run	46
28	Scenario 1: macrofaunal assemblages at 500-m plot, 10-yr run	47
29	Scenario 1: macrofaunal assemblages at 5-m plot, 10-yr run	48
30	Scenario 2: cumulative deposition of total discharged material at 5-m plot, 1-yr run	49

FIGURES (continued)

Number		Page
31	Scenario 2: sediment disturbance regime, 1-yr run	51
32	Scenario 2: net accumulation of sediment at 5 and 50-m plots, 1-yr run	52
33	Scenario 2: fraction of sediment from bulk mud discharge in top 5-cm layer at 50-m plot, 1-yr run	52
34	Scenario 2: macrofaunal assemblages at control plot, 1-yr run	54
35	Scenario 2: macrofaunal assemblages at 5-m plot, 1-yr run	55
36	Scenario 2: macrofaunal assemblages at 50-m plot, 1-yr run	56
37	Scenario 2: macrofaunal assemblages at 3,000-m plot, 1-yr run	57
38	Scenario 2: cumulative deposition of total discharged material at 50-m plot, 6-yr run	58
39	Scenario 2: net accumulation of discharged material at 5 and 50-m plots, 6-yr run	58
40	Scenario 2: fraction of sediment from bulk mud discharge in top 5-cm layer at 1,500-m plot, 6-yr run	59
41	Scenario 2: macrofaunal assemblages at control plot, 6-yr run	60
42	Scenario 2: macrofaunal assemblages at 5-m plot, 6-yr run ...	61
43	Scenario 2: macrofaunal assemblages at 3,000-m plot, 6-yr run	62
44	Scenario 3: cumulative deposition of discharged material at 3,000-m plot, 1-yr run	65
45	Scenario 3: net accumulation of sediment at 5-m plot, 1-yr run	65
46	Scenario 3: sediment disturbance regime, 1-yr run	66
47	Scenario 3: fraction of sediment from bulk mud discharge in top 5-cm layer at 3,000-m plot, 1-yr run	66

FIGURES (continued)

Number		Page
48	Scenario 3: macrofaunal assemblages at control plot, 1-yr run	68
49	Scenario 3: macrofaunal assemblages at 5-m plot, 1-yr run	69
50	Scenario 3: macrofaunal assemblages at 50-m plot, 1-yr run	70
51	Scenario 3: cumulative deposition of discharged material at 3,000-m plot, 10-yr run	72
52	Scenario 3: net accumulation of sediment at 5-m plot, 10-yr run	72
53	Scenario 3: fraction of sediment from bulk mud discharge in top 5-cm layer at 3,000-m plot, 10-yr run	73
54	Scenario 3: macrofaunal assemblages at control plot, 10-yr run	74
55	Scenario 3: macrofaunal assemblages at 5-m plot, 10-yr run	75
56	Scenario 3: macrofaunal assemblages at 50-m plot, 10-yr run	76
57	Scenario 3: macrofaunal assemblages at 500-m plot, 10-yr run	77
58	Scenario 4: net accumulation of sediment at 5 and 50-m plots, 20-yr run	80
59	Scenario 4: macrofaunal assemblages at 50-m plot, 20-yr run	80
60	Scenario 4: macrofaunal assemblages at 500-m plot, 20-yr run	81
61	Effect of eliminating resuspension mortality on macrofaunal assemblages at control plot, 6-yr run of Scenario 2	83
62	Effect of eliminating resuspension mortality on macrofaunal assemblages at 5-m plot, 6-yr run of Scenario 2	84
63	Effect of eliminating resuspension mortality on macrofaunal assemblages at 3,000-m plot, 6-yr run of Scenario 2	86

FIGURES (continued)

Number		Page
64	Scenario 2: early successional macrofaunal assemblage at 1,500-m plot, 6-yr run	88=7
65	Effect of different hydrocarbon contents and toxicities of drilling mud on early successional macrofaunal assemblage at 1,500-m plot, 6-yr run of Scenario 2	88
D-1	Mortality rates for meiofaunal assemblage as a function of depth of burial	153
D-2	Mortality rates for pioneer macrofaunal assemblage as a function of depth of burial	153
D-3	Mortality rates for late successional macrofaunal assemblage as a function of depth of burial	154
D-4	Derivation of estimated mortality curve for pioneer macrofaunal assemblage buried by "natural" sediments	155
D-5	Derivation of estimated mortality curve for pioneer macrofaunal assemblage buried by "exotic" sediments	156
D-6	Derivation of estimated mortality curve for late successional macrofaunal assemblage buried by "natural" sediments	157
D-7	Derivation of estimated mortality curve for late successional macrofaunal assemblage buried by "exotic" sediments	158
D-8	Daily survival rate of juvenile *Mysidopsis* as a function of concentration of whole P-1 drilling mud	164
D-9	Daily survival rate of juvenile *Mysidopsis* as a function of the square of concentration of whole P-1 drilling mud	164
D-10	Daily survival rate of *Palaemonetes* larvae as a function of concentration of whole P-1 drilling mud	166
D-11	Daily survival rate of *Palaemonetes* larvae as a function of the square of concentration of whole P-1 drilling mud	166
D-12	Relative toxicity of various muds compared to P-1 mud as a function of No. 2 oil concentration	168

FIGURES (concluded)

Number		Page
D-13	Benthic community survival rates as a function of depth of sediment disturbance	172
D-14	Division in doubling time as a function of sediment hydrocarbon concentration	179
D-15	Division in doubling time as a function of proportion sand in the sediment	181

TABLES

Number		Page
1	Summary of Scenario 1 conditions	25
2	Summary of Scenario 2 conditions	50
3	Summary of Scenario 3 conditions	64
4	Summary of Scenario 4 conditions	79
5	Summary of scenario behavior	90
B-1	Water column, drilling, and discharge parameters	104
B-2	Source of discharged drilling material	106
B-3	Average density and particle size distribution of discharged material	106
C-1	General factors influencing sediment dynamics	131
C-2	Size class distribution of natural sediment	131
C-3	Initial conditions for sediment disturbance processes	133
C-4	Mean interval until next disturbance for an event occurring in a given month	134
C-5	Other characteristics of disturbance events	135
C-6	Mean magnitude of disturbance events in cm	137
D-1	"Community sensitivity" coefficients estimated by subgroup participants	160
D-2	Concentrations (ppm) of whole P-1 mud resulting in various survival rates of juvenile *Mysidopsis* for exposures of different length	162

TABLES (concluded)

Number		Page
D-3	Constant daily survival rates corresponding to the combinations of survival rate and exposure duration shown in Table D-2	162
D-4	Concentrations (ppm) of whole P-1 mud resulting in various survival rates of *Palaemonetes* larvae for exposures of different length	165
D-5	Oil concentrations of various drilling muds and their relative toxicity to *Palaemonetes* larvae	167
D-6	Basic parameters for the population growth model	177

ACKNOWLEDGMENTS

This report describes the results of a collaborative effort by workshop participants. Although the following participants deserve the credit for the accomplishments of the workshop, the authors bear full responsibility for any errors the model or report may contain.

Dr. Robert C. Ayers, Jr.
Exxon Production Research Company
N-20 P.O. Box 2189
Houston, TX 77001

Mr. James Barkuloo
U.S. Fish and Wildlife Service
1612 June Avenue
Panama City, FL 32405

Dr. Donald F. Boesch
Louisiana Universities Marine Consortium
Star Route Box 541
Chauvin, LA 70344

Mr. Maynard Brandsma
Consulting Engineer
P.O. Box 374
Durango, CO 81301

Mr. James Cimato
Branch of Offshore Studies
Minerals Management Service, MS 644
Washington, DC 20240

Dr. Bruce Cox
Marathon Oil Co.
P.O. Box 629
Littleton, CO 80122

Dr. Thomas W. Duke
U.S. Environmental Protection Agency
Environmental Research Laboratory
Sabine Island
Gulf Breeze, FL 32561

Dr. Ray Emerson
Minerals Management Service
3841 Chinisk Bay Drive
Anchorage, AK 99502

Dr. Eugene Gallagher
Woods Hole Oceanographic Institute
Woods Hole, MA 02543

Dr. Joy Geisalman
Minerals Management Service
P.O. Box 1159
Anchorage, AK 99510

Mr. Raymond Hanson
Sohio Alaska Petroleum Company
Pouch 6-612
Anchorage, AK 99507

Ms. Michelle Hiller
U.S. Environmental Protection Agency (EN-336)
401 M Street SW
Washington, DC 20460

Mr. Donald Honeyman
ARCO Alaska Inc.
Box 360
Anchorage, AK 99510

Mr. Duane Karna
U.S. Environmental Protection Agency
Region X (MS 521)
1200 6th Avenue
Seattle, WA 98101

Mr. Theodore Landry
U.S. Environmental Protection Agency
Region 1
Water Quality Branch
J.F.K. Federal Building
Boston, MA 02203

Dr. Douglas Lipka
U.S. Environmental Protection Agency (RD-682)
401 M Street SW
Washington, DC 20460

Dr. Donald Maurer
Southern California Ocean Study Consortium
California State University
Room PH1-217
Long Beach, CA 90840

Dr. David McGrail
Texas A&M University
Department of Oceanography
College Station, TX 77843

Dr. Jerry Neff
Battelle
New England Marine Research Laboratory
397 Washington Street
Duxbury, MA 02332

Dr. Robert Ozretich
U.S. Environmental Protection Agency
Marine Sciences Center
Newport, OR 97635

Dr. Gary Petrazzuolo
Technical Resources, Inc.
10215 Fernwood Road, Suite 408
Bethesda, MD 20817

Dr. Fred Piltz
Pacific OCS Office
Minerals Management Service
1340 West Sixth Street
Los Angeles, CA 90017

Dr. K. Ranga Rao
University of West Florida
Biology Department
Pensacola, FL 32514

Dr. James P. Ray
Shell Oil Company
P.O. Box 4320
Houston, TX 77210

Mr. Douglas Redburn
Alaska Dept. of Environmental Conservation, Pouch "O"
3220 Hospital Drive
Juneau, AK 99811

Mr. Maurice O. Rinkel
Florida Institute of Oceanography
830 First Street, South
St. Petersburg, FL 33701

Mr. Reginald Rogers
U.S. Environmental Protecton Agency
Region IV
345 Courtland Street
Atlanta, GA 30365

Dr. Theodore Sauer, Jr.
Exxon Production Research Company
P.O. Box 2189
Houston, TX 77005

Dr. G. D. Sharma
Alaska Seagrant College
University of Alaska
Chapman Building, Room 306
Fairbanks, AK 99701

Mr. Robert Vickery
U.S. Environmental Protection
Agency
Region VI
First International Building
1201 Elm Street
Dallas, TX 75270

Mr. Richard Walentowicz
U.S. Environmental Protection
Agency (WH-585)
401 M Street, SW
Washington, DC 20460

This work was conducted under an Interagency Agreement between the U.S. Environmental Protection Agency and the U.S. Fish and Wildlife Service and was partially supported by an Interagency Agreement between the U.S. Environmental Protection Agency and the Minerals Management Service. Workshop facilities and supporting logistics were handled by Technical Resources, Inc. Partial support for meetings was provided by the Offshore Operators Committee (OOC) and the Alaska Oil and Gas Association (AOGA).

As facilitators of the workshop, the authors are especially indebted to Dr. G. Petrazzuolo and Ms. J. Watson of Technical Resources, Inc., for coordinating the workshop arrangements and to members of the project Steering Committee (Dr. R. Ayers, Mr. J. Cimato, Dr. T. Duke, and Dr. G. Petrazzuolo) for providing perceptive and consistent direction.

INTRODUCTION

Oil and gas exploration/production at marine sites has been accompanied by concern over potential environmental impacts resulting from the discharge of spent drilling muds and cuttings. This concern has led to a broad array of publicly and privately sponsored research, beginning in the mid-1970's. In order to focus available information on the complex, interdisciplinary problems of fate and effect of drilling fluids discharged in the marine environment, a collaborative modeling effort was initiated, utilizing the Adaptive Environmental Assessment (AEA) process.

ADAPTIVE ENVIRONMENTAL ASSESSMENT WORKSHOPS

The Adaptive Environmental Assessment methodology was developed by environmental scientists and systems analysts at the University of British Columbia and the International Institute for Applied Systems Analysis in Austria. The approach is organized around a series of 3- to 5-day workshops that define information needs and promote a common understanding of the issues. These workshops are followed by periods of information collection, analysis, and synthesis. The workshops are attended by groups of participants, drawn from key agencies and interests, who collectively represent a range of scientific expertise, management responsibility, and decisionmaking authority. These individuals are not only involved in the workshops, but undertake some of the key tasks of information collection, analysis, and guidance between workshops.

The focus of AEA workshops is the construction and refinement of a quantitative, dynamic simulation model of the system under study. Early in a particular application, the <u>process</u> of building a model is usually of greater

benefit than the model itself. Development of a simulation model enables participants to view their expertise in the context of the whole system, thereby promoting interdisciplinary communication and understanding. Simulation models require explicit information; in building a model, participants must be precise about their assumptions. Conceptual uncertainties about system behavior are exposed objectively and questions that must be addressed in order to understand system responses to management activities are identified. A large part of the value of such a simulation modeling workshop is that it provides a neutral structure or framework for focused communication among participants representing a diverse set of public and private interests.

OBJECTIVES

This report describes the formulation and representative behavior of a simulation model developed at a workshop held June 21-23, 1983, at Breckenridge, Colorado. This workshop was the second AEA workshop on the topic of drilling fluids. The focus of this second workshop was on refinement and extension of the previous effort in the areas of fate and effects on soft-bottom benthic communities. Specific objectives of the workshop were:

(1) To develop a model for potential impacts that adequately quantifies selected indicators as measures of impact and qualifies these estimates in terms of their levels of error or uncertainty; and

(2) To produce modeling algorithms that are compatible with the microprocessor capabilities of prospective users.

The effort was directed at developing a model that would be:

(1) Straightforward, in order to be understood by a variety of users;

(2) More technically credible than the initial model; and

(3) Useful to regulators at both State and Federal levels.

Participants were identified to contribute technical expertise in the following areas:

(1) Water column dispersion;

(2) Bottom dynamics/sediment transport processes;

(3) Burial effects;

(4) Toxicity/bioaccumulation; and

(5) Community re-establishment following disturbance.

At the workshop, we concentrated on the objective of a straightforward, useful, and technically credible model capable of representing a wide variety of geographical locations. The model described here is implemented on a main-frame computer. The possibility of implementation on mini- or micro-computers has been delayed until it is established that the model has the requisite technical credibility and management utility.

RELATIONSHIP TO PREVIOUS WORK

The earlier workshop held at Gulf Breeze, Florida, in September, 1981, resulted in a preliminary simulation model applicable to the discharge of drilling muds and cuttings in the Gulf of Mexico. That model (Auble et al. 1982) had four components or submodels:

(1) A Discharge/Fate submodel that dealt with characteristics of the discharge and subsequent dilution and deposition of discharged material;

(2) A Water Column Effects submodel that simulated the response of plankton populations;

(3) A Soft Bottom Effects submodel that simulated the response of soft-bottom benthic communities (assuming the discharge took place over this type of community); and

(4) A Hard Bottom Effects submodel that simulated the response of coral (assuming the discharge took place over this type of community).

The model described here is a major revision of the Discharge/Fate and Soft Bottom Effects portions of the earlier model. Effort was concentrated in these areas because of their relative importance in terms of evaluating environmental impacts and the potential for accomplishing substantial improvement in the model. Principal changes from the earlier model include:

(1) A different conceptualization and more mechanistic treatment of plume dynamics and sediment deposition;

(2) The addition of calculations simulating bottom sediment redistribution and dynamics;

(3) A different conceptualization of soft-bottom benthic communities;

(4) Refined treatments of the processes of burial, toxicity, growth, and recolonization; and

(5) Much greater ability to represent different geographical regions.

Despite the considerable refinements incorporated in the current model, it still represents a compromise between detailed, mechanistic representations and oversimplified, but easily understood, calculations. Specifically, this model does not attempt to duplicate the detail of plume dynamics represented in models such as the one developed by the Offshore Operators Committee

(Brandsma et al. 1980). Rather, the emphasis here is to connect an acceptable representation of fate processes with an acceptable representation of effects processes to produce a model that allows examination of the behavior of a coupled system.

SCOPE OF REPORT

Changes from the earlier AEA-workshop model were extensive. Thus, this report is formulated as a complete and independent description of the revised model. The MODEL DESCRIPTION section outlines the spatial and temporal scales of the model and summarizes the calculations and connections of various sub-models.

The MODEL BEHAVIOR section presents output from four cases, or scenarios, and discusses model behavior. These scenarios are not intended to represent predictions about specific sites, but rather to provide understanding of how factors that vary geographically can influence the simulated fate and effect of discharged drilling muds and cuttings. The four scenarios are:

(1) A shallow (5 m), cold environment with ice cover during a substantial fraction of the year, such as might be encountered in the Beaufort Sea, Alaska;

(2) A shallow (20 m), temperate environment, such as might be encountered in the Gulf of Mexico;

(3) A deeper (80 m), temperate environment, such as might be encountered in the Gulf of Mexico; and

(4) A very deep (1,000 m) environment, such as might be encountered on the Atlantic slope.

Several model limitations or uncertainties are examined by varying selected parameter values and assumptions. The body of the report concludes with a DISCUSSION section summarizing the areas of understanding and uncertainty regarding drilling fluids and cuttings in the marine environment revealed by this modeling effort.

Appendices A through D contain the explicit equations and parameter values used in the various submodels, along with a discussion of their limitations and uncertainties. The appendices thus repeat some of the points summarized in the MODEL DESCRIPTION section in the main body of the report. The complete sets of parameter values used to represent the four cases, or scenarios, for which output is presented are described.

MODEL DESCRIPTION

MODEL BOUNDS

The model is a set of coupled difference equations formulated with a daily time step. The daily time step is used for all simulations; however, some outputs display only periodic values of the state variables (e.g., every 30th day) to avoid exceedingly complex graphs. For numerical simplicity, a simulated year is assumed to consist of 360 days (12 months, each containing 30 days).

The model represents a series of seven discrete 1-m^2 plots at specified distances along a transect in one direction away from a discharge point (Figure 1). Parameters of the model can be set to simulate a wide variety of marine environments and discharge operations. The model does not, however, simulate the dynamics of discharge on the surface of ice.

SUMMARY OF CALCULATIONS

The model can be conceptualized as three connected submodels: Discharge and Plume Fate; Sediment Redistribution; and Benthic Community Effects. On each day of simulation, these submodels are executed in sequence with flows of information between submodels (Figure 2). The Benthic Community Effects submodel can be further divided into sections that calculate mortality due to burial, mortality due to toxicity, mortality due to resuspension disturbance, and growth of the community.

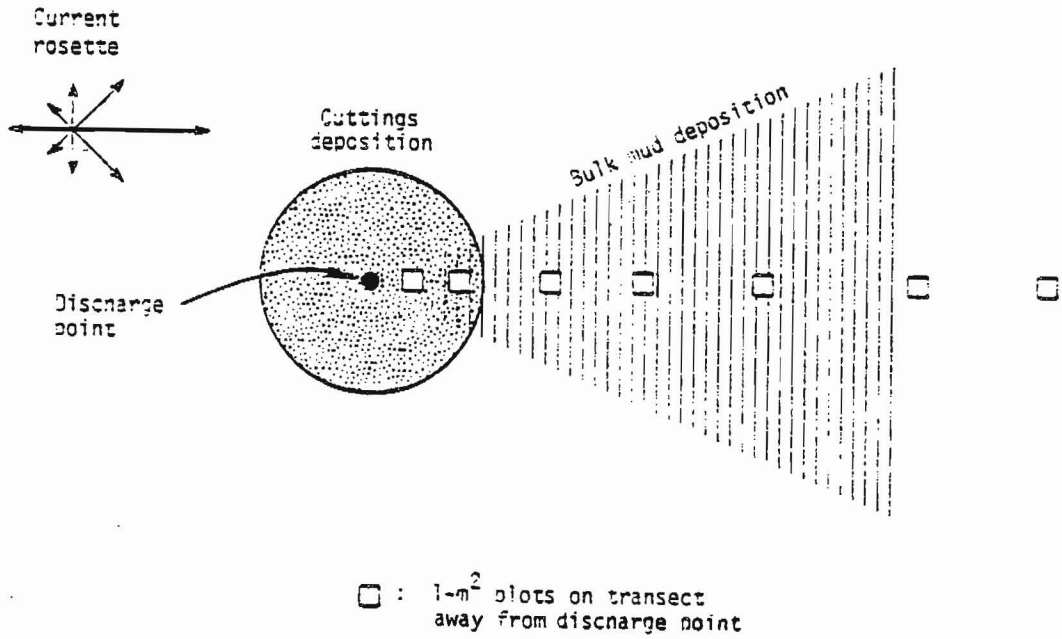

Figure 1. Digrammatic top view of a deposition pattern and the location of simulated plots. The mud plume depicted is the case in which initial deposition is displaced downcurrent from the discharge point. The current rosette would be used to estimate the probability that a bulk mud discharge falls along the simulated transect.

Discharge and Plume Fate

This submodel simulates the depth of material deposited from each discharge event at seven distances from the discharge point. The general sequence of calculations is depicted in Figure 3. Discharged materials are aggregated into three particle size classes of cuttings and three size classes of drilling mud for these calculations. Concentrations of barium, chromium, and hydrocarbons in discharged materials; ratios of solids dispersion and soluble

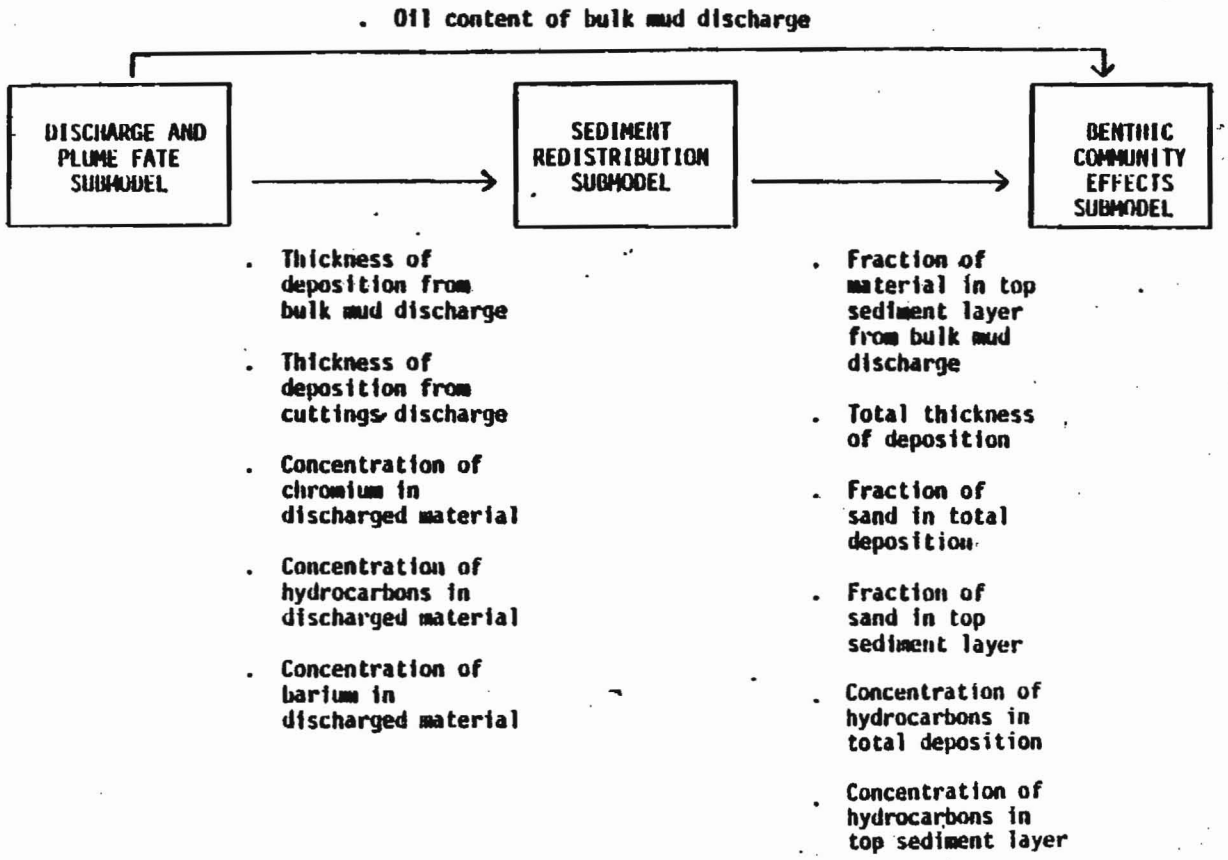

Figure 2. Information exchanges between submodels.

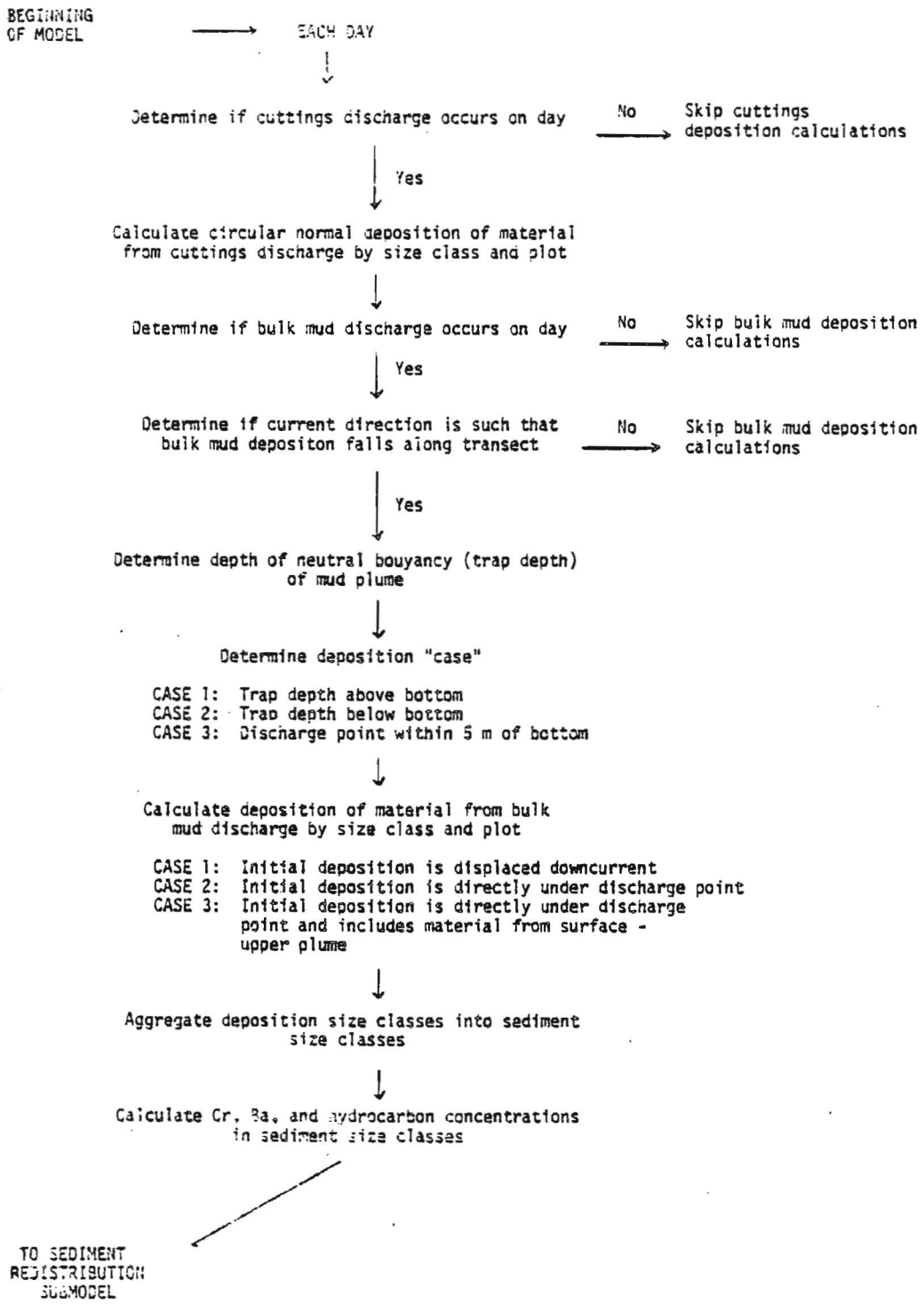

Figure 3. General sequence of calculations concerning discharge and fate.

dilution in the surface plume; and whether or not muds and cuttings discharged are deposited along the transect chosen for evaluating biological effects are also determined. The model can be easily parameterized to represent different geographical areas (e.g., water depth, current velocity and rosette, density stratification, well depth, and total solids discharged), different drilling fluids (e.g., density and chromium and hydrocarbon concentrations), and different discharge procedures (e.g., amount, frequency, rate, and predilution).

Material from a bulk mud discharge is deposited along the transect chosen for evaluating biological effects on any day when both a bulk mud discharge occurs and the direction of the prevailing current is along the transect. The occurrence of a bulk mud discharge event is determined from a frequency of discharge specified as model input. The probability that a discharge occurs on the transect is estimated from a current rosette for the geographical area being simulated (Figure 1). On days when discharged materials fall on the transect, the mud deposition variables are calculated. Deposition of material from solids control equipment discharges (designated here as cuttings discharges) is calculated on all days when such discharges occur, regardless of current direction, because of the circular normal representation described below.

Material from the cuttings (or solids control equipment) discharge is assumed to be distributed on the bottom according to the circular normal probability density function (Figure 4). The standard deviation of this function for each particle size class is a function of the particle settling rate, the current velocity, and an angle of repose constraint on the cuttings pile. The amount of cuttings deposited in a given area is calculated as the product of the total cuttings discharged and an approximation of the double integration of the probability density function, using the coordinates of the area (assuming the discharge point is at coordinates 0,0) as the limits of integration.

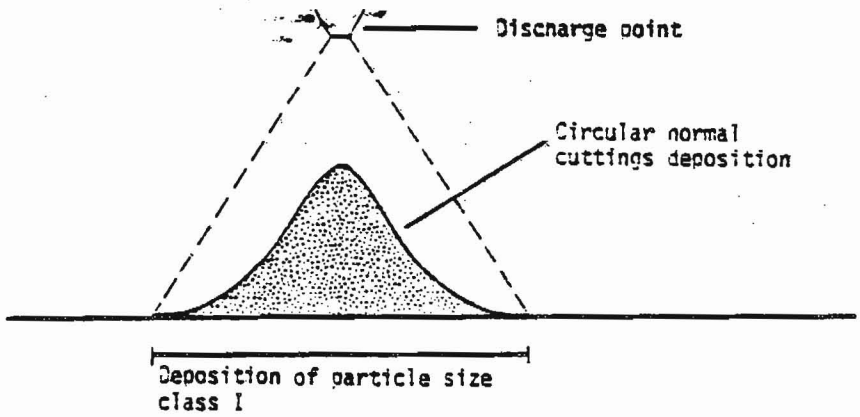

Figure 4. Diagrammatic cross section of deposition of material from cuttings deposition. Total deposition consists of the superposition of three size classes.

Deposition of material from the bulk mud discharge is dependent on the behavior of the plume between the discharge point and the bottom (Figures 5 and 6). Two general cases are considered: (1) the mud plume impacts the bottom and collapses; and (2) dynamic collapse of the mud plume occurs at a trap depth above the bottom. A third special case is considered for shallow water areas where the plume impacts the bottom, but where water is so shallow that the mud plume and surface-upper plume are mixed. The trap depth, or depth of neutral buoyancy, is calculated as a function of discharge momentum, discharge density difference, ambient crossflow velocity, and ambient density stratification. For the first case, each size class of material is deposited from the point of plume impact out to a distance determined from the particle settling rate, the height of the mud cloud created when the plume impacts the bottom, and the bottom current velocity (Figure 5). As the mud cloud moves downcurrent, its width increases due to entrainment of seawater. The same

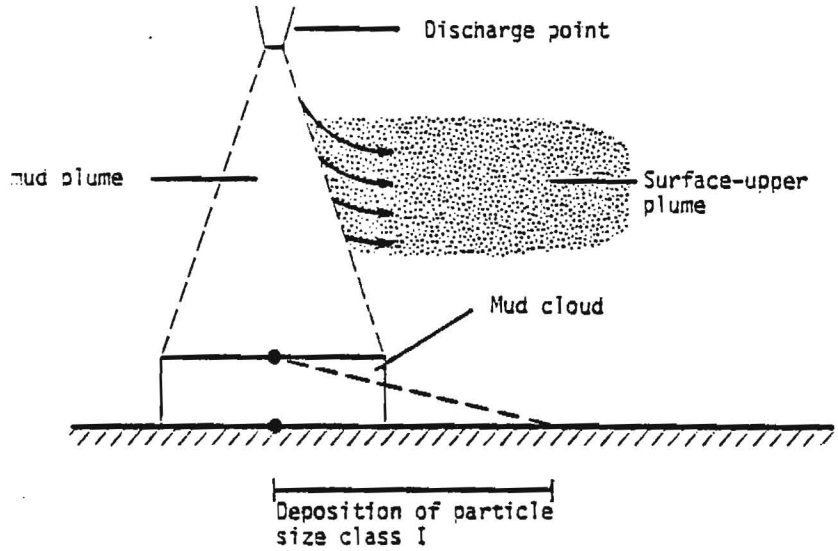

Figure 5. Diagrammatic cross section of mud plume dynamics for case 1: mud plume impacts bottom and collapses. Total deposition is the superposition of three size classes.

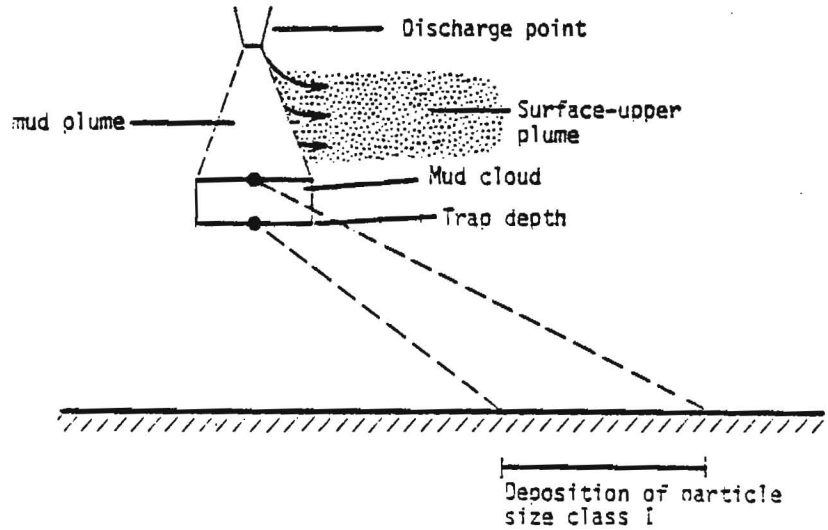

Figure 6. Diagrammatic cross section of mud plume dynamics for case 2: dynamic collapse of mud plume at a trap depth above the bottom. Total deposition is the superposition of three size classes.

amount of material is assumed to be deposited in each 1-m strip that the cloud passes over downcurrent. However, because the mud cloud is increasing in size, the depth of deposited material decreases with distance from the discharge point. Deposition for the second general case is calculated in a similar way, except that the area of depósition is offset from the point of discharge (Figure 6). This occurs because the mud cloud forms at the trap depth and particles settling from it are carried downcurrent before impacting the bottom. In geographic areas and during times of the year when ice is present, current velocities and effective water depths are decreased to simulate discharge under ice.

Concentrations of barium, chromium, and hydrocarbons in the mud discharge are calculated by assuming that they are associated proportionally with the amount of material in each particle size class. The model will, however, allow these materials to be partitioned between soluble and adsorbed phases and selectively partitioned among size classes (e.g., proportionally more associated with small particles due to greater surface area).

Sediment Redistribution

The calculations of sediment dynamics basically consist of a bookkeeping (Figure 7) of the movements of various types of sediment at each 1-m^2 plot along the transect (Figure 1). The general sequence of sediment redistribution calculations is depicted in Figure 8. The sediment profile at each plot is partitioned into three layers:

(1) A top layer with a fixed thickness of 5 cm;

(2) A bottom layer of variable thickness, increasing as a result of net deposition and decreasing as a result of net erosion; and

(3) Underlying natural sediment.

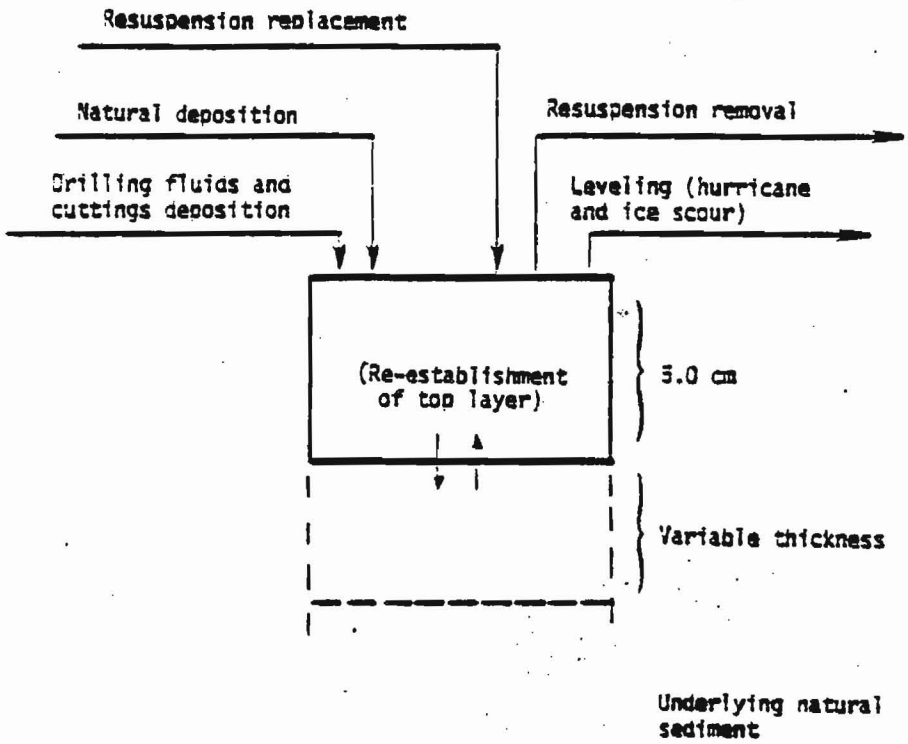

Figure 7. Conceptualization of sediment dynamics at a plot.

Each layer is assumed to be completely mixed. Outflows of sediment consist of leveling, due to hurricane and ice scour events, and resuspension. Inflows of sediment consist of deposition of discharged drilling mud and cuttings, deposition of natural sediment associated with high river discharge (e.g., during snow melt in Alaska), and replacement of sediment associated with resuspension events.

If the topography of the bottom has not been altered, the resuspension caused by disturbance events is generally assumed to result in no net change in the total amount of sediment (measured as thickness in cm) at a given plot. Rather, the multiple, individual resuspensions associated with a disturbance event are conceptualized as removing a given thickness of sediment at the plot and replacing that thickness with natural sediment. There are several ways in

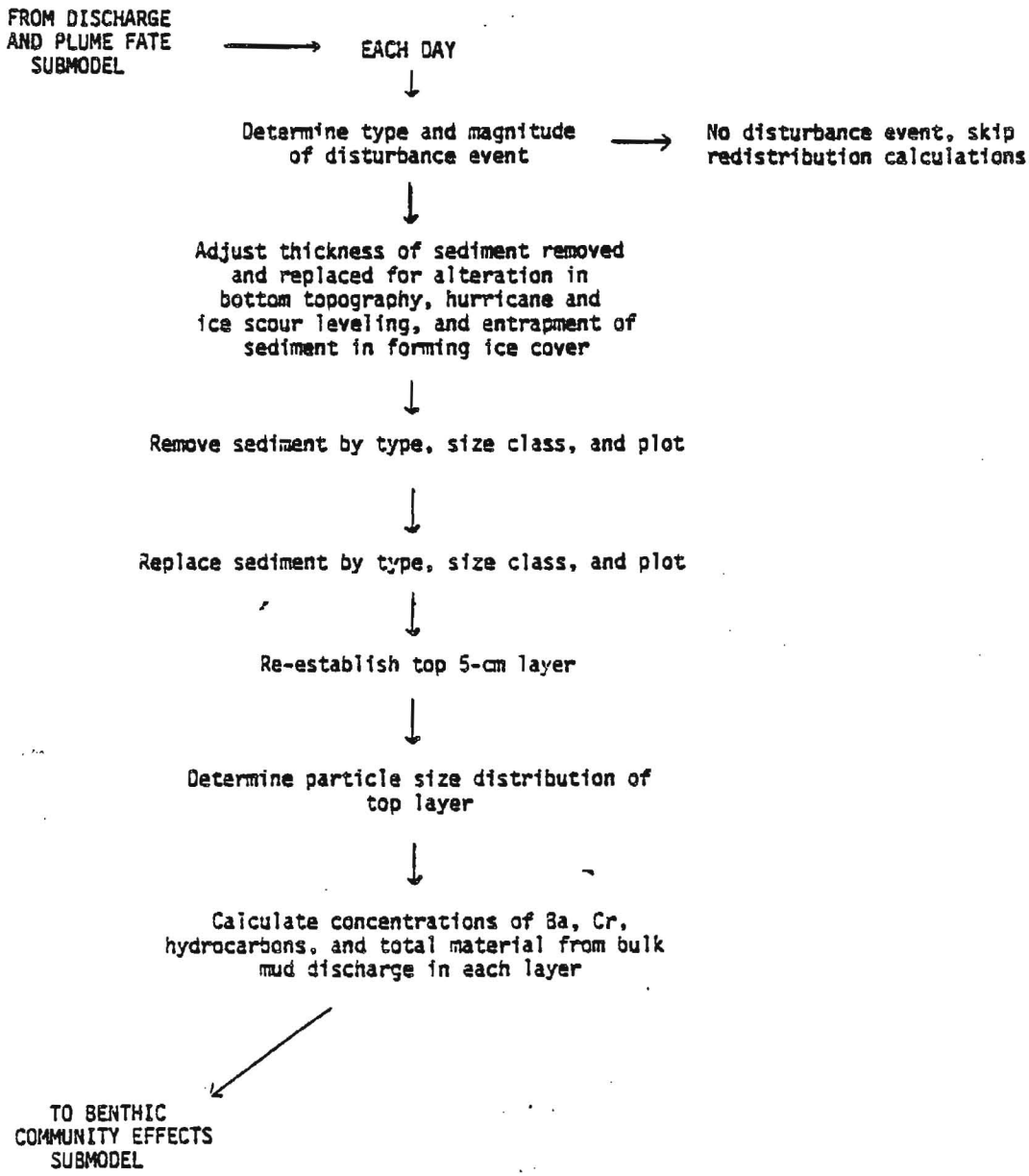

Figure 8. General sequence of calculations concerning sediment redistribution.

which a change in total sediment height may result from a disturbance event: (1) when the topography of the bottom has been altered, the amounts of sediment removed and replaced are adjusted as a function of the altered topography (e.g., a thick pile erodes more quickly than a thin pile); (2) when the size class distribution at the plot differs from that of natural sediment and the disturbance event is specified as differentially affecting the two size classes; (3) during ice formation when some fraction of the resuspended material is entrapped or frozen in the ice; and (4) in a hurricane or ice scour event when leveling may occur. Leveling due to hurricane and ice scour events is calculated and described separately from the resuspension process.

Deposition of drilling muds and cuttings is provided by the Discharge and Plume Fate submodel. The magnitude and timing of other events are determined by sampling from statistical distributions of the thicknesses of sediment disturbed and intervals between events. The basic sediment variable represents cm of sediment distinguished by distance from discharge point, layer (top 5-cm layer and bottom layer), size class (silt and clay, and sand), and type (natural, bulk mud discharge, and cuttings discharge).

After inflows and outflows of the various kinds of sediment are calculated for a given day, the top 5-cm layer is re-established. Summary indicators (thickness of layers, proportion of sand, chromium concentration, hydrocarbon concentration, and fraction of material from the mud discharge in the top sediment layer) are then calculated by summing over the various kinds of sediment and applying the appropriate densities and concentrations specified for the different types and size classes of sediment.

Benthic Community Effects

The model conceptualized at the workshop assumes that the benthic community is composed of three species assemblages: (1) a meiofaunal assemblage; (2) a pioneer or early successional macrofaunal assemblage; and (3) a late successional macrofaunal assemblage. This section of the model calculates

numbers of individuals per m^2 in each of these assemblages under the conditions generated by the discharge and sediment redistribution portions of the model, at each of the seven locations along a transect away from the discharge point (Figure 1). On any day of simulation (Figure 9), the number of individuals in each species assemblage may change as a result of four processes: (1) mortality due to burial by deposited mud and cuttings or natural sediments; (2) mortality due to the toxicity of deposited mud and cuttings; (3) mortality due to resuspension events, such as storms and ice movement; and (4) population growth due to both asexual reproduction and larval recruitment.

Burial. On each day of simulation, a mortality rate for each species assemblage is calculated as a function of the depth of sediment deposited on that day and the similarity between the particle size distribution of the deposited sediment and that of natural sediment of the site. For each species assemblage, workshop participants derived two curves relating depth of deposited sediment to mortality: one for "indigenous" sediments and one for "exotic" sediments (e.g., drilling mud and cuttings). An example of this mortality relationship is depicted in Figure 10 for the late successional macrofaunal assemblage. The model chooses between these two curves based on the sand content of the deposited material. If the difference between the proportion of sand in the deposited material and in indigenous material exceeds a user-specified value, the "exotic" mortality functions are used; otherwise, the "indigenous" mortality functions are selected. These mortality rates are adjusted by multiplying the mortality rate by a user-specified estimate of relative community sensitivity. This "community sensitivity" factor, which essentially shifts the mortality curves upward or downward along the y-axis, was included for possible use in the submodel because data may not be available to estimate separate mortality curves for all environments. The community sensitivity coefficients represent participants' estimates of the greater sensitivity of continental shelf and slope communities relative to the shallow water responses. The adjusted mortality rates are multiplied by the number of individuals present to determine the number of individuals that die. A new estimate of the number of individuals present is then obtained by subtraction.

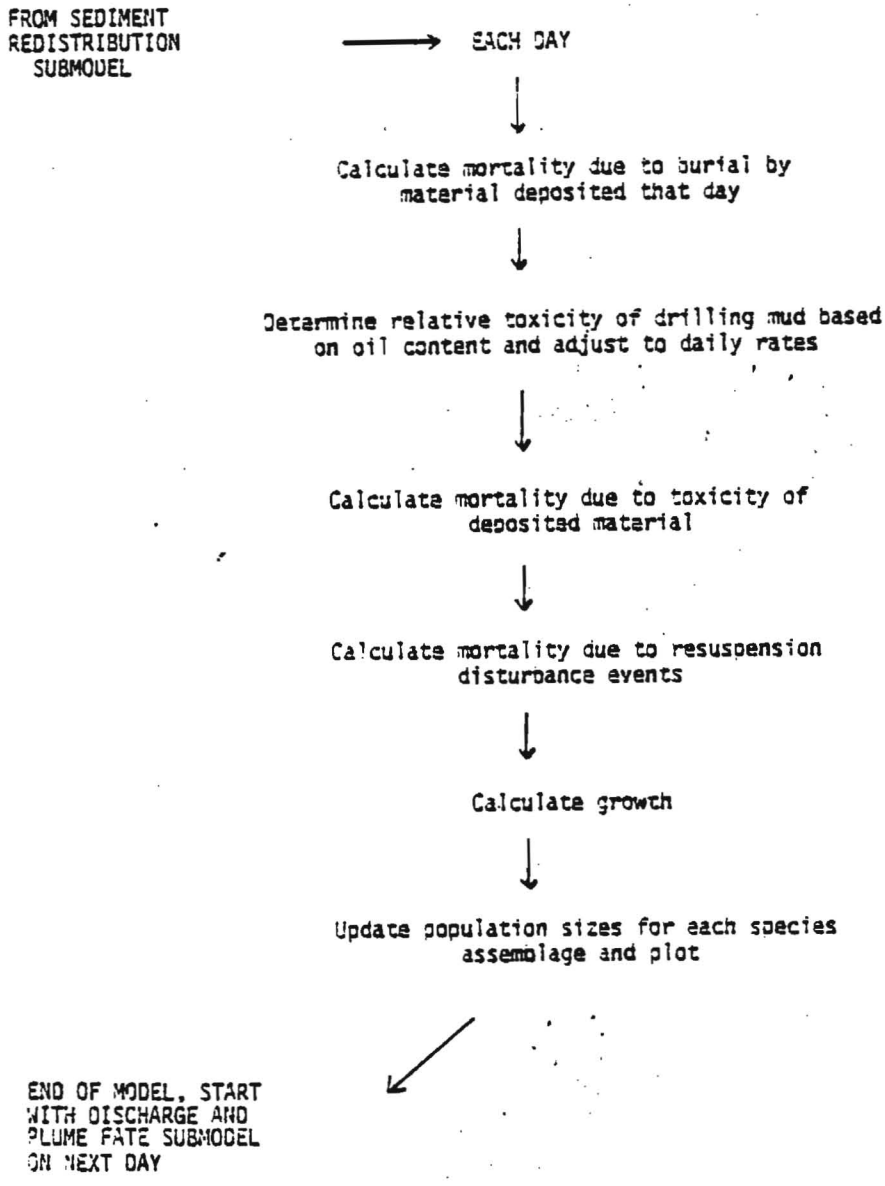

Figure 9. General sequence of calculations concerning benthic community effects.

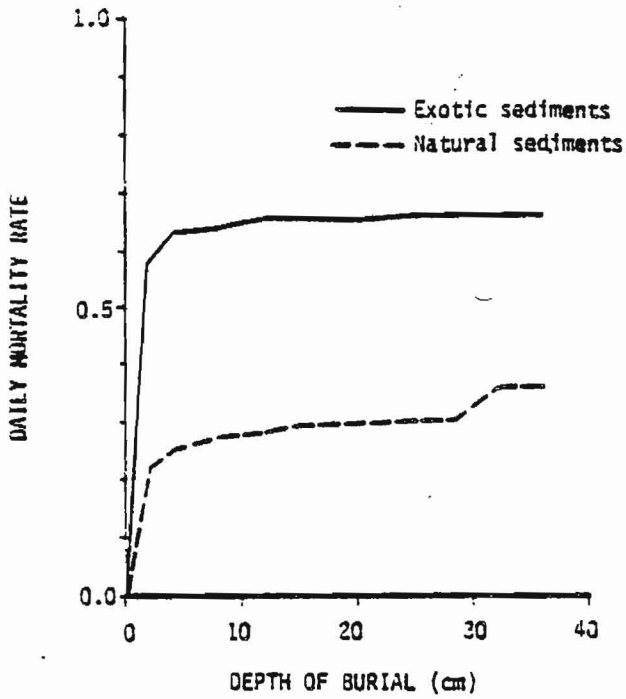

Figure 10. Mortality rates for late successional macrofaunal assemblage as a function of depth of burial.

Toxicity. Following removal of animals due to burial, the Benthic Community Effects submodel computes additional mortality associated with the toxicity of deposited materials. Because composite toxicity data are not available for the three species assemblages considered in the model, a single species for which data are available is chosen to represent each assemblage. The model presently uses data for *Mysidopsis* sp. (an opossum shrimp) to represent the early successional macrofaunal assemblage and *Palaemonetes* sp. (a grass shrimp) to represent the late successional macrofaunal assemblage. Suitable data for a representative of the meiofaunal assemblage are not presently available. Thus, no output is presented for population response of the meiofaunal assemblage, although the model could be used to examine the results of hypothesized toxicity relationships. All of the toxicity data can be easily changed to represent different geographic locations or to incorporate new information as it becomes available. For example, species that are more or less sensitive can be substituted when appropriate data is available.

Four basic steps are involved in the calculation of mortality due to the toxic effects of deposited materials: (1) developing an acute toxicity relationship between daily survival and concentration for a reference mud; (2) adjusting the acute toxicity relationship if the mud considered in the model is other than the reference mud; (3) adjusting the acute toxicity relationship if the model communities are subjected to a chronic exposure; and (4) determining the daily survival rate from the exposure concentration produced by the Sediment Redistribution submodel.

Although the model operates on a daily time step, laboratory toxicity tests for spent drilling muds do not typically include 24-hr exposures. Relationships between exposure concentrations and daily survival for a reference mud are, therefore, derived in the following way. Laboratory test results are often reported as the concentrations that result in a series of survival (or mortality) rates (e.g., 90, 70, 50, 30, and 10%) for a series of one or more exposures of varying duration (e.g., 48, 72, and 96 hr). These results are often arrived at through probit analysis of the raw test data. For each combination of survival rate and exposure duration, a corresponding daily survival rate is calculated, assuming that the rate of loss is constant over the duration of the exposure. For example, a survival rate of 0.7 for a 96-hr exposure produces a constant daily survival rate of 0.915 (i.e., $0.915^4 = 0.7$). Daily survival rates calculated in this manner are plotted against the corresponding concentrations and fitted with a single curve using regression techniques. A linear relationship can usually be obtained by squaring the values of the independent variable (concentration).

The toxicity relationship derived in this manner for a reference mud is adjusted if the mud being simulated is other than the reference mud. Available information indicates a relatively strong correlation between the toxicity of a particular mud and its hydrocarbon content. A relationship is, therefore, calculated in which the independent variable is hydrocarbon concentration and the dependent variable is the ratio of the 96-hr LC_{50} for a given hydrocarbon content and the 96-hr LC_{50} of the reference mud. For example, if this

relationship indicates a ratio of 2 for the mud being simulated, then the slope of the basic toxicity curve is divided by 2.

Changes in toxicity due to long term or chronic exposure are incorporated in a similar way. Workshop participants indicated that a useful regulatory rule-of-thumb is that chronic exposure to one-tenth of a given concentration will result in about the same survival as an acute exposure to the given concentration. This is implemented in the model by dividing the slope of the basic toxicity relationship by a user-specified factor (nominally set at 0.1) if organisms are continuously exposed to drilling muds for periods exceeding a user-specified length (nominally set at 28 days). A daily survival rate for each species assemblage is calculated from the slope and intercept of the adjusted toxicity relationship and the adjusted exposure concentration produced by the Sediment Redistribution submodel.

Resuspension. Each of the three species assemblages is also subjected to a third mortality factor, associated with resuspension or movement of sediments during events such as storms and ice scouring. Intensity of these events is measured by the thickness of sediment disturbed (calculated by the Sediment Redistribution submodel). Mortality rates for each species assemblage for various thicknesses of disturbance were estimated by workshop participants.

Growth. Growth of the meiofaunal and late successional species assemblages is represented with logistic equations (Pielou 1977) of the form:

$$dN_1/dt = N_1 (r_1 - s_1N_1) \quad (1)$$

$$dN_3/dt = N_3 (r_3 - s_3N_3) \quad (2)$$

where N_1, N_3 = number of individuals per m^2 in the meiofaunal and late successional macrofaunal species assemblages, respectively

r_1, r_3 = potential per capita growth rates for each assemblage in the absence of competition

s_1, s_3 = reductions in the potential per capita growth rates per individual present

For the early successional or pioneer macrofaunal assemblage, the growth equation is modified slightly to represent the competitive effect of individuals of the late successional macrofaunal assemblage:

$$dN_2/dt = N_2 (r_2 - s_2N_2 - k_2N_3) \quad (3)$$

where N_2 = number of individuals per m^2 in the pioneer macrofaunal species assemblage

N_3 = number of individuals per m^2 in the late successional macrofaunal species assemblage

r_2 = potential per capita growth rate in the absence of competition

s_2 = reduction in the potential per capita growth rate per pioneer macrofaunal individual present

k_2 = reduction in the per capita growth rate of the pioneer assemblage per individual of the late successional assemblage present

Parameter values for these equations were estimated by workshop participants. In addition, participants formulated relationships that reduce the potential growth rates as functions of changes in sediment particle size distribution and contamination of the sediments by hydrocarbons.

MODEL BEHAVIOR

The basic model output consists of graphs of the daily values of variables. This section presents a variety of such graphs, portraying the behavior of variables at plots representing distances along a transect away from the discharge point. The same seven distances are used in each scenario: 5 m; 50 m; 500 m; 1,500 m; 3,000 m; 4,000 m; and a control plot that receives no deposition of discharged material. Rather than attempt to include all distances for all scenarios and variables, certain distances were selected where differences in behavior and causal connections were most apparent. Two types of graphs are included. The first type consists of all the daily values of a variable for a 1-yr run of the model. The second type of graph is used for longer model runs. In these graphs, only every thirtieth daily value is plotted (i.e., one daily value is plotted each month).

WORKSHOP SCENARIOS

Four scenarios were selected from those discussed at the workshop. These scenarios were chosen to represent a wide range of physical environments. Conditions for each scenario are summarized in the following sections. Detailed parameter values are presented in the appendices that describe the various submodels.

Scenario 1

This scenario represents a shallow, cold water, high latitude environment, such as might be encountered in the shallow Beaufort Sea. Conditions and parameter settings are summarized in Table 1; complete specifications are

Table 1. Summary of Scenario 1 conditions.

DISCHARGE	
# wells	60
time per well	30 days
start of drilling	day 10
end of drilling	day 1,810
frequency of mud discharge	daily
volume of mud discharge	200 bbl
rate of mud discharge	1,000 bbl/hr
discharge depth	surface
PHYSICAL	
water depth	5 m
average surface current	13 cm/sec
average bottom current	13 cm/sec
% of time current is in direction of transect	40%
mean amplitude of largest disturbance event	75 cm of sediment
mean amplitude of largest disturbance event occurring at least once per year	5 cm of sediment
BIOLOGICAL	
doubling time	
early successional macrofauna	6 days
late successional macrofauna	60 days
carrying capacity	
early successional macrofauna	10,000/m^2
late successional macrofauna	5,000/m^2
96-hr LC_{50} of material from bulk mud discharge	
early successional macrofauna	~ 50,000 ppm
late successional macrofauna	~ 130,000 ppm

contained in the appended submodel descriptions. In this scenario, deposition of material from the bulk mud discharge is calculated as Case 3, in which the mud plume impacts the bottom and the water is so shallow that the mud plume and surface plume are mixed.

One-year run. Drilling and discharge begin on day 10. At the end of 1 year, cumulative total deposition of discharged material is approximately 2,100 cm at 5 m, 34 cm at 50 m, and less than 0.5 cm at 500 m (Figures 11 to 13). The composition of deposited material changes with distance and season (current velocity) as a function of the different behavior (settling rates) of various particle size classes. At 5 m, over 95% of the total deposition is the large sediment (sand) size class (Figure 11). During the summer, ice-free season, current velocities are higher and less material is deposited at the 5-m plot as the discharged material is carried farther downcurrent away from the discharge point. This is especially evident in the small sediment (silt-clay) size class of material from both the bulk mud and cuttings discharges (Figure 11). At 50 m (Figure 12), the total deposition at the end of 1 year is composed of the small sediment size class from bulk mud discharges (68%), the small sediment size class from cuttings discharges (25%), and the large size class from cuttings discharges (7%). There is no material from the bulk mud discharges that corresponds to the large sediment size class (sand), and none is deposited at any plot (i.e., all of the three size classes of bulk mud material used in the fate calculations convert to the small sediment size class). At 50 m, the higher current velocities of the summer season produce a substantially lower rate of deposition of the small sediment size class of cuttings discharge as the material is distributed farther downcurrent. However, the large sediment size class of cuttings material is deposited as far as 50 m only during the period of higher current velocities.

Less than 1 cm of discharged material is deposited at the 500-m plot, and this material is mostly (82%) composed of the small sediment size class of bulk mud discharge (Figure 13). Deposition rates for this sediment size class of material from both bulk mud and cuttings discharges increase with higher current velocities (summer, ice-free season) when more material reaches this distance.

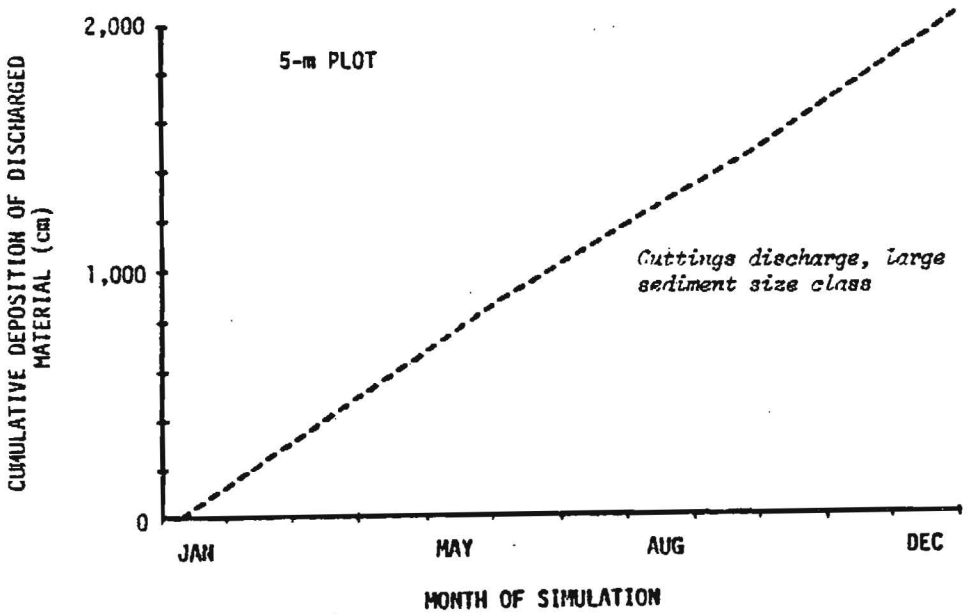

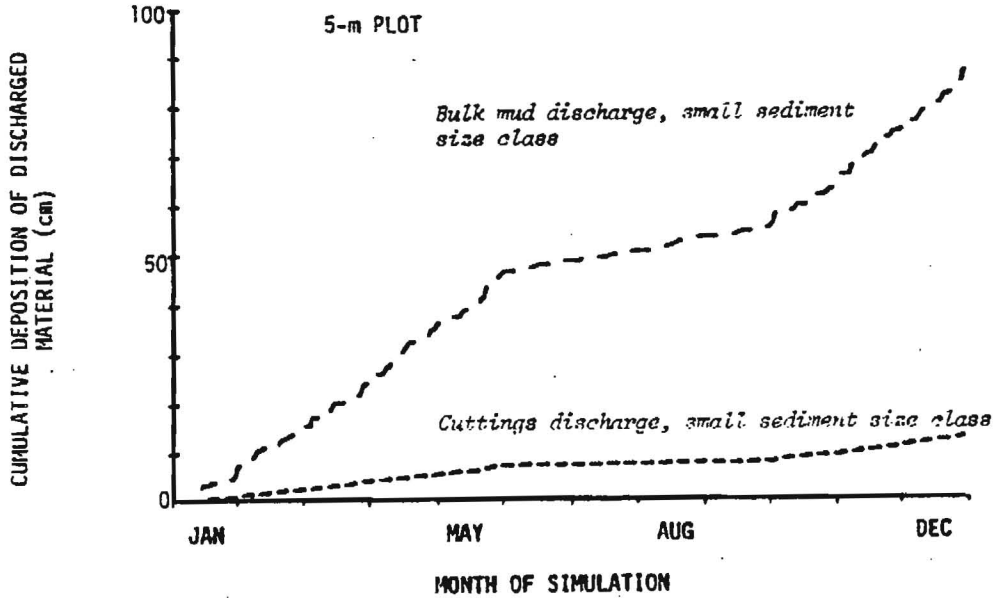

Figure 11. Scenario 1: cumulative deposition of discharged material at 5-m plot, 1-yr run.

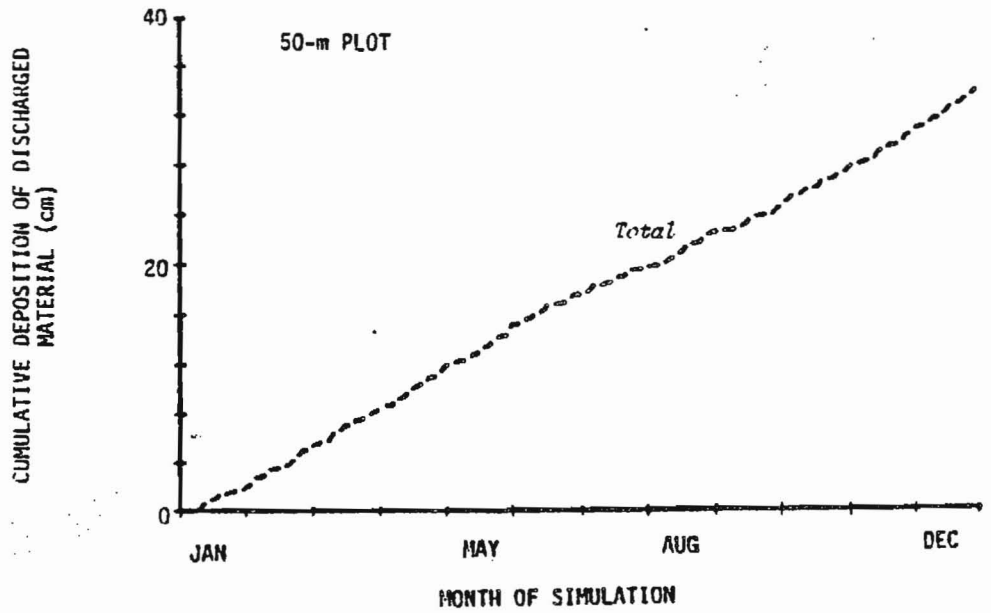

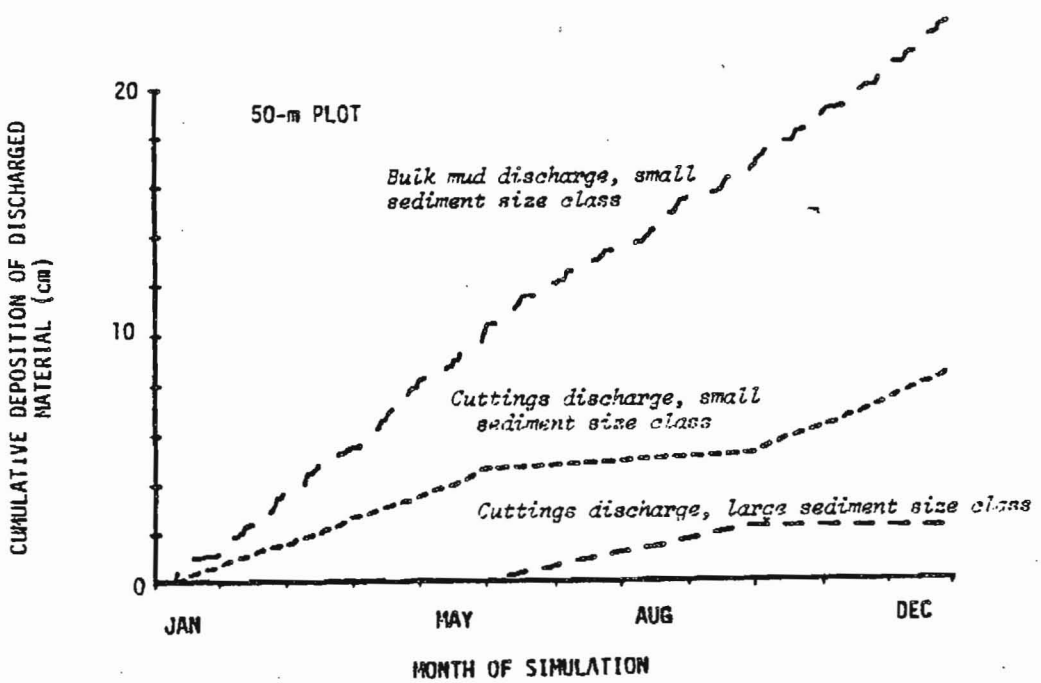

Figure 12. Scenario 1: cumulative deposition of discharged material at 50-m plot, 1-yr run.

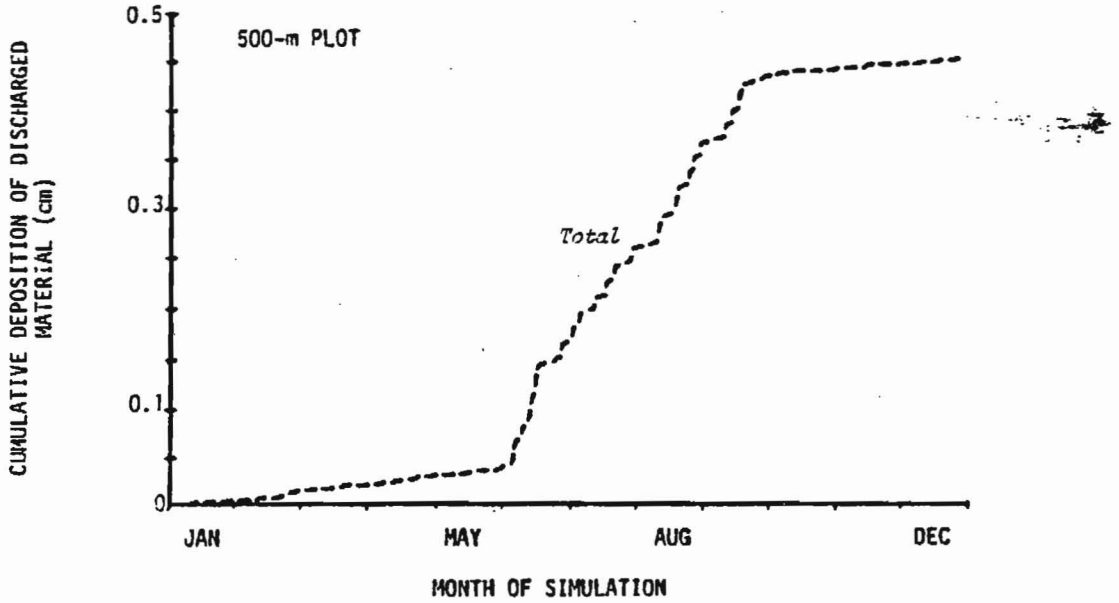

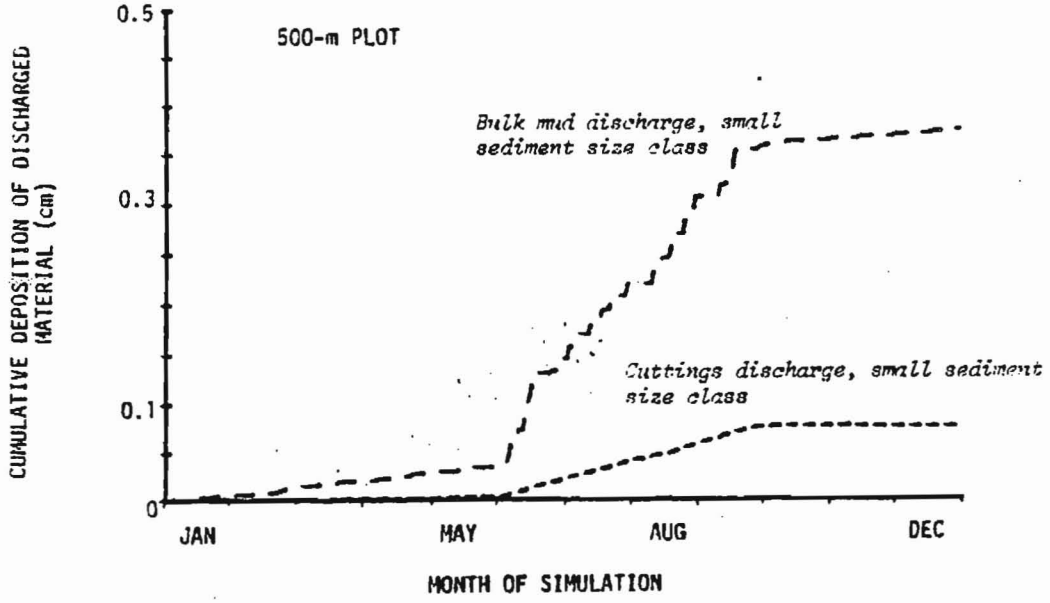

Figure 13. Scenario 1: cumulative deposition of discharged material at 500-m plot, 1-yr run.

The disturbance regime is represented in terms of the thickness of sediment disturbed as a result of various events occurring at different frequencies (Figure 14). The regime is dominated by the 75-cm ice scour event early in the year. There are also several fall events that disturb a substantial thickness (5 to 10 cm) of sediment.

The result of interaction between the sediment disturbance regime (Figure 14) and the deposition of discharged (Figures 11 to 13), as well as natural, material can be seen in the net accumulation, or thickness, of sediment (Figure 15). Major storm events are especially evident at the 5-m plot. The effects of a given disturbance are magnified by alterations in the bottom topography (e.g., a tall mound erodes more than a low mound). Thus, the thickness of net accumulation reaches a plateau at around 200 cm, despite continued deposition, because of the magnified effects of nominal wave action. At 50 m, net accumulation is much less and the alteration of bottom topography is less pronounced. As a result, net accumulation is a much higher fraction of total deposition at 50 m than at 5 m. The 10 days of natural deposition associated with snow and ice melting and high river discharge is evident in late June at both the 50 and 500-m plots, where natural deposition constitutes a significant fraction of total (natural plus discharged) deposition (Figure 15). The natural deposition in early summer is roughly balanced in the fall by erosion due to entrapment of sediment suspended during ice formation.

The fraction whole mud in the sediment (Figures 16 and 17), defined here as the volume/volume fraction of material from bulk mud discharges in the top 5-cm sediment layer, depends not only on the total deposition and disturbance fluxes that produce the pattern of net accumulation, but also on the balance between material from cuttings as opposed to bulk mud discharges. Maximum values for the fraction whole mud in the 1-yr run are: 181,000 ppm at 5 m; 236,000 ppm at 50 m; 12,600 ppm at 500 m; and 290 ppm at 1,500 m (Figures 16 and 17). Several general factors combine to explain the pattern at any given distance:

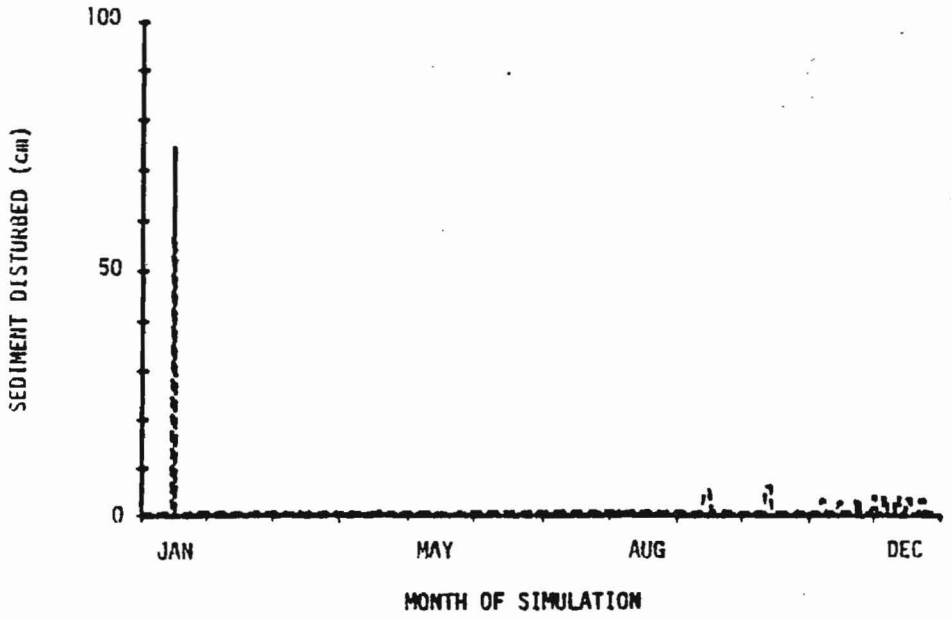

Figure 14. Scenario 1: sediment disturbance regime, 1-yr run.

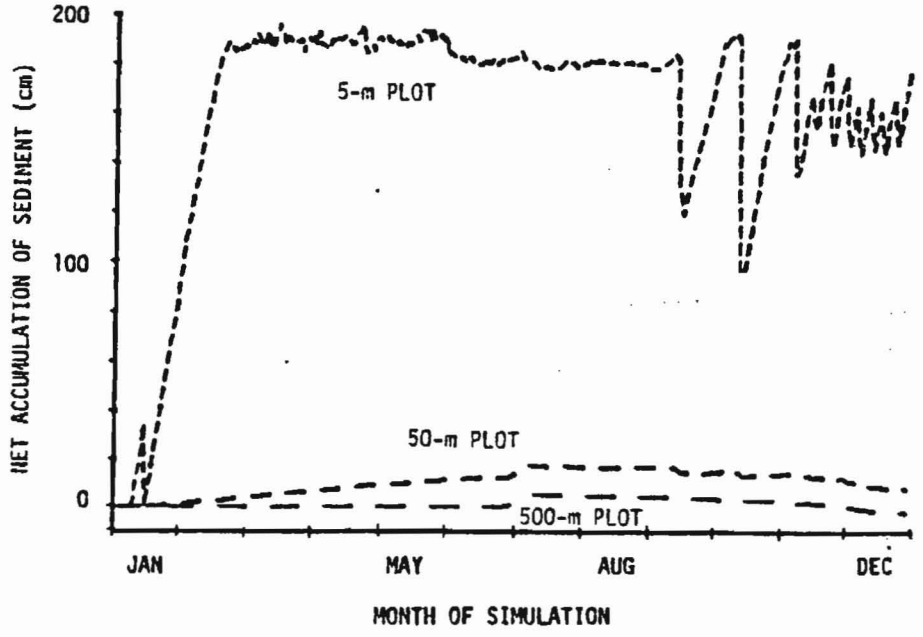

Figure 15. Scenario 1: net accumulation of sediment at 5, 50, and 500-m plots, 1-yr run.

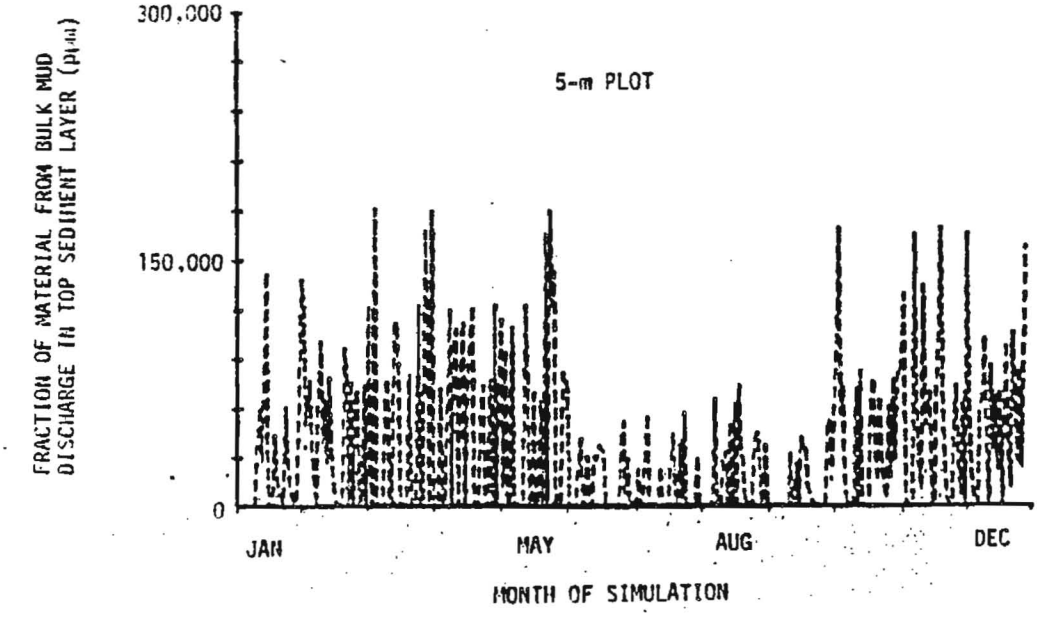

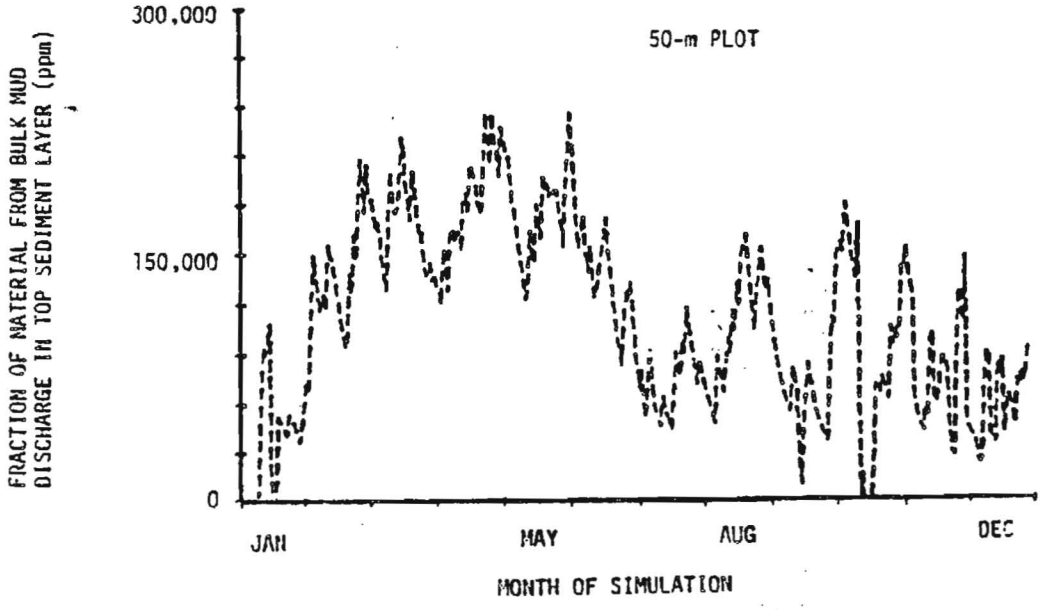

Figure 16. Scenario 1: fraction of sediment from bulk mud discharge in top 5-cm layer at 5 and 50-m plots, 1-yr run.

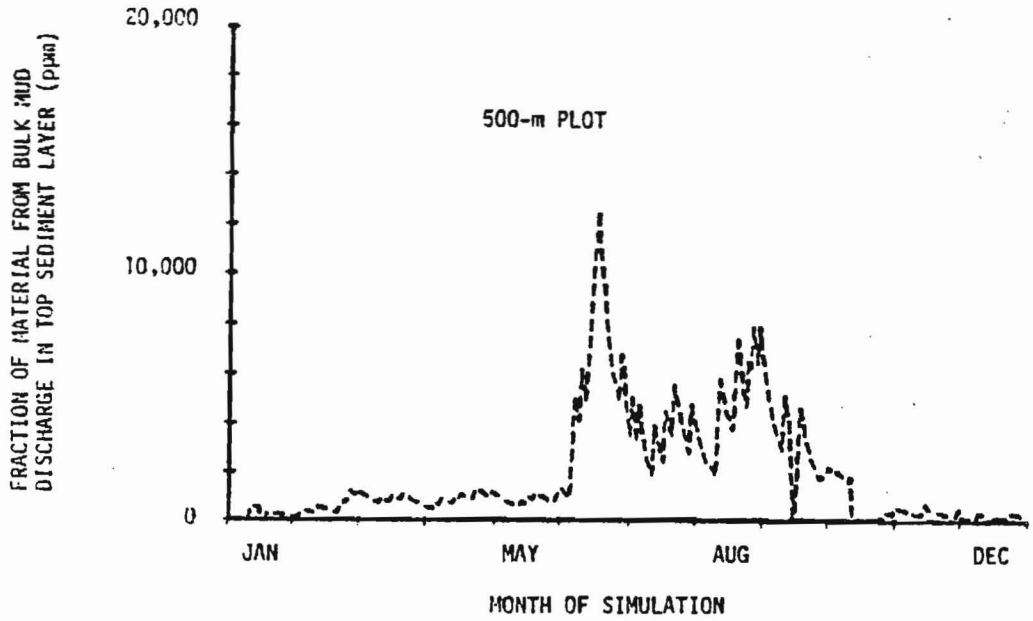

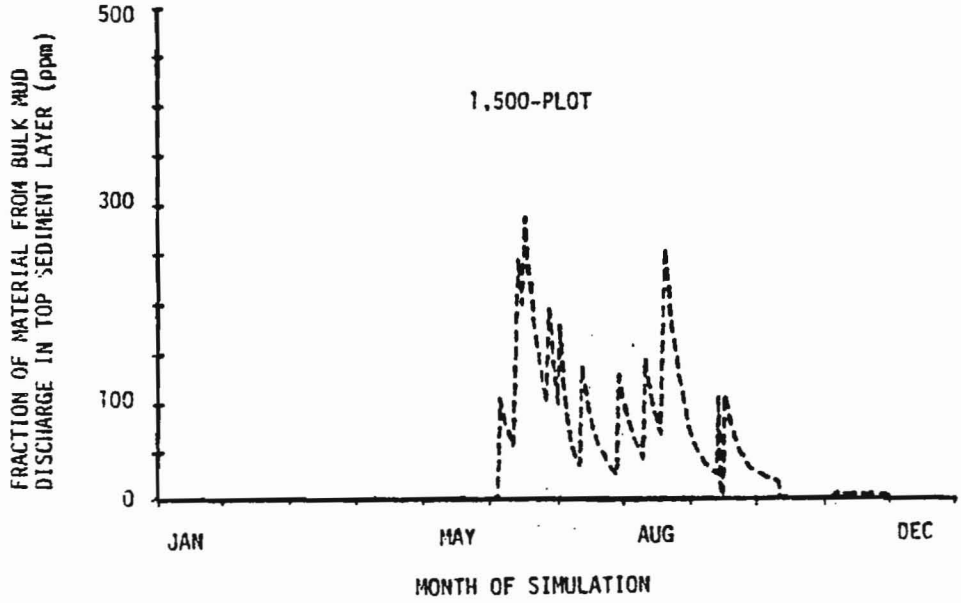

Figure 17. Scenario 1: fraction of sediment from bulk mud discharge in top 5-cm layer at 500 and 1,500-m plots, 1-yr run.

(1) Deposition of material from the bulk mud discharges (Figures 11 to 13) increases the concentration of material from the bulk mud discharge in the top 5-cm sediment layer (fraction whole mud).

(2) Removal of sediment and replacement with natural sediment due to disturbance events (Figure 14) reduces the fraction whole mud.

(3) Deposition of material from cuttings discharges (Figures 11 to 13) or natural deposition decreases the fraction whole mud.

(4) Increased current velocities spread material farther downcurrent and affect material from the bulk mud discharges more strongly than they affect material from the cuttings discharges because the bulk mud particles are generally smaller and settle more slowly. Thus, the increased current velocities during the summer period result in increased fractions whole mud at 500 and 1,500 m as more material from the bulk mud discharge reaches these distances (Figure 17). Close to the discharge point, however, increased current velocities produce lower fractions of whole mud because the balance between bulk mud and cuttings material is shifted towards a greater fraction of material originating from cuttings discharges (Figure 16).

Figures 18 through 21 depict the dynamics of early and late successional macrofaunal assemblages, in units of number per m^2. In the general calculation, the number of organisms in the assemblages changes as a result of the intrinsic growth rate (doubling time), intraspecific competition (carrying capacity), interspecific competition, disturbance mortality, burial mortality, mortality due to fraction whole mud in sediment (toxicity), reduction in growth rate due to the size class composition of sediment and deposited material, growth reduction due to the hydrocarbon content of sediment and deposited material, and limitation of growth due to temperature (ice). Assemblages are constrained to a lower bound of 1% of their carrying capacity.

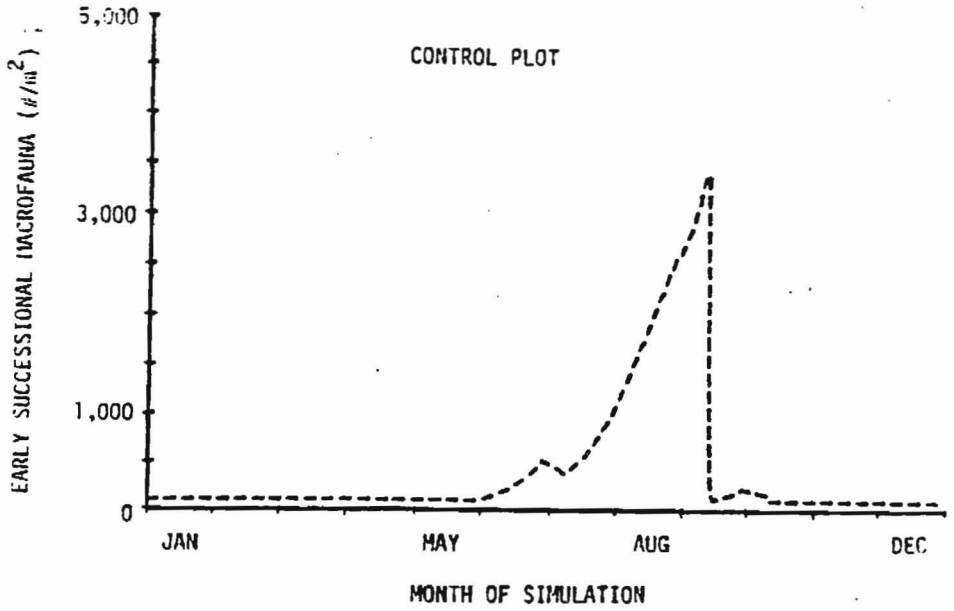

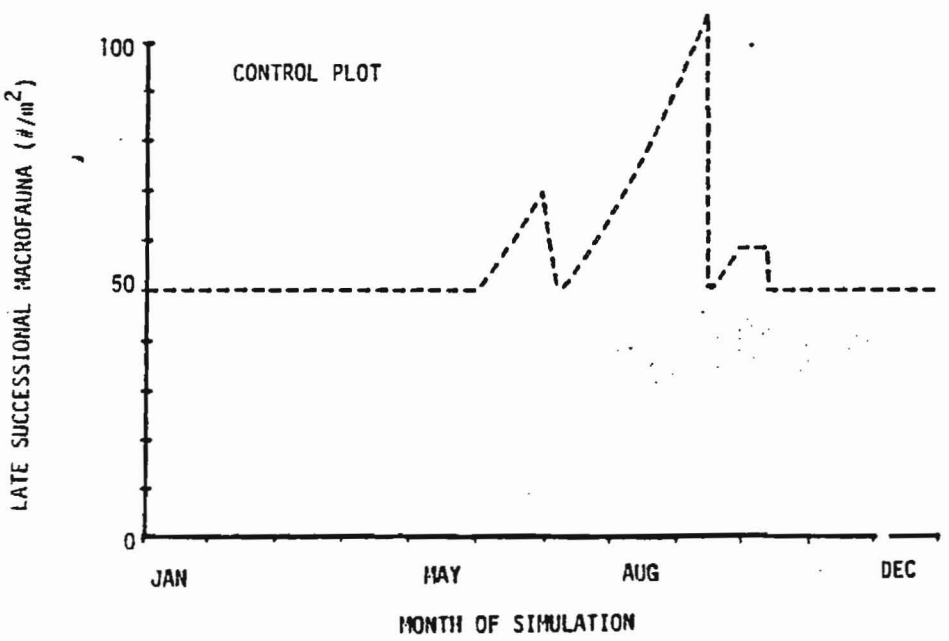

Figure 18. Scenario 1: macrofaunal assemblages at control plot, 1-yr run.

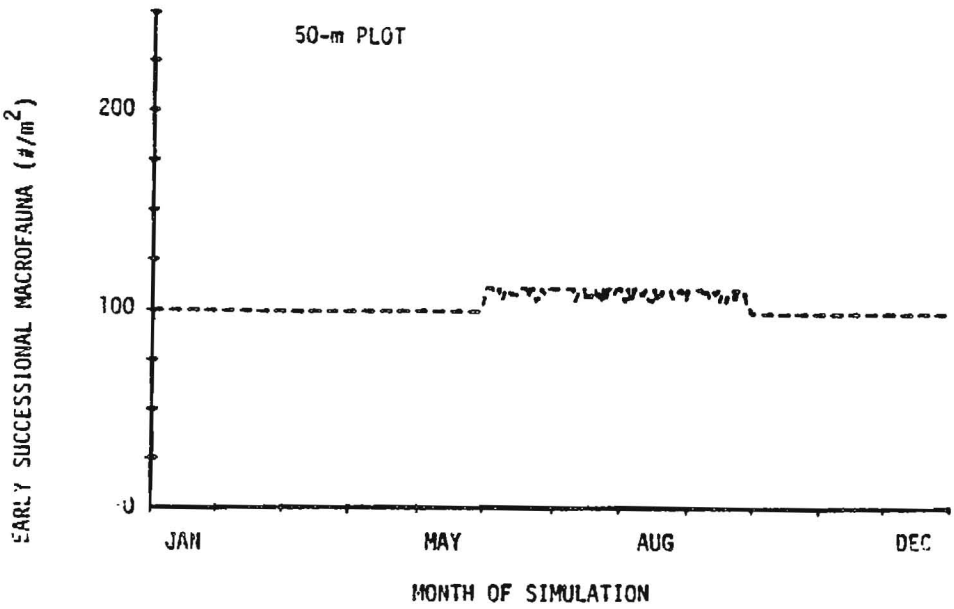

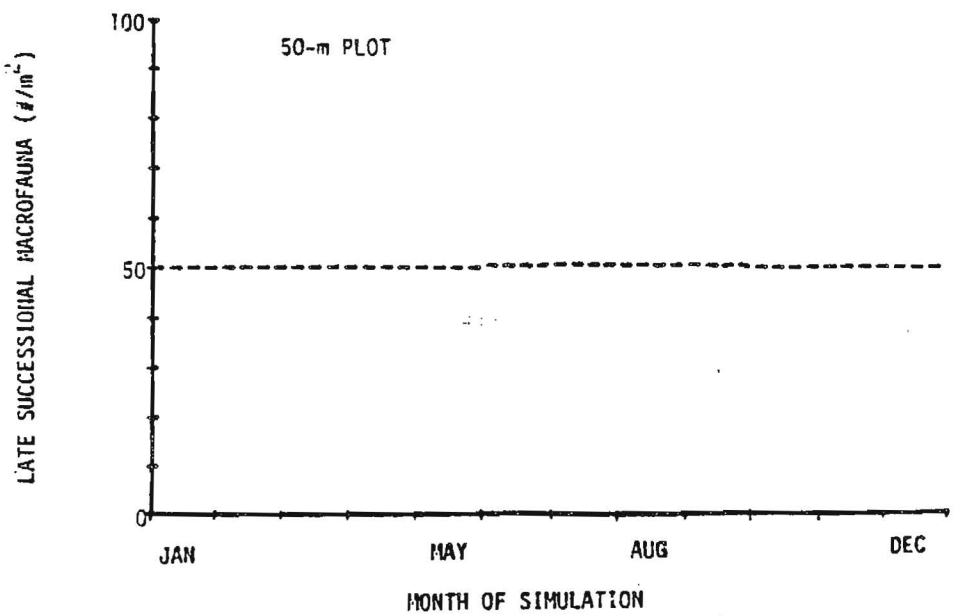

Figure 19. Scenario 1: macrofaunal assemblages at 50-m plot, 1-yr run.

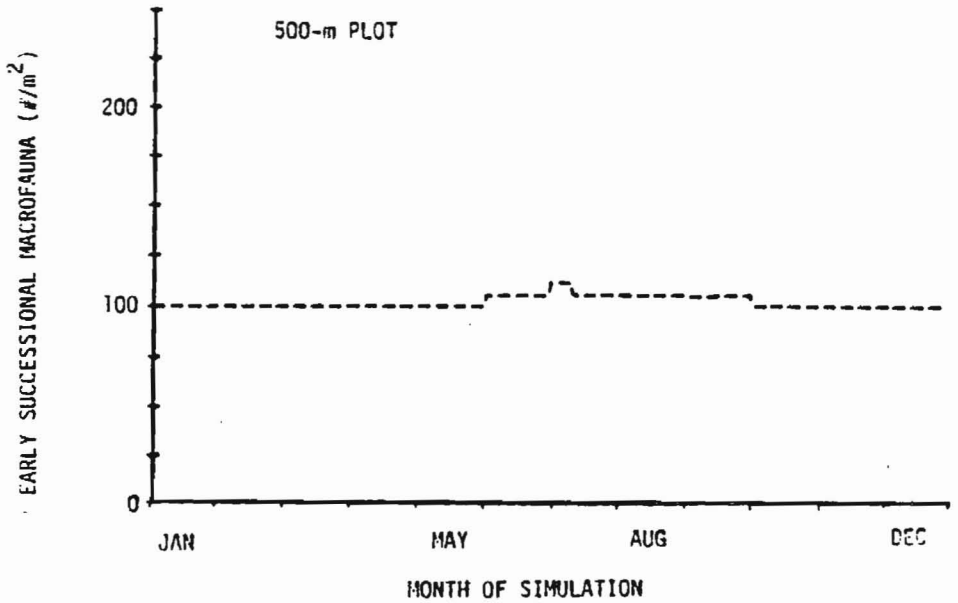

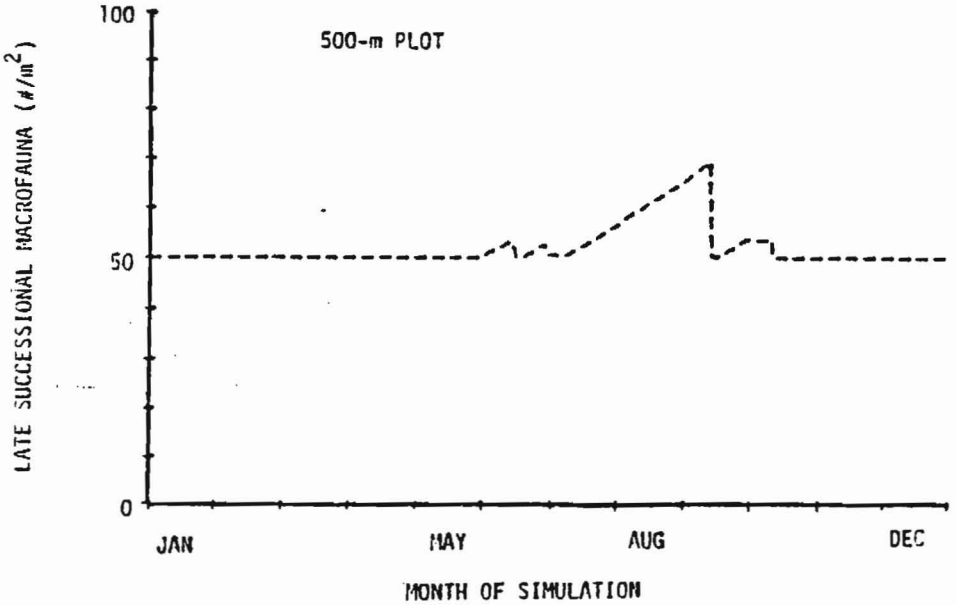

Figure 20. Scenario 1: macrofaunal assemblages at 500-m plot, 1-yr run.

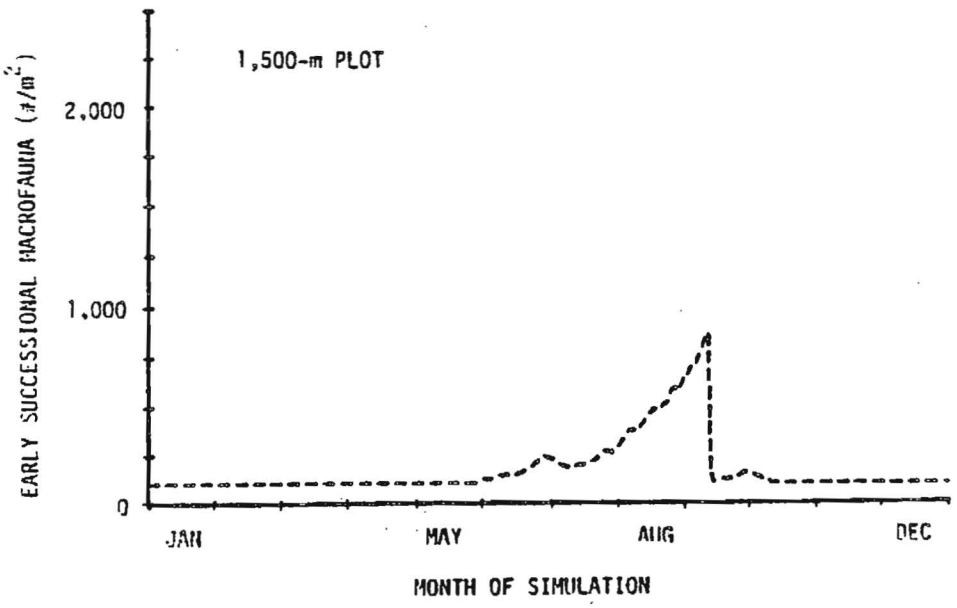

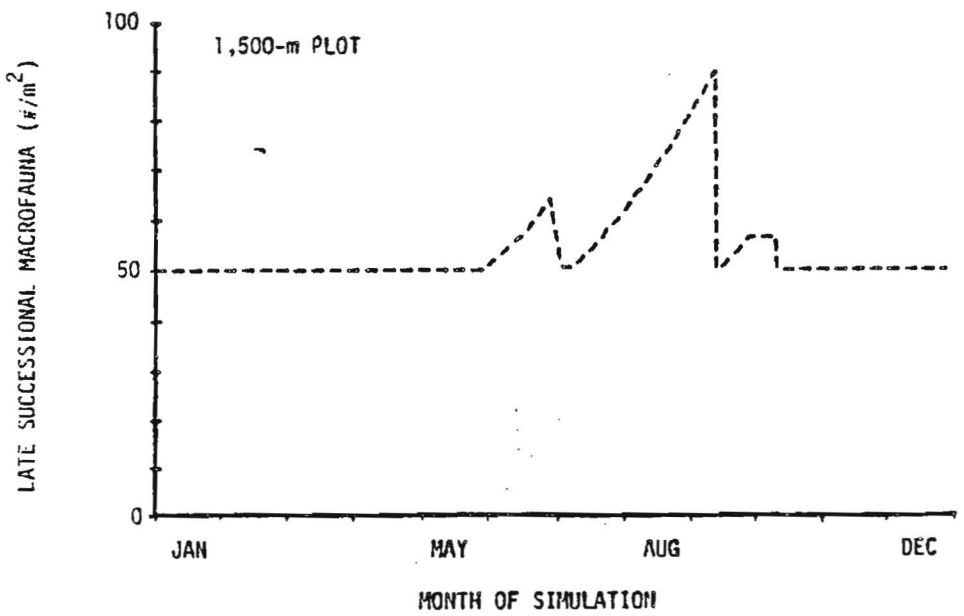

Figure 21. Scenario 1: macrofaunal assemblages at 1,500-m plot, 1-yr run.

Several factors explain many of the differences in the patterns of biological effect at various plots (Figures 18 to 21; note differences in scale):

(1) The early successional macrofaunal assemblage grows faster and has a larger carrying capacity (maximum size) than the late successional macrofaunal assemblage.

(2) The early successional macrofaunal assemblage is generally more sensitive (i.e., suffers greater mortality) to burial, disturbance, and toxicity than the late successional assemblage.

(3) The late successional macrofaunal assemblage suppresses the early successional assemblage (i.e., large numbers of late successional macrofauna reduce the growth rate of early successional macrofauna).

At the control plot (Figure 18), temperature limits growth during much of the year. Disturbance events (Figure 14) and the natural deposition in early summer result in substantial population reductions. The early successional assemblage increases significantly in the period of summer growth. However, the growing season is so short that the late successional assemblage does not achieve a significant fraction of its carrying capacity and does not exert any strong suppressing influence on the early successional assemblage.

At the 5 and 50-m plots (50-m plot depicted in Figure 19), the impacts of discharged materials (burial, toxicity, and growth rate reduction) keep both assemblages at essentially minimum sizes. At the 500-m plot, the early successional assemblage remains at approximately the minimum value, but the late successional assemblage exhibits some growth because it is less sensitive to impacts from discharged materials (Figure 20). At the 1,500-m plot, both macrofaunal assemblages display substantial growth. The early successional assemblage reaches a maximum value of about 30% of that of the control plot; the late successional assemblage achieves a value of 85% of that of the control plot. Relative to the control plot, impacts of deposition are still noticeable even at a distance of 1,500 m. This occurs for two reasons. First, greater

current velocities in the summer result in higher deposition at 1,500 m during the time when the assemblages might otherwise reach their maximum growth. Second, the growth reduction terms in the population growth equations are very sensitive to small quantities of deposited material.

Ten-year run. Drilling and associated discharges start on day 10 of the first year of simulation and continue for 5 years. The period of discharge can be identified in a plot of cumulative deposition of discharged materials as the period in which cumulative deposition increases (Figure 22). Remember that only every thirtieth (monthly) value is plotted in the graphs from multiple-year simulation runs. Cumulative deposition of total discharged material for the 5 years of discharge is 10,900 cm at the 5-m plot, 169 cm at the 50-m plot (Figure 22), and 2.3 cm at the 500-m plot. The disturbance regime interacts with deposition to limit the net accumulation of sediment to values well below the cumulative deposition of discharged material. The seasonal pattern of natural deposition during high runoff in the early summer and erosion in the fall due to entrapment of sediment in ice is evident at the control plot and can also be seen at the plots impacted by discharged material (Figure 23). Sediment thickness at the 50-m plot returns to the control trajectory in year 8 of simulation, 3 years following the cessation of drilling in year 5. The fraction whole mud in the top 5-cm sediment layer declines to trace levels at the 500 and 1,500-m plots shortly after the cessation of drilling early in year 5 (Figure 24). Significant amounts of material from the bulk mud discharge remain until late in year 7 at the 5-m plot and until late in year 6 at the 50-m plot (Figure 25). The dynamics of barium concentrations in the top sediment layer closely correspond to those of total material from the bulk mud discharge. Barium concentrations reach maximum values of approximately: 58,000 ppm at 5 m; 74,000 ppm at 50 m; 3,800 ppm at 500 m; 380 ppm at 1,500 m; and a background concentration of 300 ppm at the control plot.

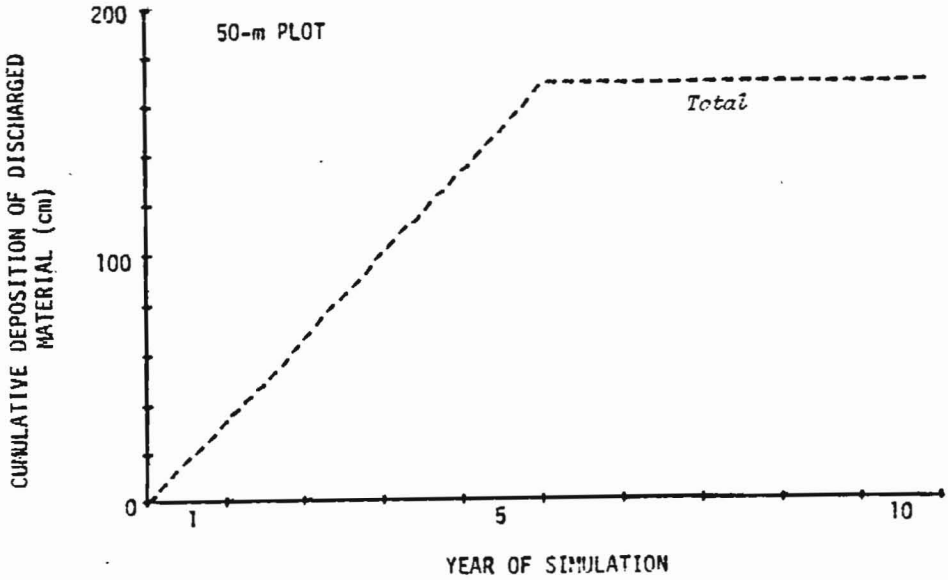

Figure 22. Scenario 1: cumulative deposition of total discharged material at 50-m plot, 10-yr run.

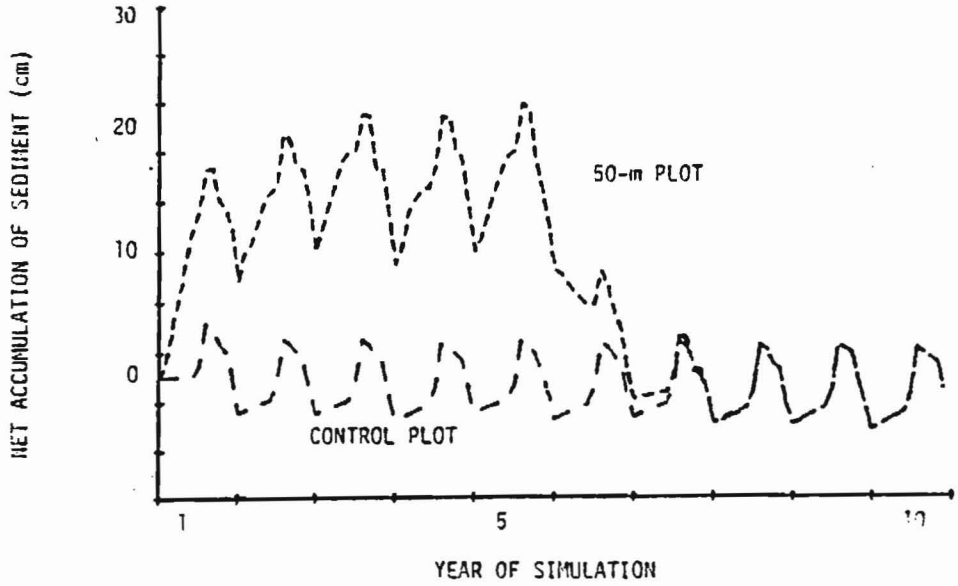

Figure 23. Scenario 1: net accumulation of sediment at 50-m and control plots, 10-yr run.

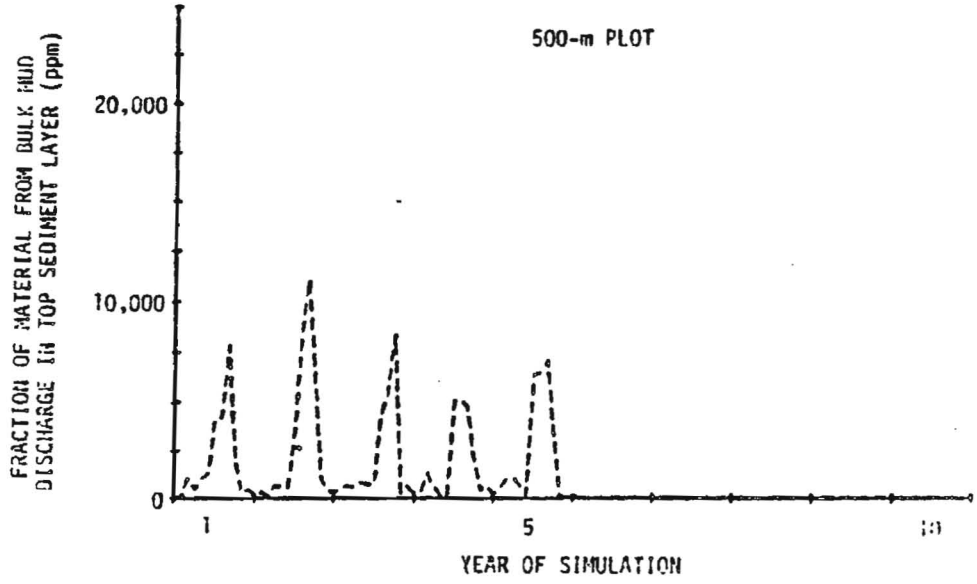

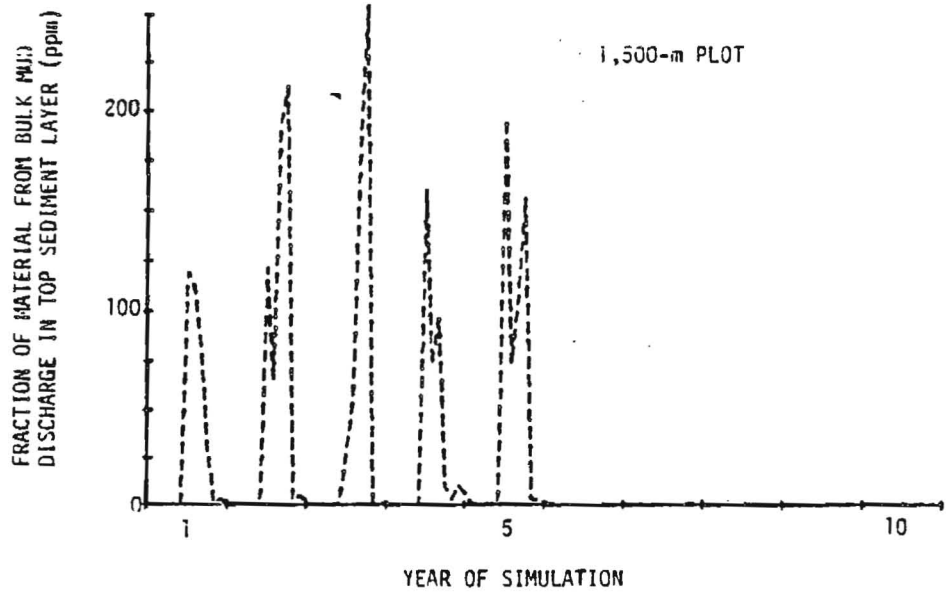

Figure 24. Scenario 1: fraction of sediment from bulk mud discharge in top 5-cm layer at 500 and 1,500-m plots, 10-yr run.

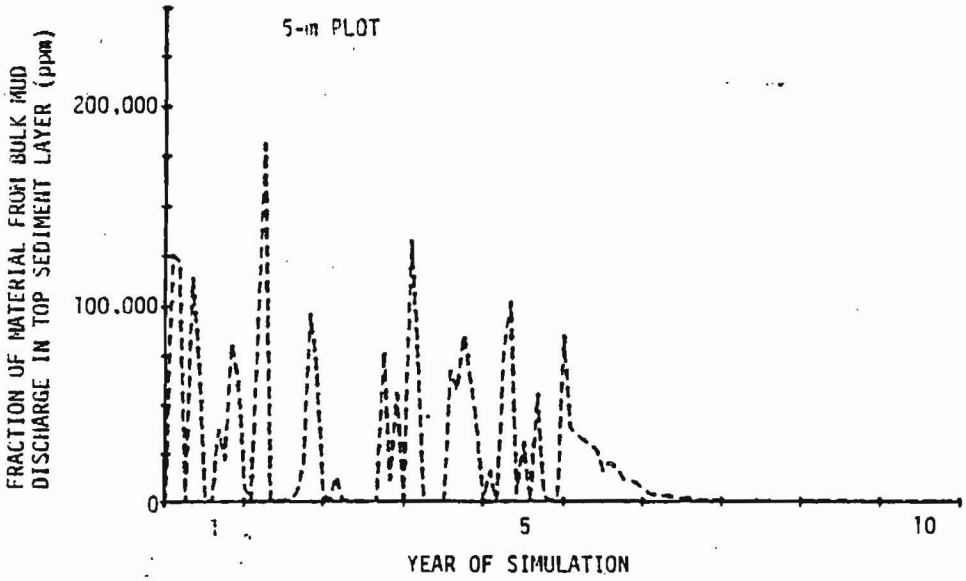

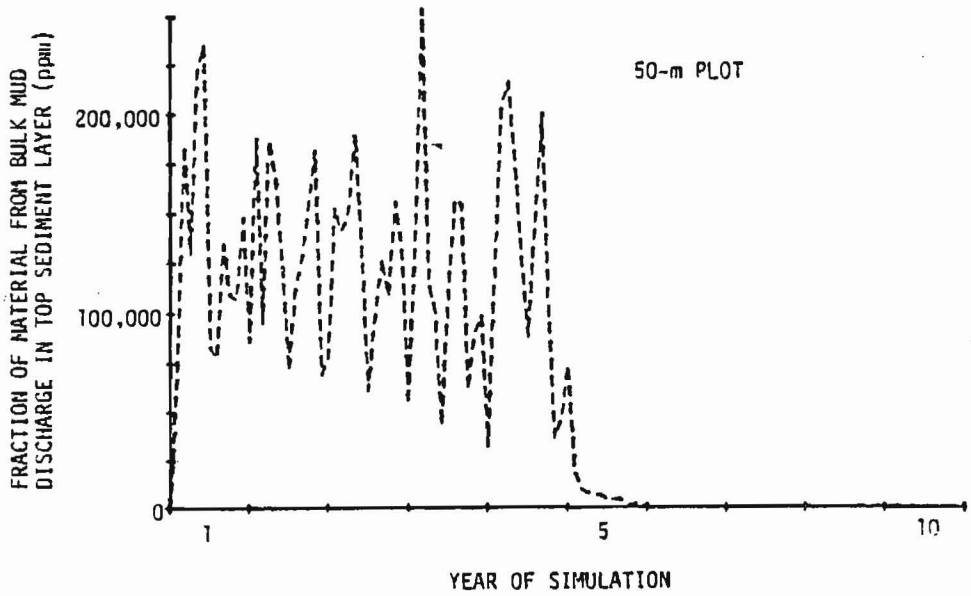

Figure 25. Scenario 1: fraction of sediment from bulk mud discharge in top 5-cm layer at 5 and 50-m plots, 10-yr run.

Impacts on populations must be evaluated with reference to the substantial intrayear (seasonal) and interyear variation at the control plot (Figure 26). Temperature limitations on growth and storms in the fall and winter basically "reset" the populations to minimum conditions each year. Succession occurs each growing season, with the most rapid initial growth by early successional macrofauna. Variation in the timing and intensity of disturbance events results in year-to-year variation in the growth patterns. Recovery at plots impacted by discharged material follows the decline of fraction whole mud in the top 5-cm sediment layer (Figures 24 and 25). At the 500 and 1,500-m plots, macrofaunal populations fully recover in year 6 of the simulation (Figures 27 and 28). At the 5-m plot, late successional macrofauna, which are less sensitive to the toxicity of whole mud, demonstrate substantial recovery in year 6. However, recovery to control trajectories is not achieved for both populations until year 7 at the 5-m plot (Figure 29).

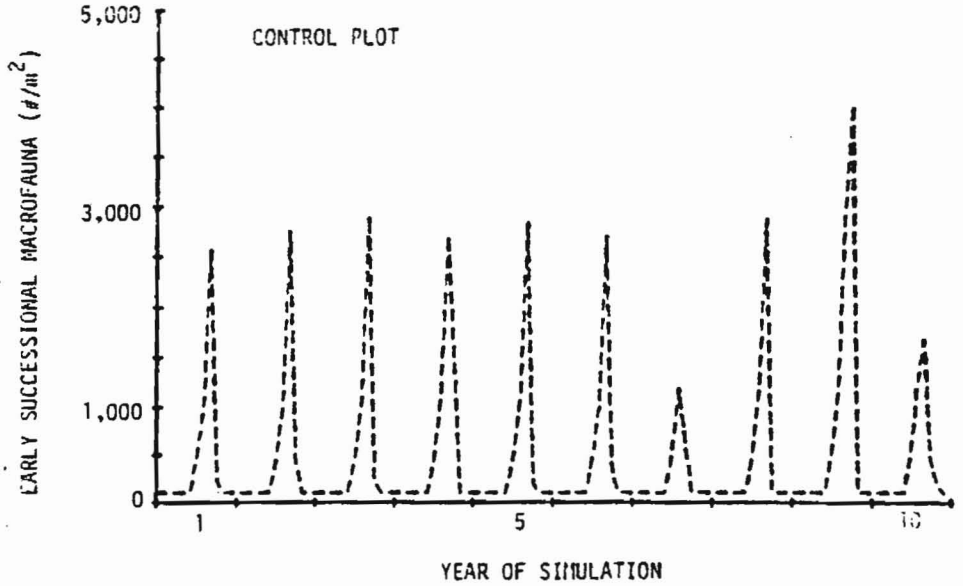

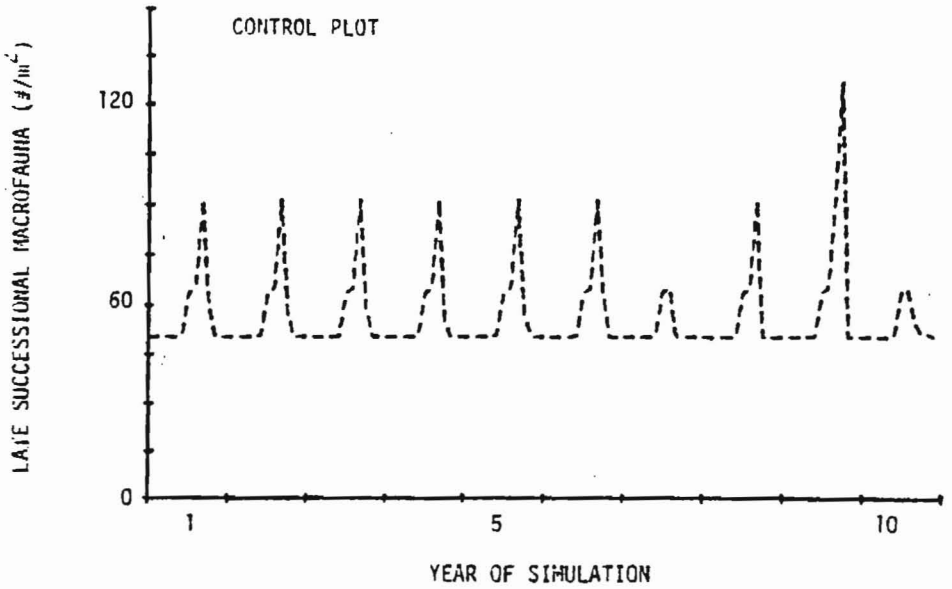

Figure 26. Scenario 1: macrofaunal assemblages at control plot, 10-yr run.

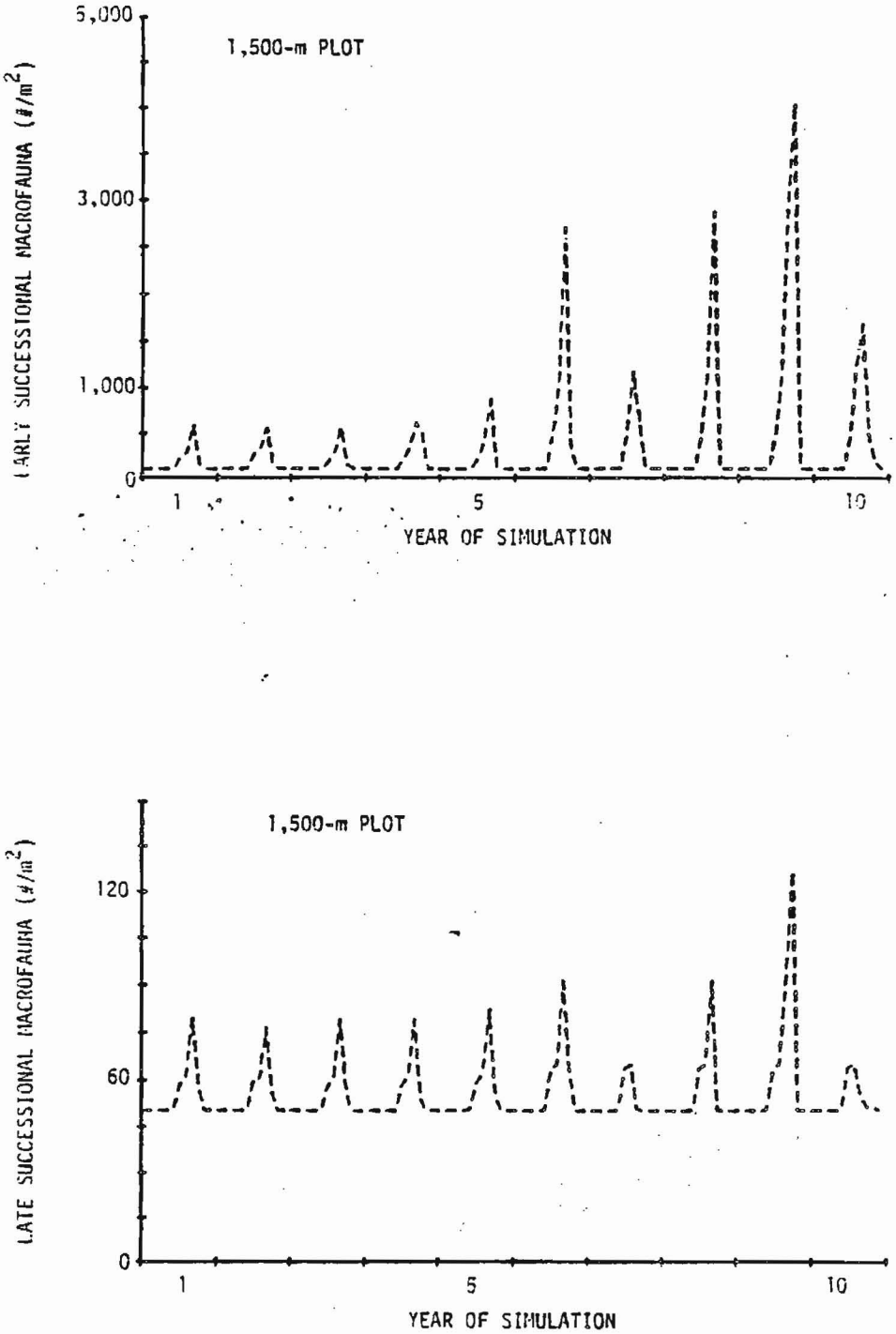

Figure 27. Scenario 1: macrofaunal assemblages at 1,500-m plot, 10-yr run.

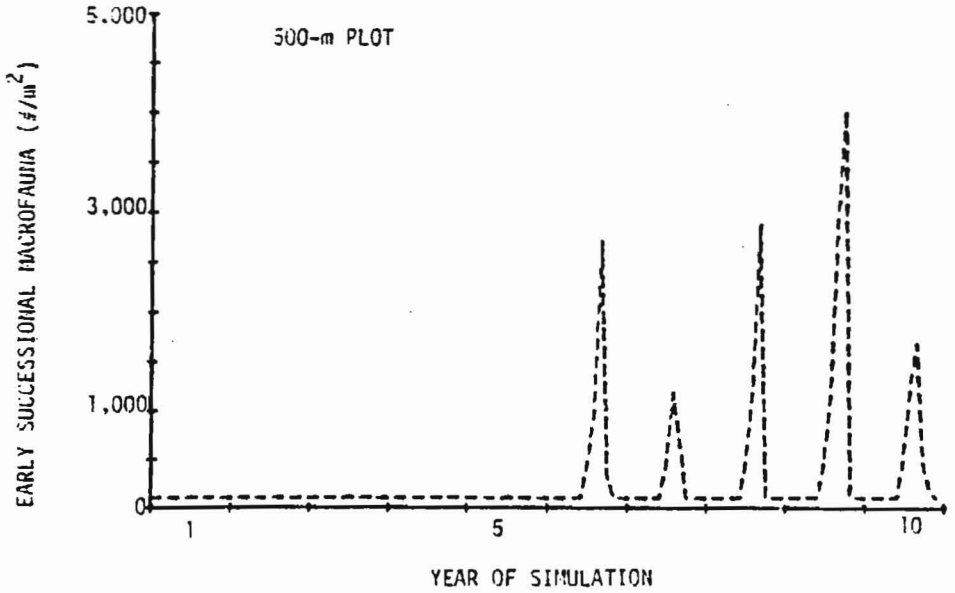

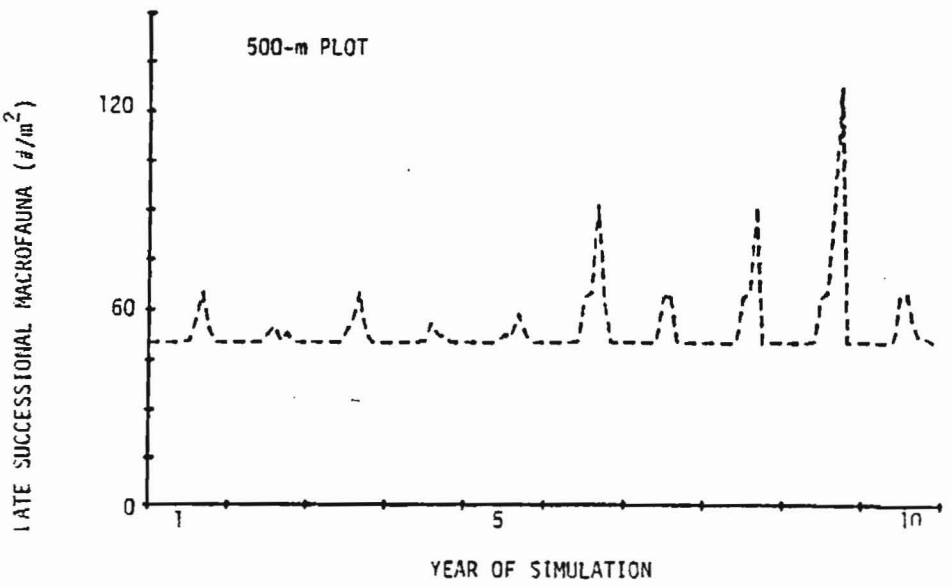

Figure 28. Scenario 1: macrofaunal assemblages at 500-m plot, 10-yr run.

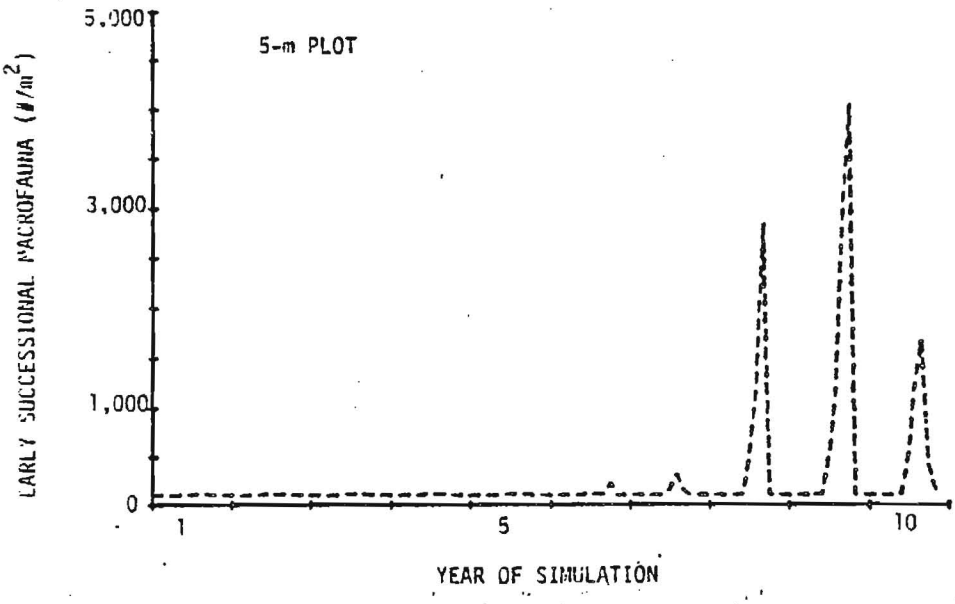

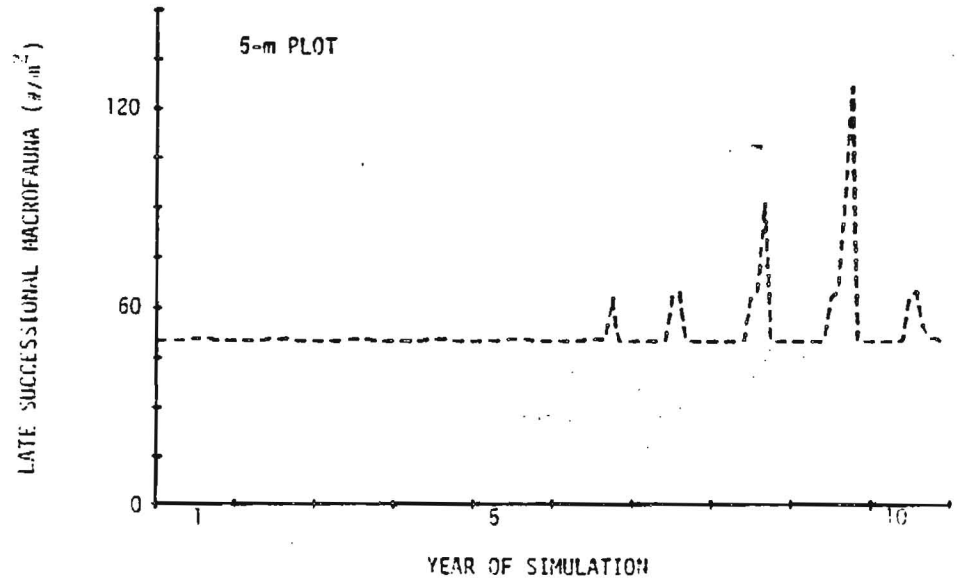

Figure 29. Scenario 1: macrofaunal assemblages at 5-m plot, 10-yr run.

Scenario 2

This scenario represents a shallow, temperate environment, such as might be encountered in the Gulf of Mexico. Conditions and parameter settings are summarized in Table 2; complete specifications are contained in the appended submodel descriptions. Deposition of material from the bulk mud discharges in this scenario is calculated according to Case 1, in which the mud plume impacts the bottom and collapses.

One-year run. Drilling and discharge begin on day 10. At the end of 1 year, cumulative total deposition of discharged material is approximately: 1,700 cm at 5 m; 5 cm at 50 m; 80 mm at 500 m; 14 mm at 1,500 m; 0.1 mm at 3,000 m; and 0.05 mm at 4,000 m (5-m plot depicted in Figure 30). At 5 m, over 99% of total deposition is the large sediment size class of material from the cuttings discharges; at 500 m, over 91% of total deposition is the small sediment size class of material from the bulk mud discharges.

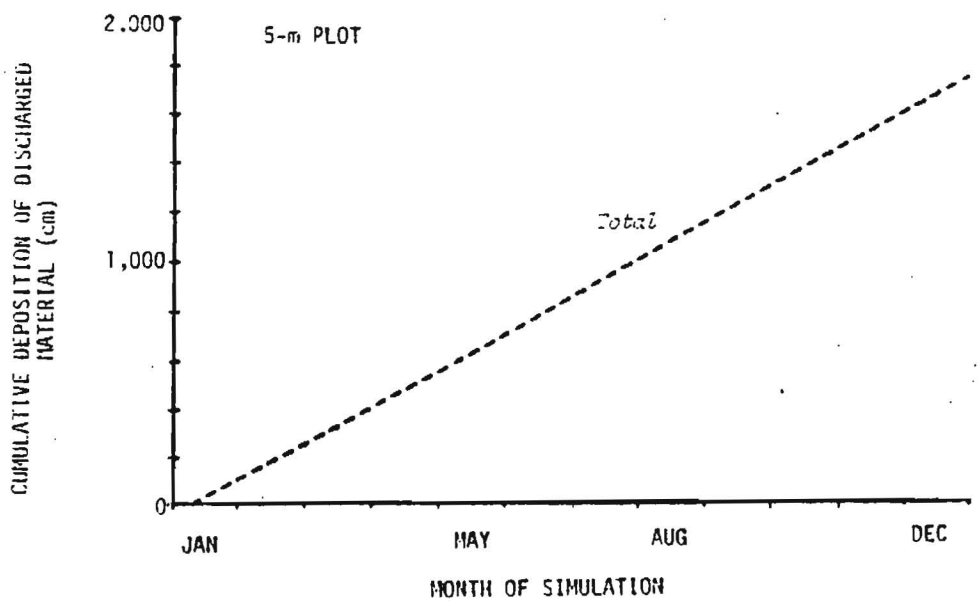

Figure 30. Scenario 2: cumulative deposition of total discharged material at 5-m plot, 1-yr run.

Table 2. Summary of Scenario 2 conditions.

DISCHARGE	
# wells	20
time per well	45 days
start of drilling	day 10
end of drilling	day 910
frequency of mud discharge	daily
volume of mud discharge	200 bbl
rate of mud discharge	1,000 bbl/hr
discharge depth	surface
PHYSICAL	
water depth	20 m
average surface current	25 cm/sec
average bottom current	10 cm/sec
% of time current is in direction of transect	40%
mean amplitute of largest disturbance event	17.5 cm of sediment
mean amplitude of largest disturbance event occurring at least once per year	7 cm of sediment
BIOLOGICAL	
doubling time	
early successional macrofauna	6 days
late successional macrofauna	60 days
carrying capacity	
early successional macrofauna	10,000/m^2
late successional macrofauna	5,000/m^2
96-hr LC_{50} of material from bulk mud discharge	
early successional macrofauna	~ 50,000 ppm
Late successional macrofauna	~ 130,000 ppm

The sediment disturbance regime is characterized by tidal action in the spring and summer, a late summer hurricane, and numerous fall and winter storms (Figure 31). The disturbance regime and deposition interact to produce a net accumulation approaching 2 m at the 5-m plot, but only several cm at the 50-m plot (Figure 32; note effects of storms and late summer hurricane). The fraction of the top 5-cm sediment layer consisting of material from bulk mud discharges reaches maximum values of approximately: 22,000 ppm at 5 m; 32,000 ppm at 50 m; 6,600 ppm at 500 m; 1,200 ppm at 1,500 m; and 70 ppm at 3,000 m (50-m plot depicted in Figure 33). Concentrations are higher at 50 m than at 5 m, despite very similar depositions of material from bulk mud discharges at the two distances, because of much greater deposition of cuttings material, and consequent dilution, at the closer plot.

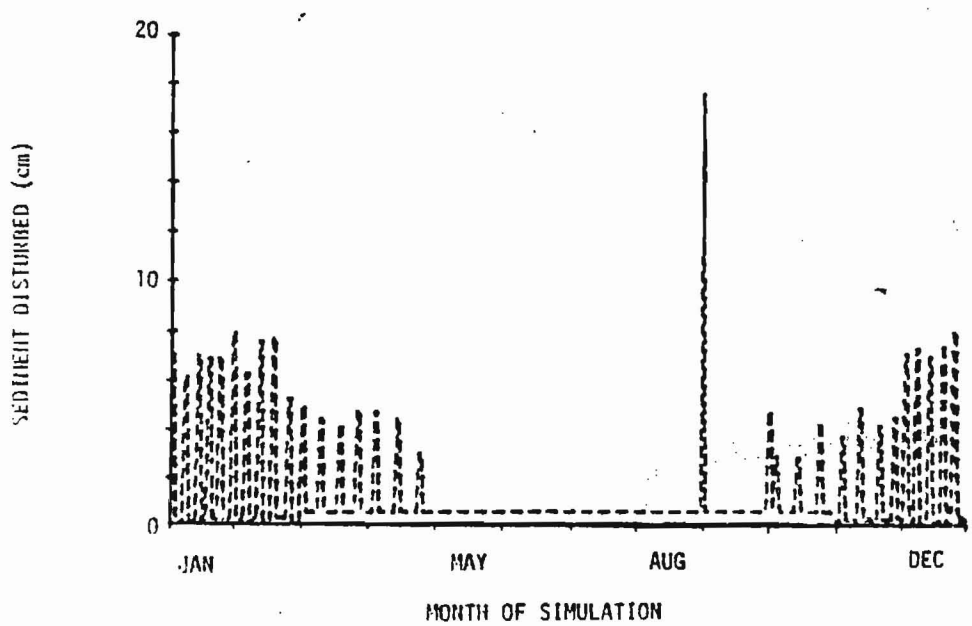

Figure 31. Scenario 2: sediment disturbance regime, 1-yr run.

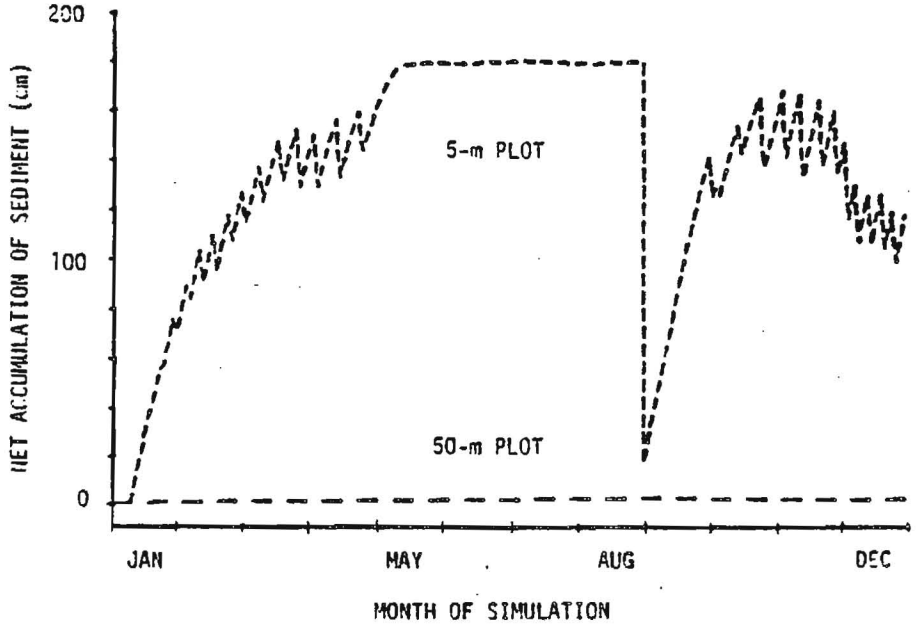

Figure 32. Scenario 2: net accumulation of sediment at 5 and 50-m plots, 1-yr run.

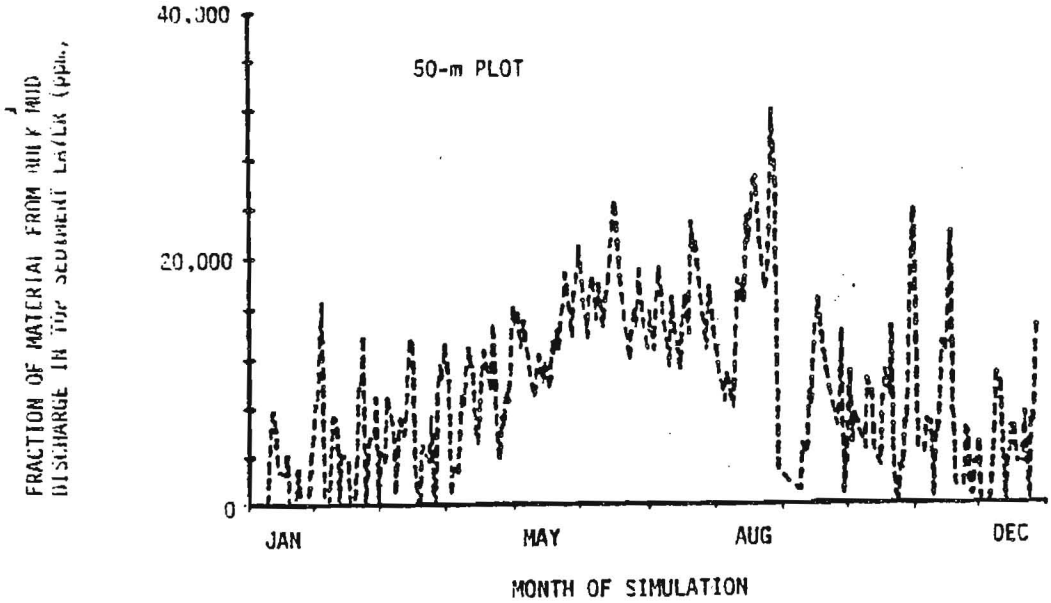

Figure 33. Scenario 2: fraction of sediment from bulk mud discharge in top 5-cm layer at 50-m plot, 1-yr run.

Macrofaunal assemblages are suppressed by disturbance events throughout the fall and winter (Figures 34 to 37). Early successional macrofauna increase rapidly in the spring and summer, reach a peak, and decline due to suppression effects from the more slowly increasing late successional macrofauna. Both assemblages are affected by the late summer hurricane.

At the 5-m plot, both macrofaunal assemblages are essentially completely suppressed by the impacts of deposited materials (Figure 35). At the 50-m plot, both macrofaunal assemblages are strongly suppressed, although some growth is evident immediately following storm events that reduce the fraction whole mud in the sediment and, thus, the mortality from toxicity (Figure 36). At the 3,000-m plot, macrofauna exhibit growth more similar to the control plot, although the impacts of deposited materials are still sufficient to slow the rates of population increase (e.g., the early successional macrofauna do not reach an inflection point due to suppression by late successional macrofauna) and to reduce the maximum population numbers (Figure 37).

Six-year run. Drilling and associated discharges continue for 2.5 years after starting on day 1 of the first year (Figure 38). Disturbance events reduce the net accumulation of total deposited material (Figure 39) and the fraction whole mud in the top sediment layer (Figure 40) to near zero within approximately 1 year following the cessation of discharge. The exact timing of these reductions is a function of the magnitude and timing of disturbance events; different sequences of random numbers might generate somewhat faster or slower reductions. The patterns of barium concentrations in the top sediment layer closely correspond to the patterns of the fraction of total material from the bulk mud discharge. Barium concentrations reach maximum values of approximately: 8,200 ppm at 5 m; 3,100 ppm at 50 m; 2,200 ppm at 500 m; 610 ppm at 1,500 m; 320 ppm at 3,000 m; 310 ppm at 4,000 m; and a background concentration of 300 ppm at the control plot.

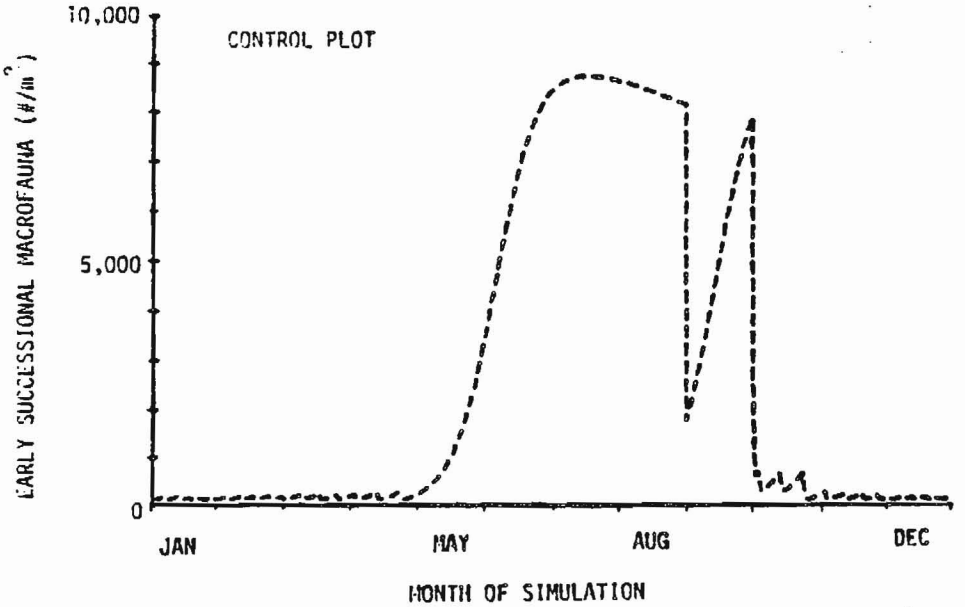

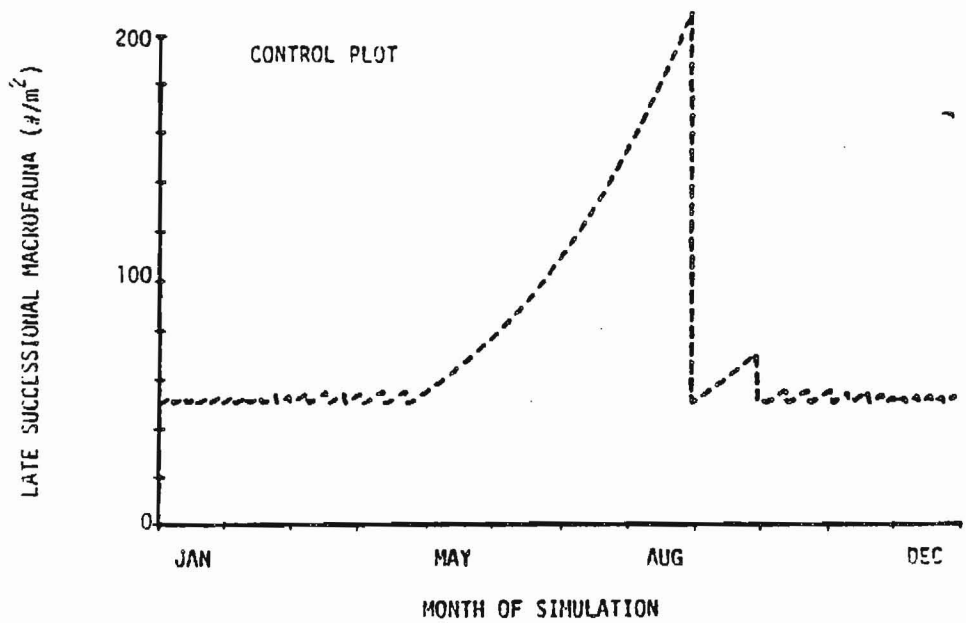

Figure 34. Scenario 2: macrofaunal assemblages at control plot, 1-yr run.

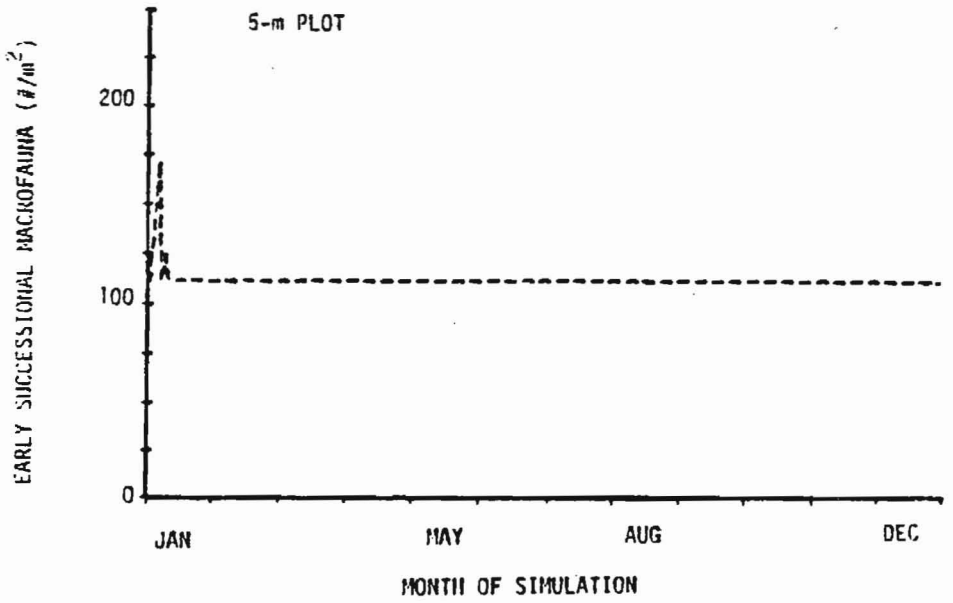

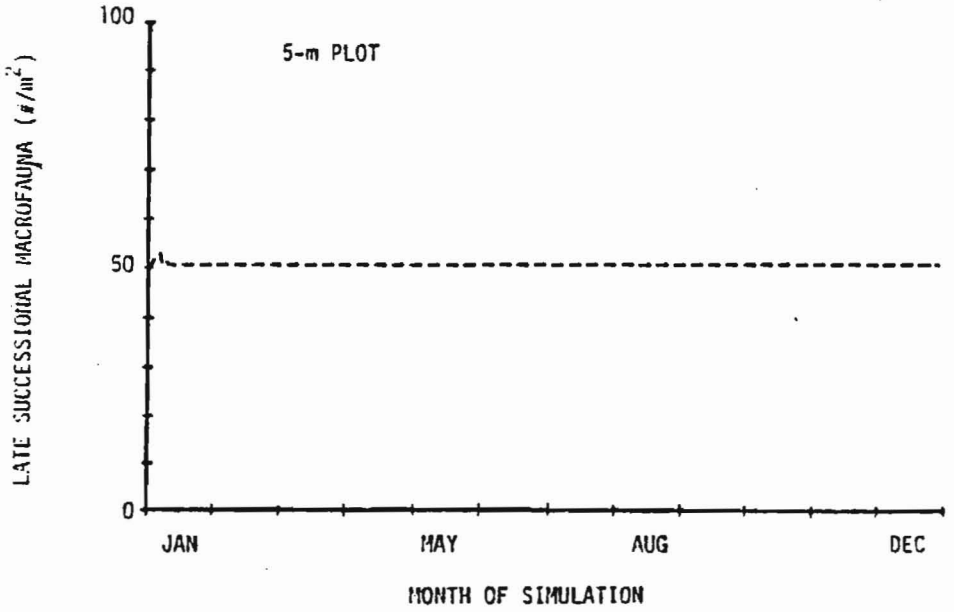

Figure 35. Scenario 2: macrofaunal assemblages at 5-m plot, 1-yr run.

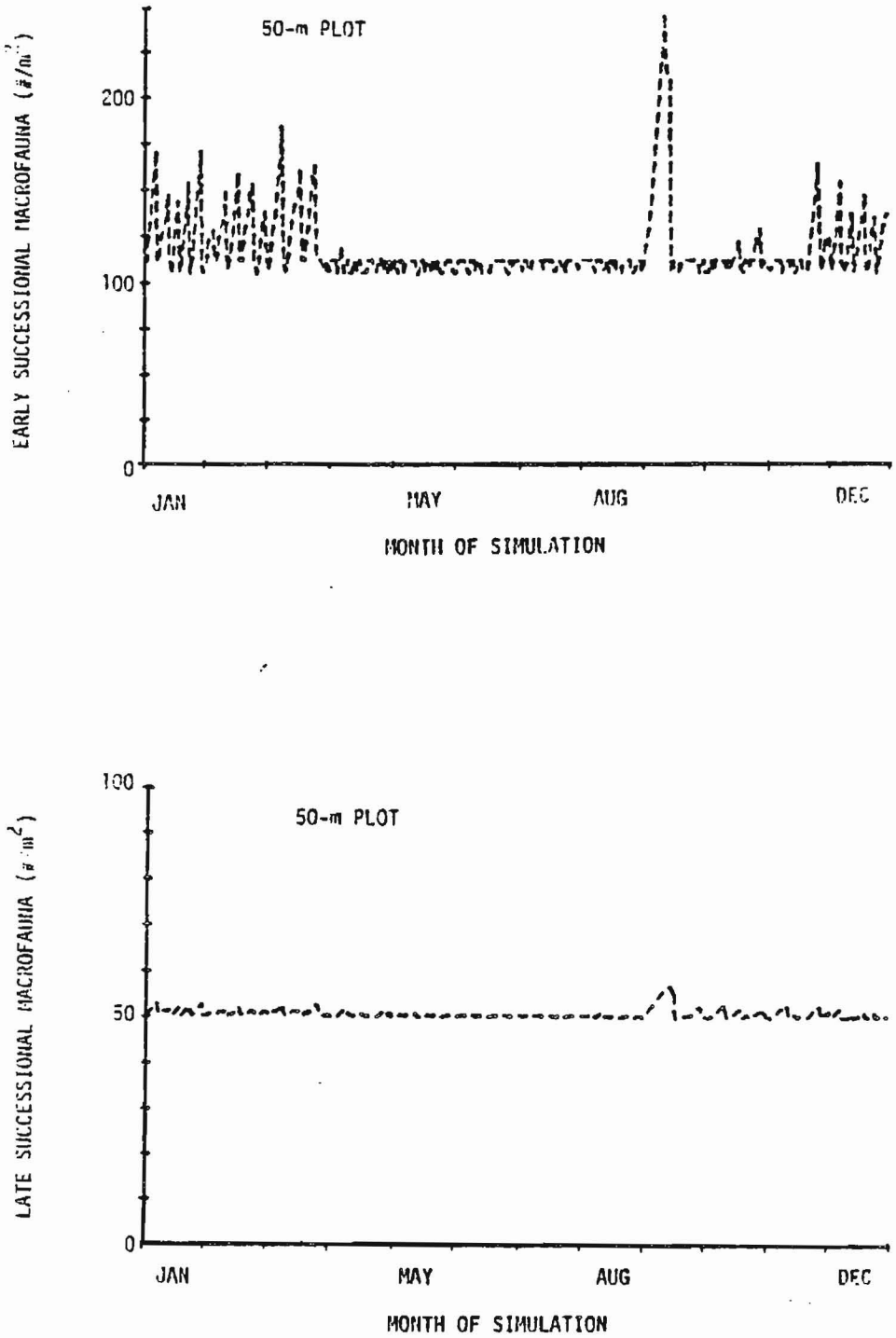

Figure 36. Scenario 2: macrofaunal assemblages at 50-m plot, 1-yr run.

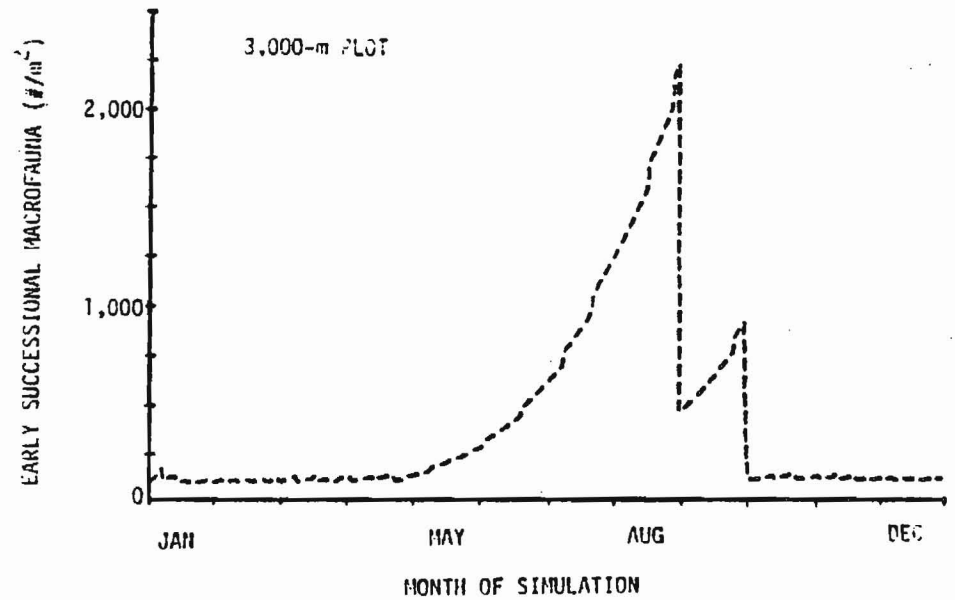

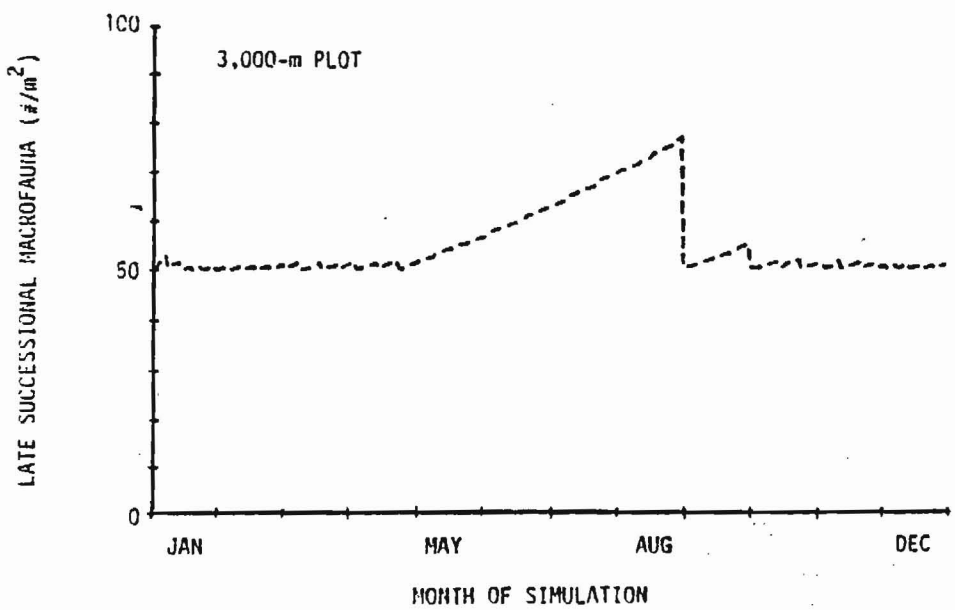

Figure 37. Scenario 2: macrofaunal assemblages at 3,000-m plot, 1-yr run.

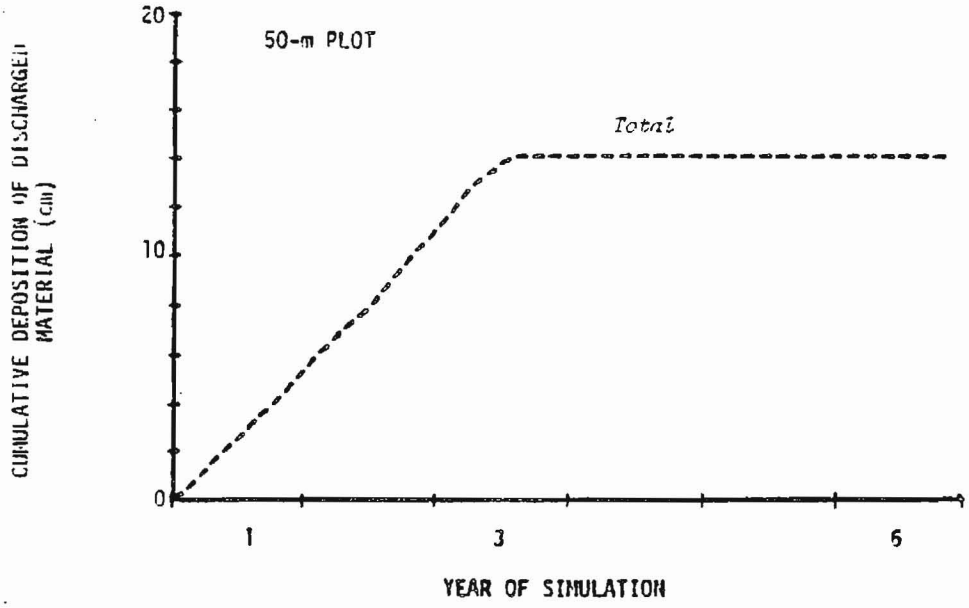

Figure 38. Scenario 2: cumulative deposition of total discharged material at 50-m plot, 6-yr run.

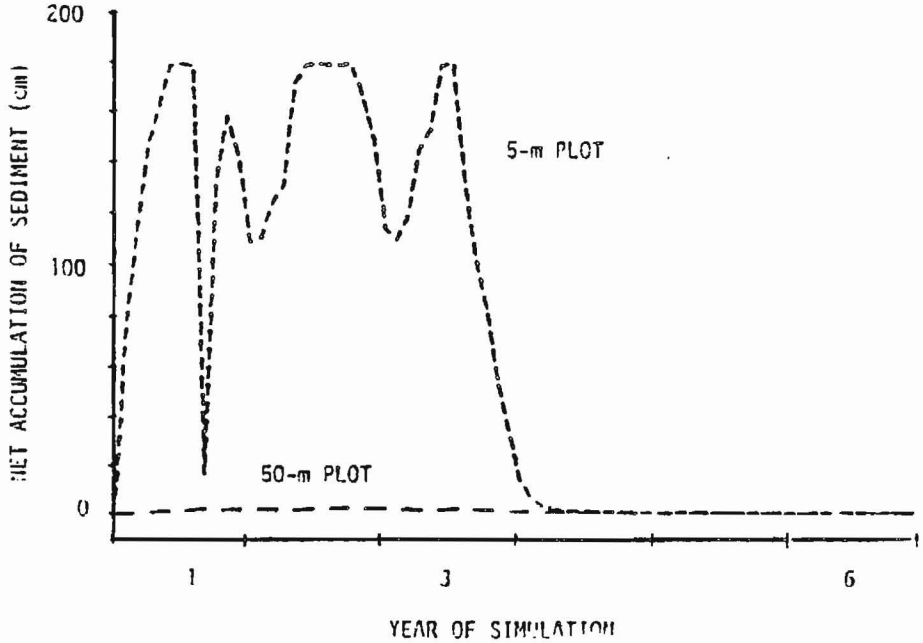

Figure 39. Scenario 2: net accumulation of discharged material at 5 and 50-m plots, 6-yr run.

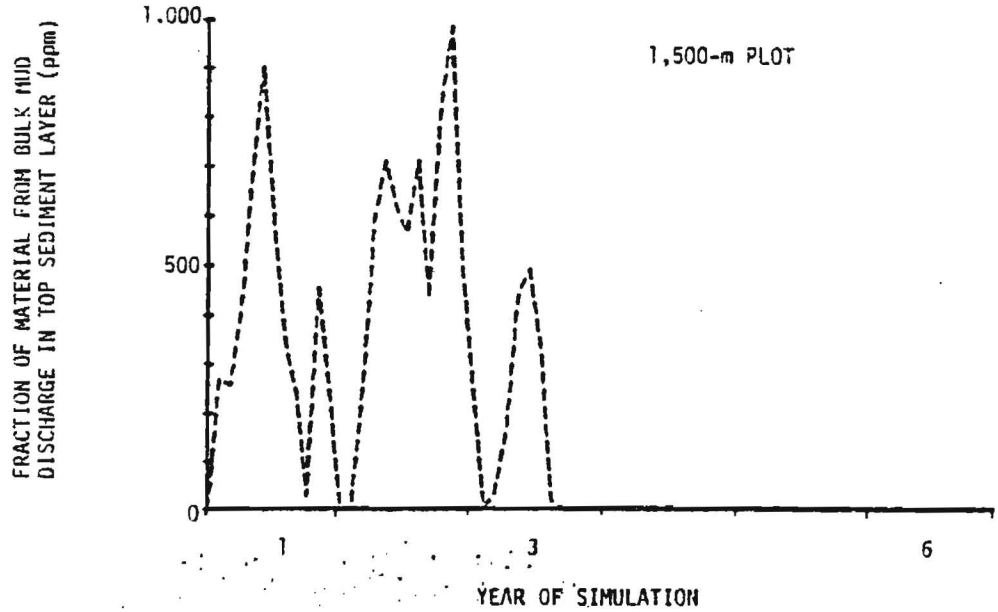

Figure 40. Scenario 2: fraction of sediment from bulk mud discharge in top 5-cm layer at 1,500-m plot, 6-yr run.

Macrofaunal assemblages at the control plot exhibit a distinct annual cycle with effects of a large, late summer storm evident in years 1 and 4 (Figure 41). At the 5-m plot, both assemblages are essentially completely suppressed while drilling occurs, exhibit a very slight recovery late in year 3, and fully recover by late summer of year 4 (Figure 42). At the 3,000-m plot, where much less discharged material is deposited, both assemblages have substantial growth during the period while discharge is occurring and recover very quickly (reaching levels close to those at the control plot) in year 3 when drilling and discharges cease (Figure 43).

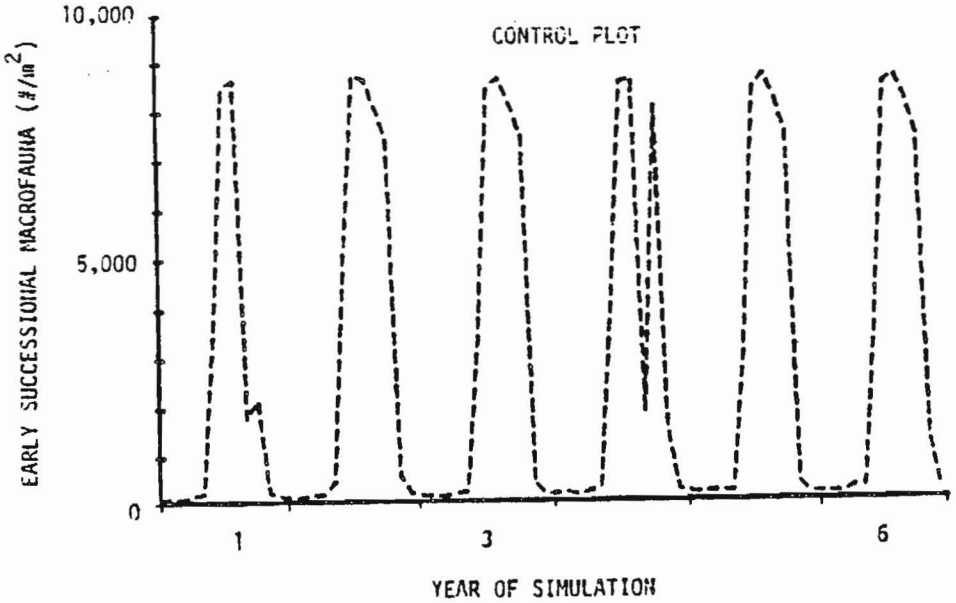

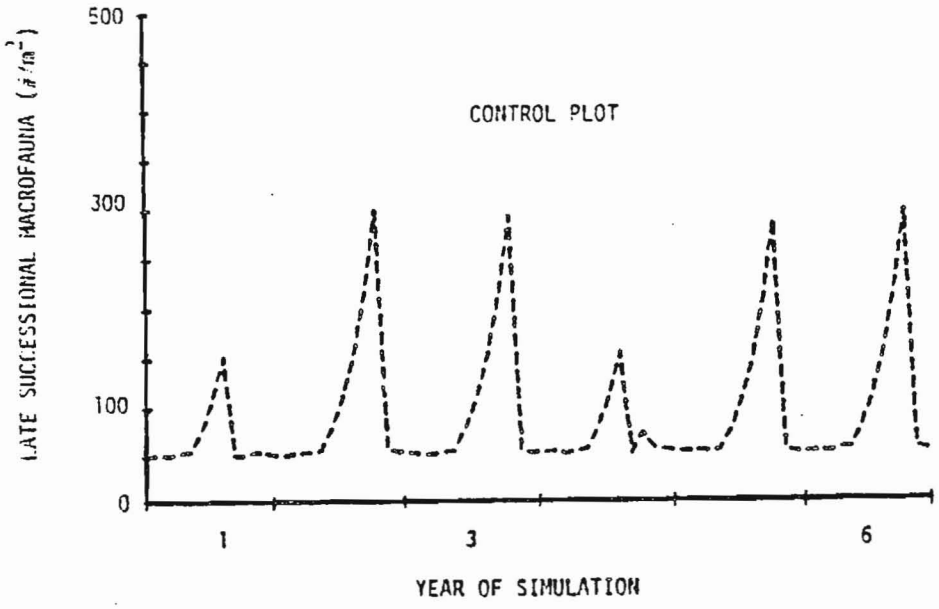

Figure 41. Scenario 2. macrofaunal assemblages at control plot, 6-yr run.

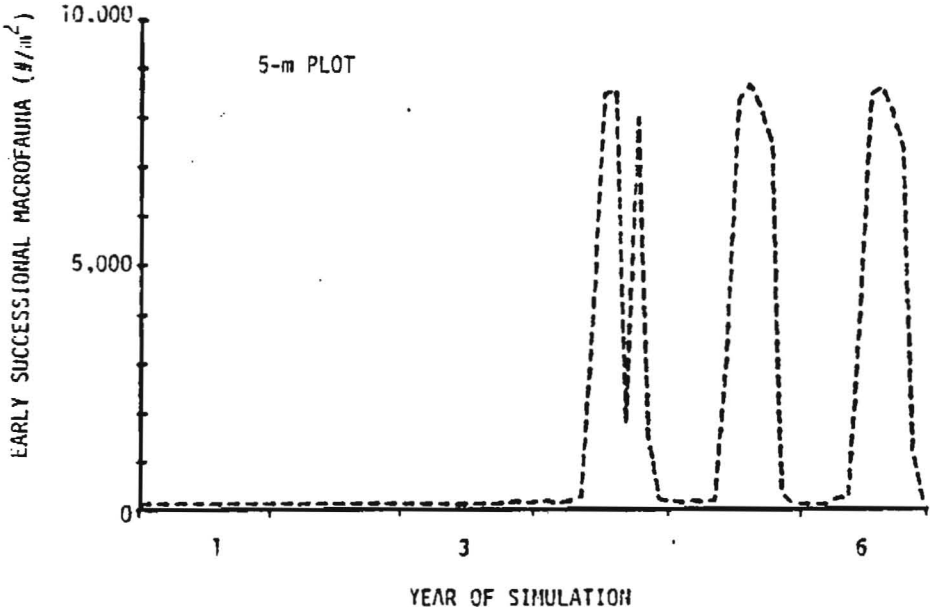

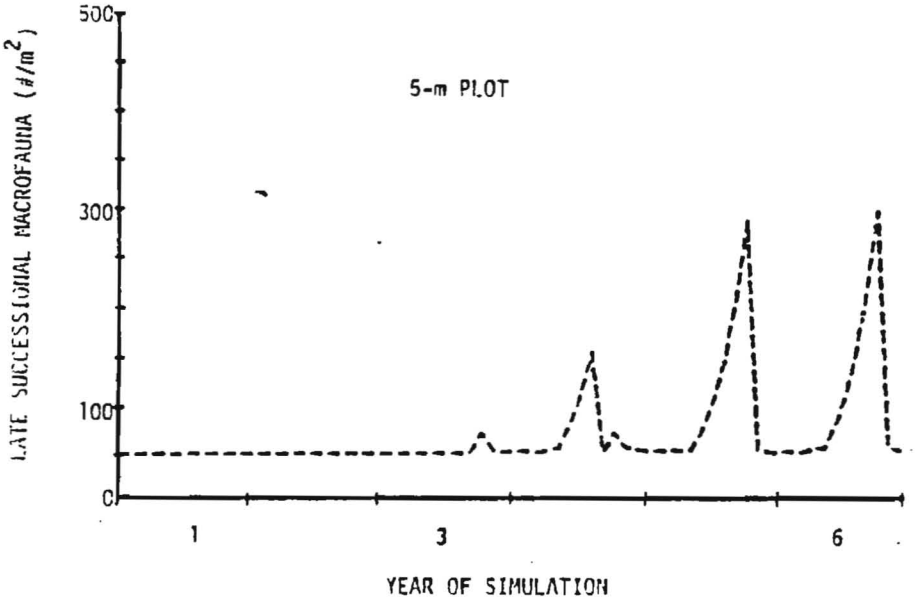

Figure 42. Scenario 2: macrofaunal assemblages at 5-m plot, 6-yr run.

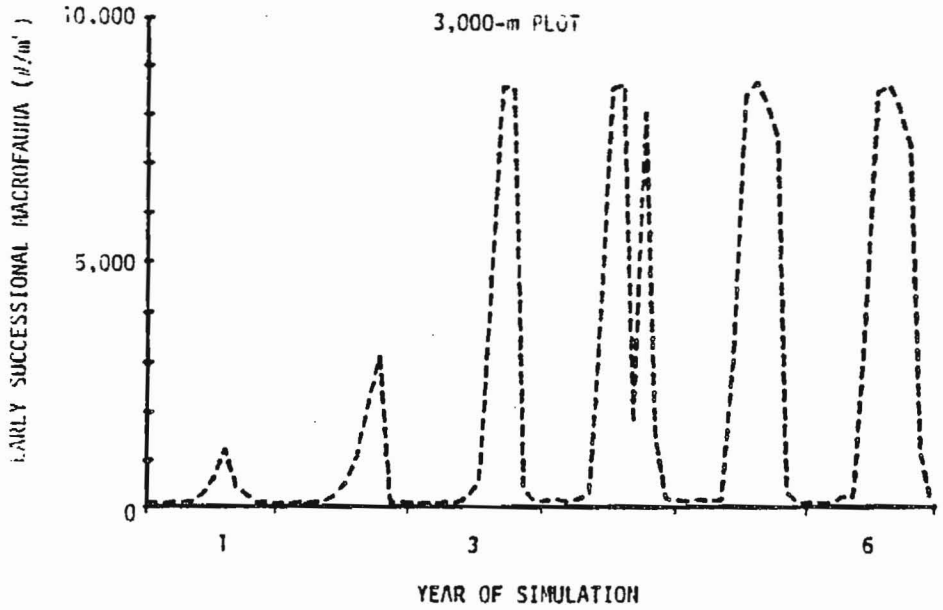

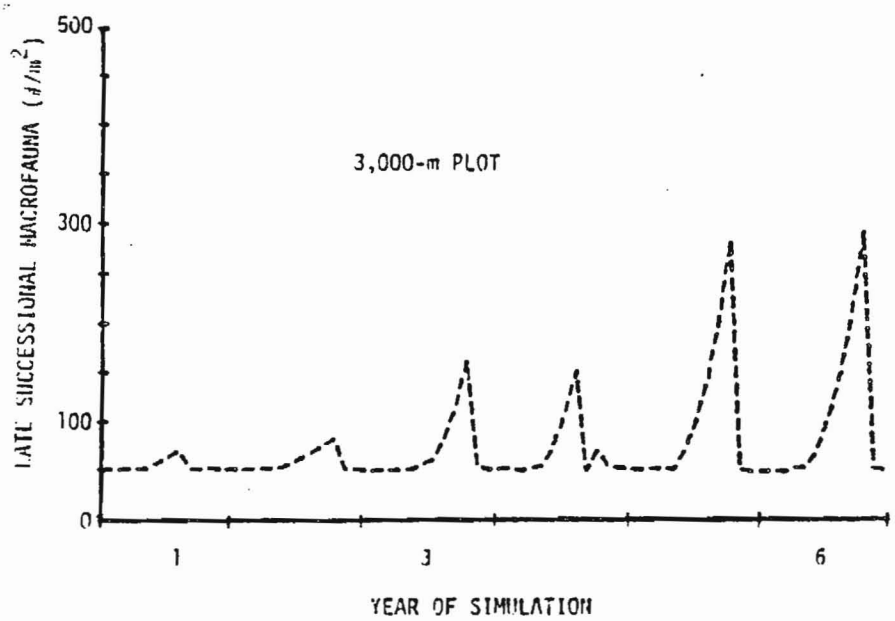

Figure 43. Scenario 2: macrofaunal assemblages at 3,000-m plot, 6-yr run.

Scenario 3

This scenario represents a deeper, temperate environment, such as might be encountered in the Gulf of Mexico. Conditions and parameter settings are summarized in Table 3; complete specifications are contained in the appended submodel descriptions. In this scenario, deposition of material from the bulk mud discharges is calculated according to Case 2, in which dynamic collapse of the mud plume occurs at a trap depth above the bottom.

One-year run. Drilling and discharge begin on day 10. At the end of 1 year, cumulative total deposition of discharged material is approximately: 1,700 cm at 5 m; 6 mm at 50 m; and less than 1 mm at 500, 1,500, 3,000, and 4,000 m. At the 5, 50, and 500-m plots, all the deposited material is from the cuttings discharges. Material from the bulk mud discharges is carried beyond these plots by the current as it settles. Furthermore, because of variation in current velocity, plots may receive depositions from only some of the bulk mud discharges. A stair-step pattern of deposition from bulk mud discharges is, thus, overlain on the more continuous deposition of material from cuttings discharges (Figure 44). Deposition at the 5-m plot is large enough to produce a net accumulation very similar to that simulated for the shallower water environment of Scenario 2 (Figures 45 and 32). The pattern of sediment disturbance (Figure 46) is very similar to that of Scenario 2 (Figure 32); the intensity of the events is much less, however, reflecting the deeper water conditions (80 m in Scenario 3 versus 20 m in Scenario 2).

The fraction of material from bulk mud discharges reaches maximum values around 600 ppm at 1,500 and 3,000 m and approximately 400 ppm at 4,000 m. No deposition of material from the bulk mud discharges occurs at the plots closer to the discharge point. The pattern for fraction whole mud in the top sediment layer reflects the diluting action of disturbance events on the stair-step pattern of the deposition of this material (Figure 47).

Table 3. Summary of Scenario 3 conditions.

DISCHARGE	
# wells	40
time per well	45 days
start of drilling	day 10
end of drilling	day 1,810
frequency of mud discharge	Daily
volume of mud discharge	200 bbl
rate of mud discharge	1,000 bbl/hr
discharge depth	5 m
PHYSICAL	
water depth	80 m
average surface current	15 cm/sec
average bottom current	5 cm/sec
% of time current is in direction of transect	70%
mean amplitude of largest disturbance event	2 cm of sediment
mean amplitute of largest disturbance event occurring at least once per year	1.5 cm of sediment
BIOLOGICAL	
doubling time	
early successional macrofauna	20 days
late successional macrofauna	120 days
carrying capacity	
early successional macrofauna	10,000/m^2
late successional macrofauna	10,000/m^2
96-hr LC_{50} of material from bulk mud discharge	
early successional macrofauna	~ 50,000 ppm
late successional macrofauna	~ 130,000 ppm

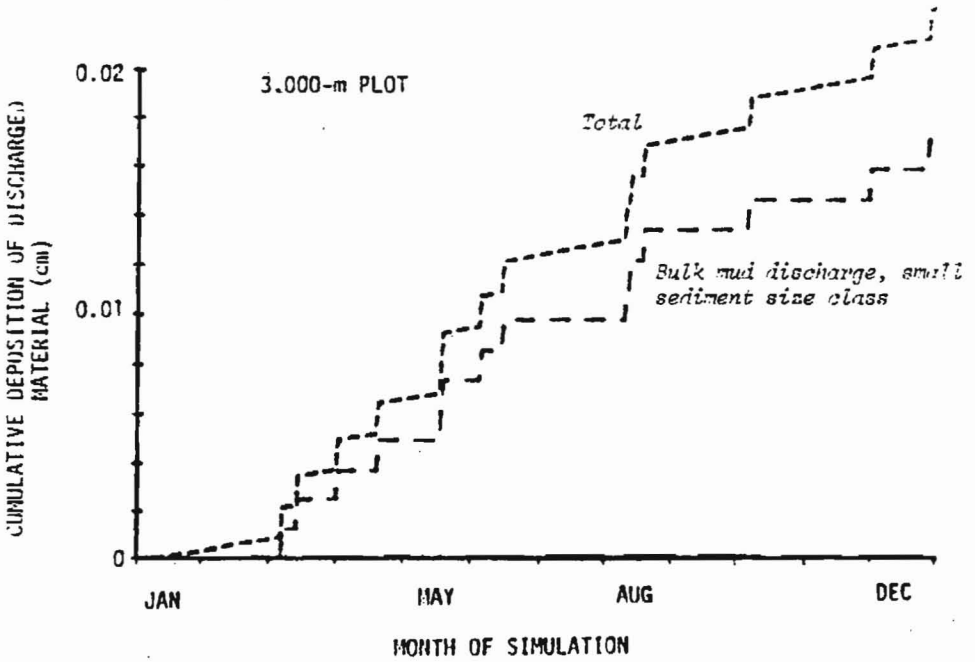

Figure 44. Scenario 3. cumulative deposition of discharged material at 3,000-m plot, 1-yr run.

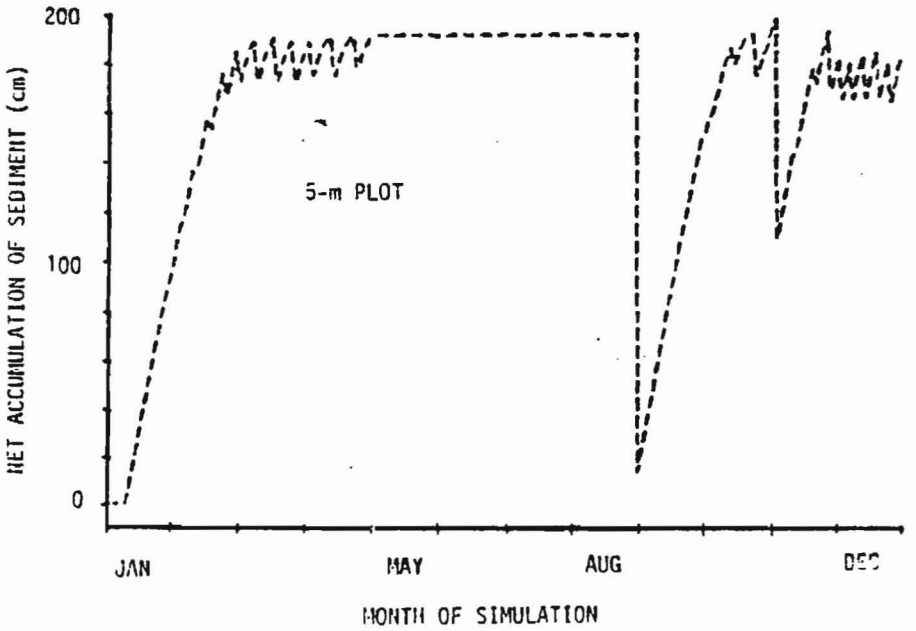

Figure 45. Scenario 3: net accumulation of sediment at 5-m plot, 1-yr run.

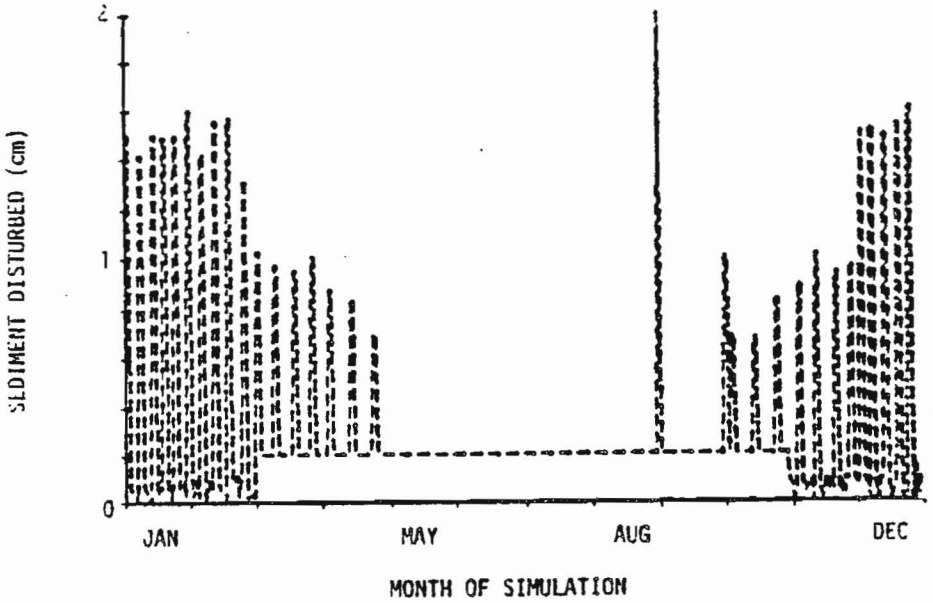

Figure 46. Scenario 3: sediment disturbance regime, 1-yr run.

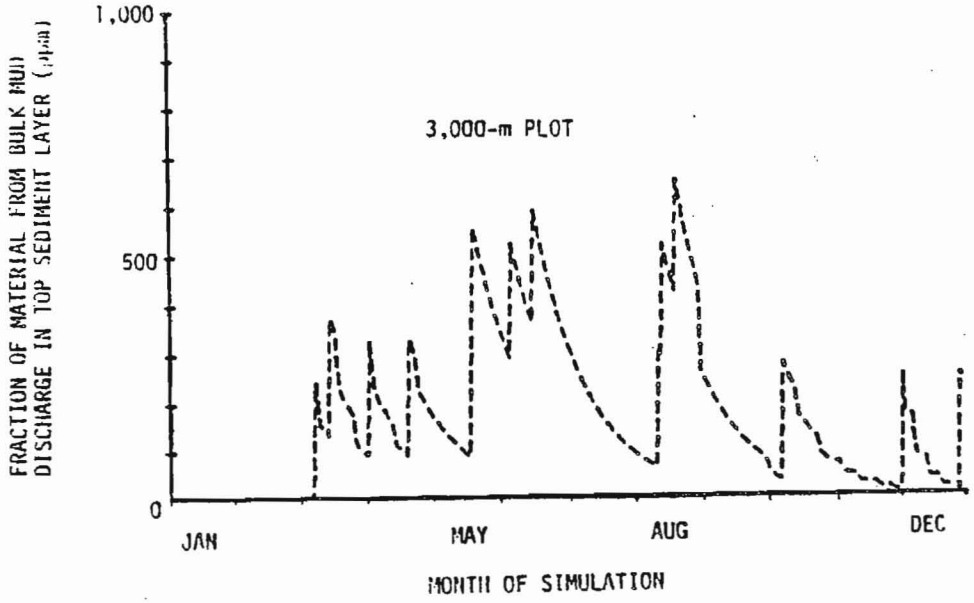

Figure 47. Scenario 3: fraction of sediment from bulk mud discharge in top 5-cm layer at 3,000-m plot, 1-yr run.

Macrofaunal assemblages at the control plot are suppressed by disturbance events in the fall and winter, with substantial population growth occurring by late summer (Figure 48). At the 5-m plot, both populations are essentially completely suppressed by the physical impacts of deposited material (Figure 49). At the 50-m plot, the amount of deposited material and its physical impacts are substantially less, allowing approximately 50% of the growth simulated for the control plot (Figures 50 and 47).

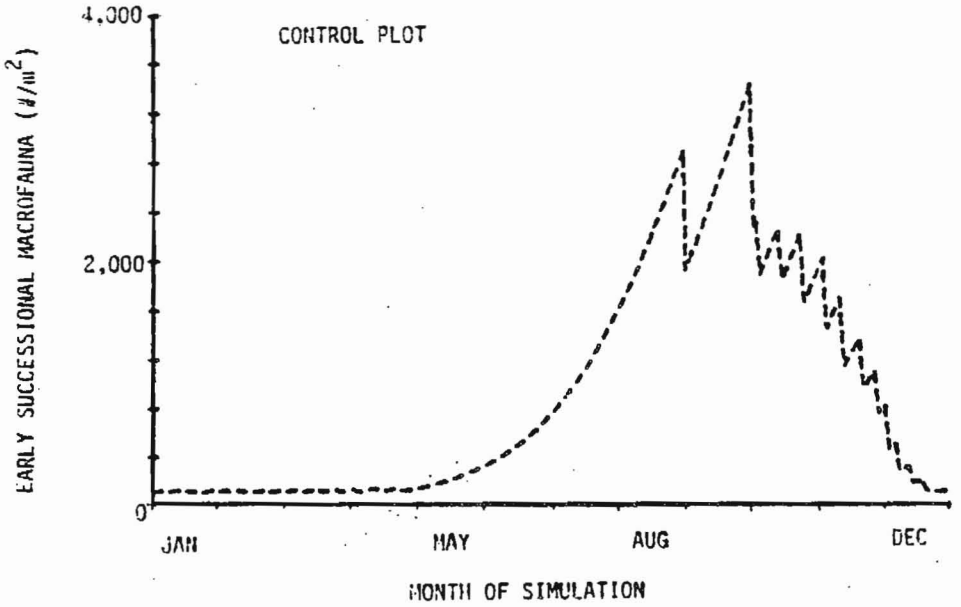

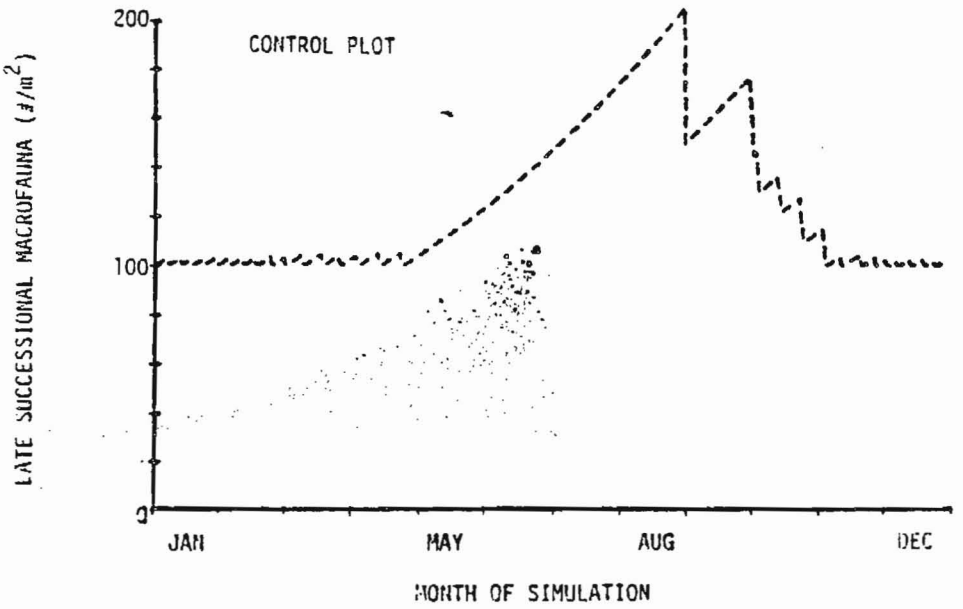

Figure 48. Scenario 3: macrofaunal assemblages at control plot, 1-yr run.

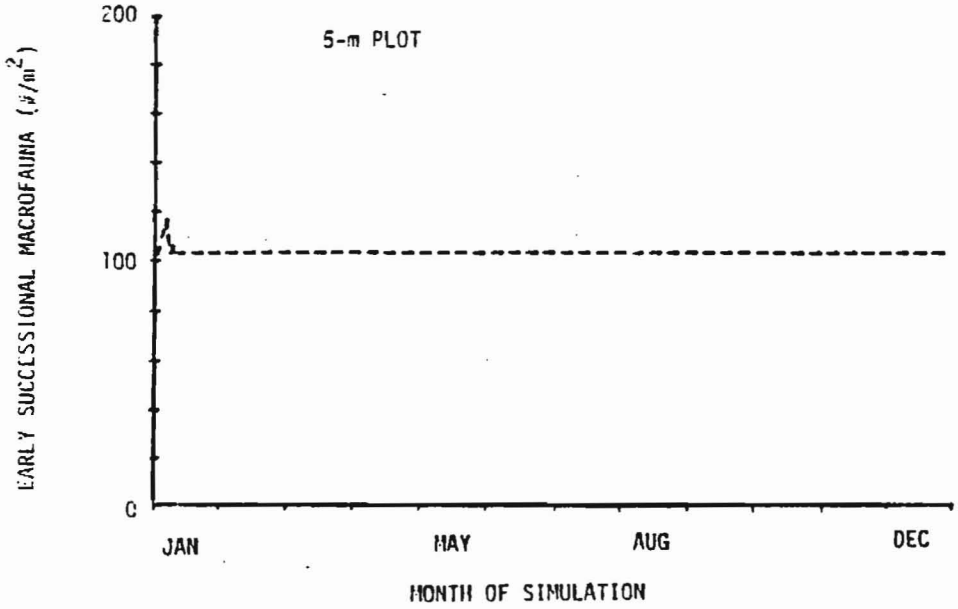

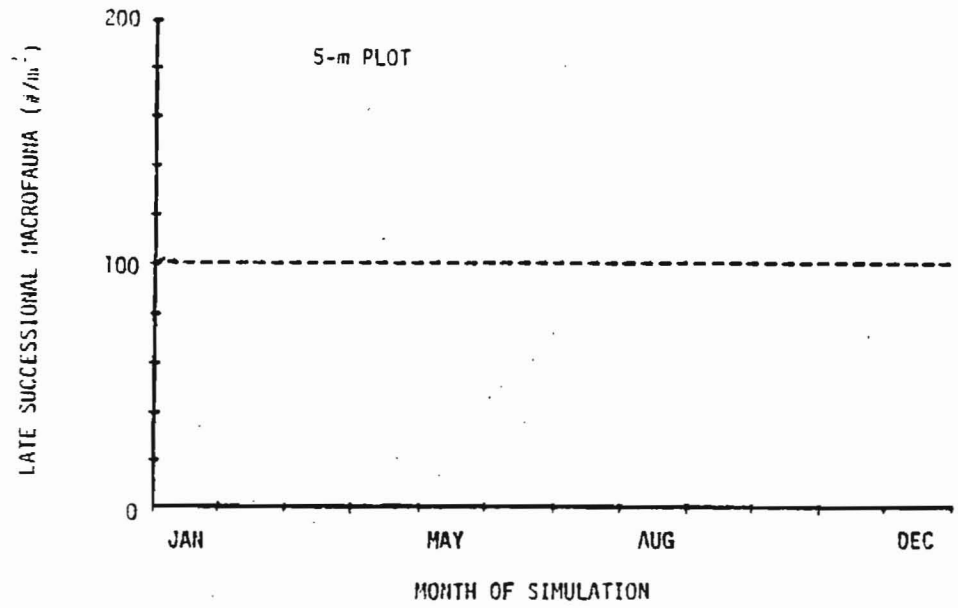

Figure 49. Scenario 3: macrofaunal assemblages at 5-m plot, 1-yr run.

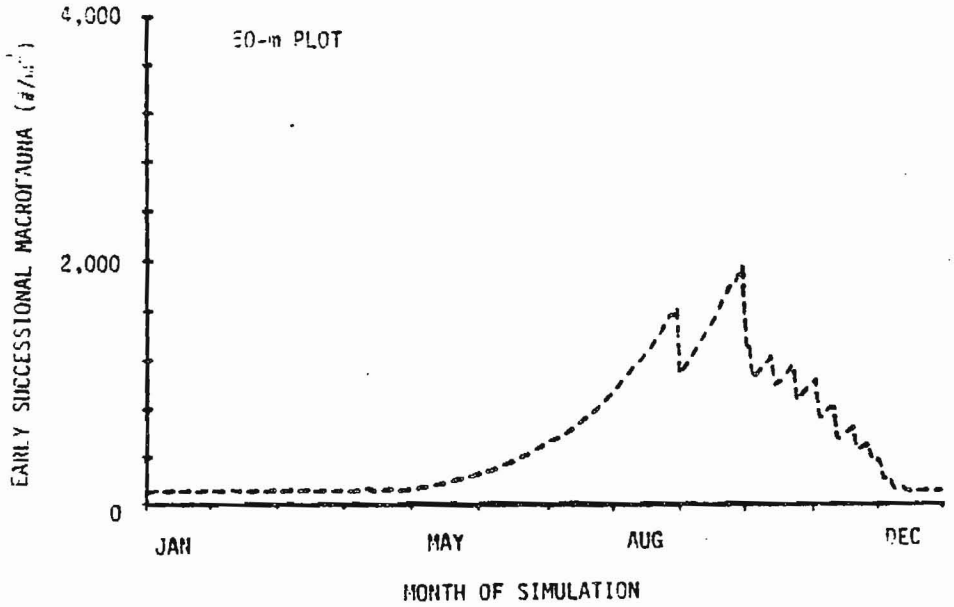

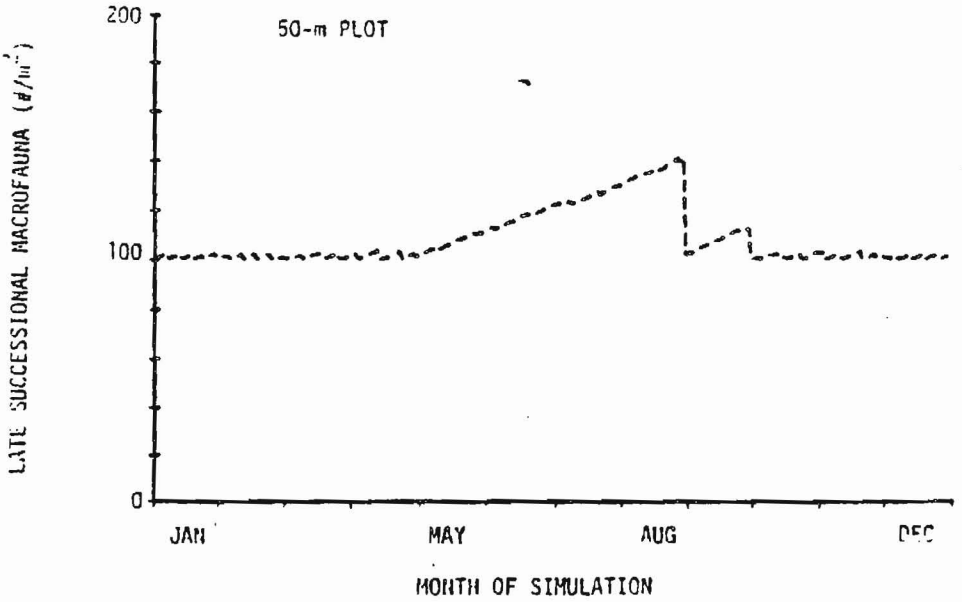

Figure 50. Scenario 3: macrofaunal assemblages at 50-m plot, 1-yr run.

Ten-year run. Drilling and discharge begin on day 10 of the first year and continue for 5 years (Figure 51). Deposited material is eroded and diluted more slowly than in Scenario 2 because of the lower intensity of disturbance events and, to some extent, because of when drilling stops relative to the randomly scheduled, low-frequency hurricanes (Figure 52). Enough disturbance occurs, however, to reduce the fraction whole mud in the top sediment layer to very low levels within a year after discharge ceases at the more remote plots where some, relatively small, deposition of this material occurs (Figure 53). The dynamics of sediment barium concentrations closely correspond to those of fraction whole mud. Maximum sediment barium concentrations are approximately 460 ppm at 1,500 and 3,000 m and 410 ppm at 4,000 m, with no increase above the background concentration of 300 ppm at 5, 50, and 500 m because of the downcurrent displacement of material from the bulk mud discharges.

As in Scenario 2, macrofaunal assemblages at the control plot exhibit a strong annual cycle (Figures 54 and 41). At the 5-m plot, deposition of material from the cuttings discharges is large enough to suppress the populations while drilling occurs (Figure 55). There is no material from the bulk mud discharges at this plot and, hence, no mortality from toxicity. However, the physical impacts of altered particle size composition and greater disturbance intensity associated with gradual erosion of the altered bottom topography result in population sizes at the 5-m plot that are significantly lower than those at the control plot for 3 to 4 years following the cessation of drilling. At the 50 and 500-m plots, the amount of deposited material is much less. Differences from the control plot are correspondingly less while drilling occurs, and recovery is much faster following the cessation of drilling (Figures 56 and 57). At the greater distances that receive deposition of material from bulk mud discharges and, thus, toxicity impacts on the populations, the amount of material is small and the populations are suppressed by less than 5% from the levels simulated at the control plot.

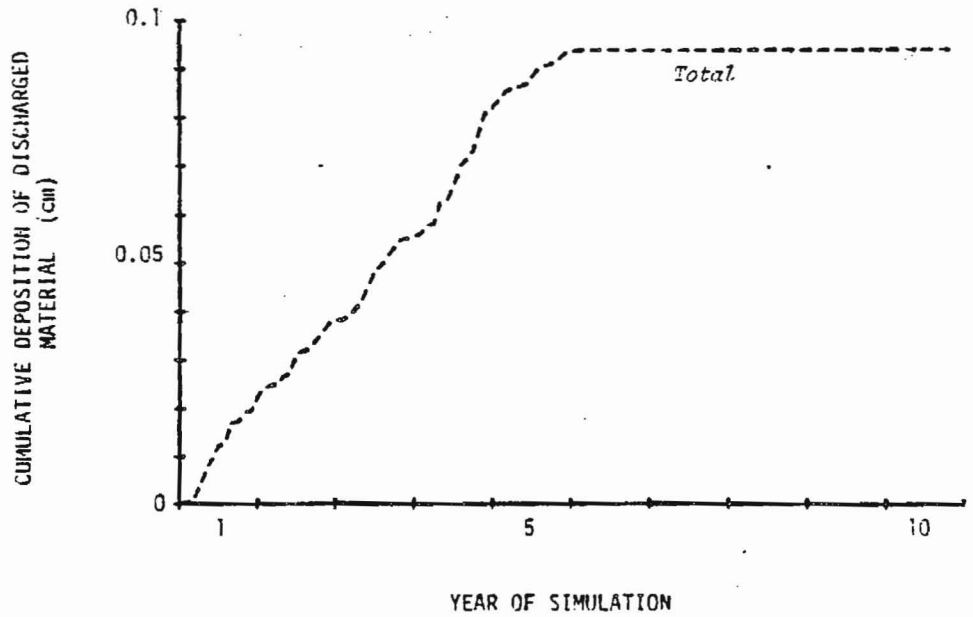

Figure 51. Scenario 3: cumulative deposition of discharged material at 3,000-m plot, 10-yr run.

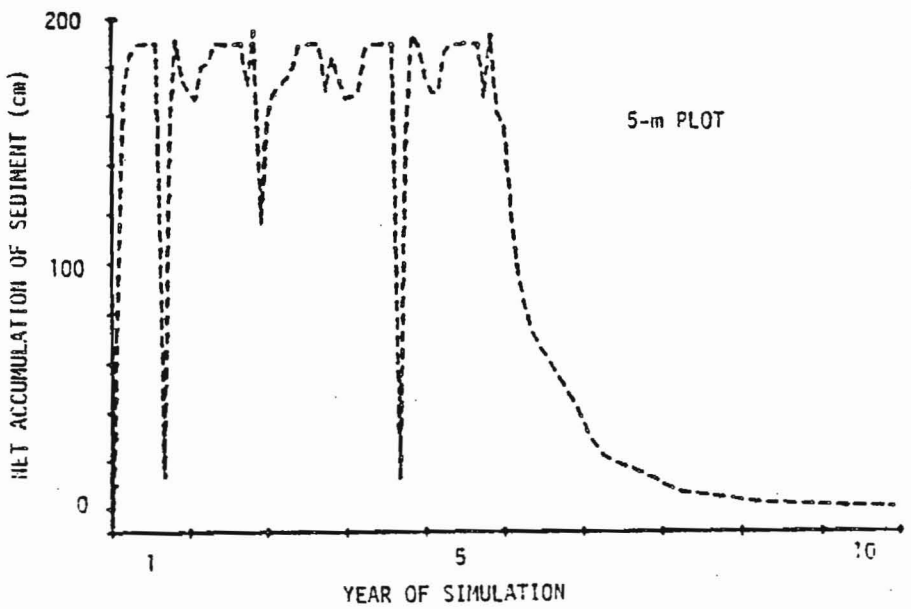

Figure 52. Scenario 3: net accumulation of sediment at 5-m plot, 10-yr run.

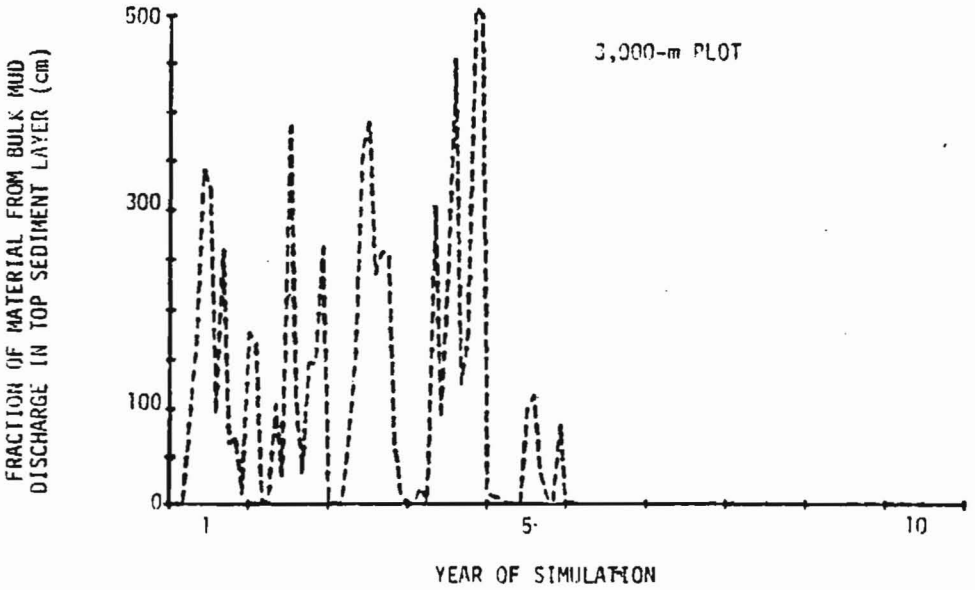

Figure 53. Scenario 3: fraction of sediment from bulk mud discharge in top 5-cm layer at 3,000-m plot, 10-yr run.

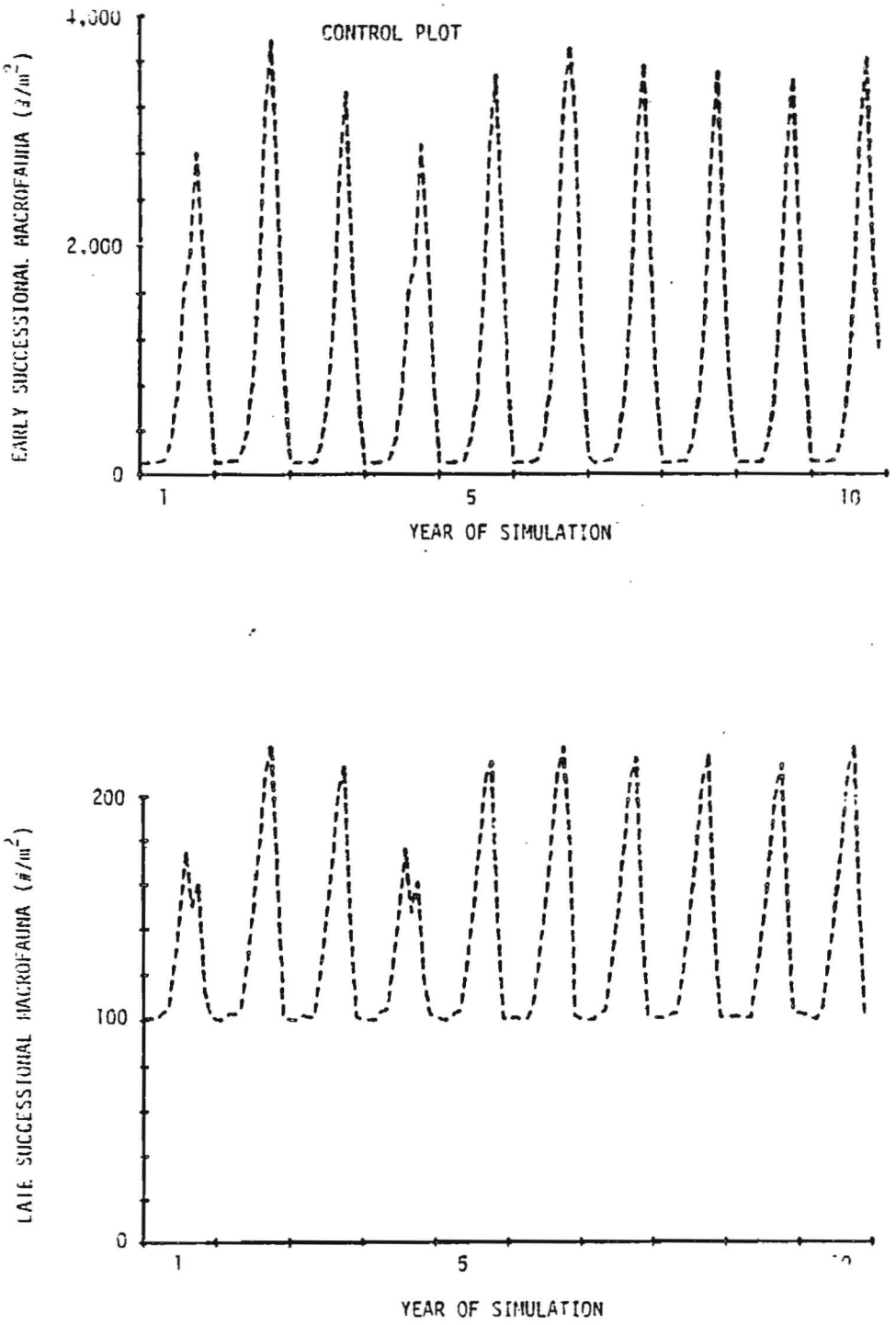

Figure 54. Scenario 3: macrofaunal assemblages at control plot, 10-yr run.

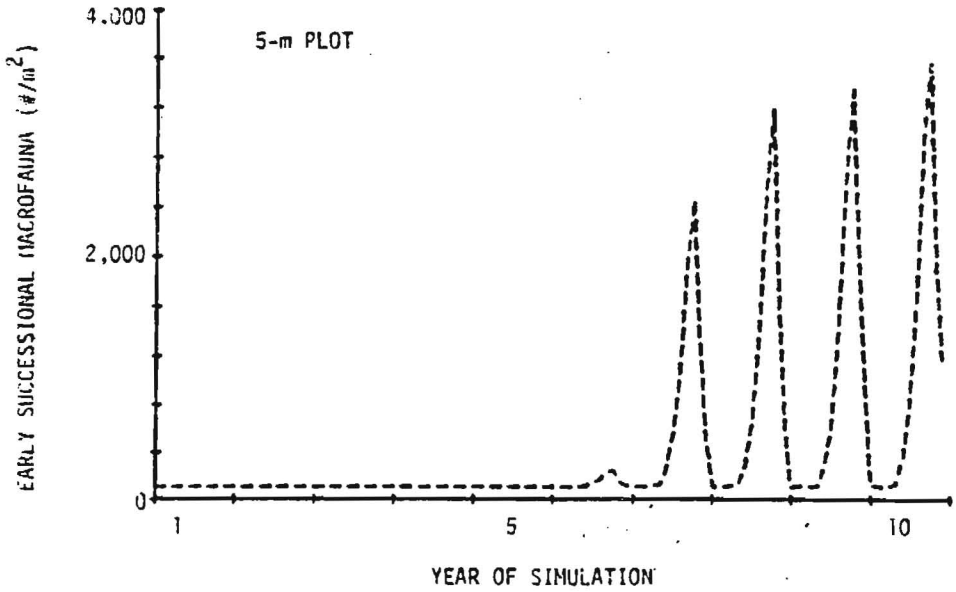

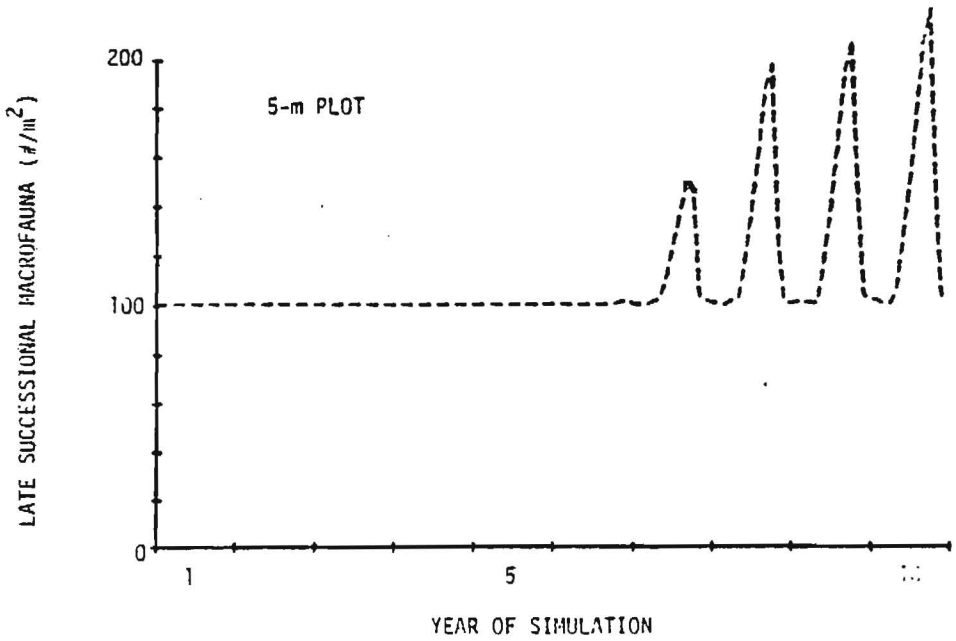

Figure 55. Scenario 3: macrofaunal assemblages at 5-m plot, 10-yr run.

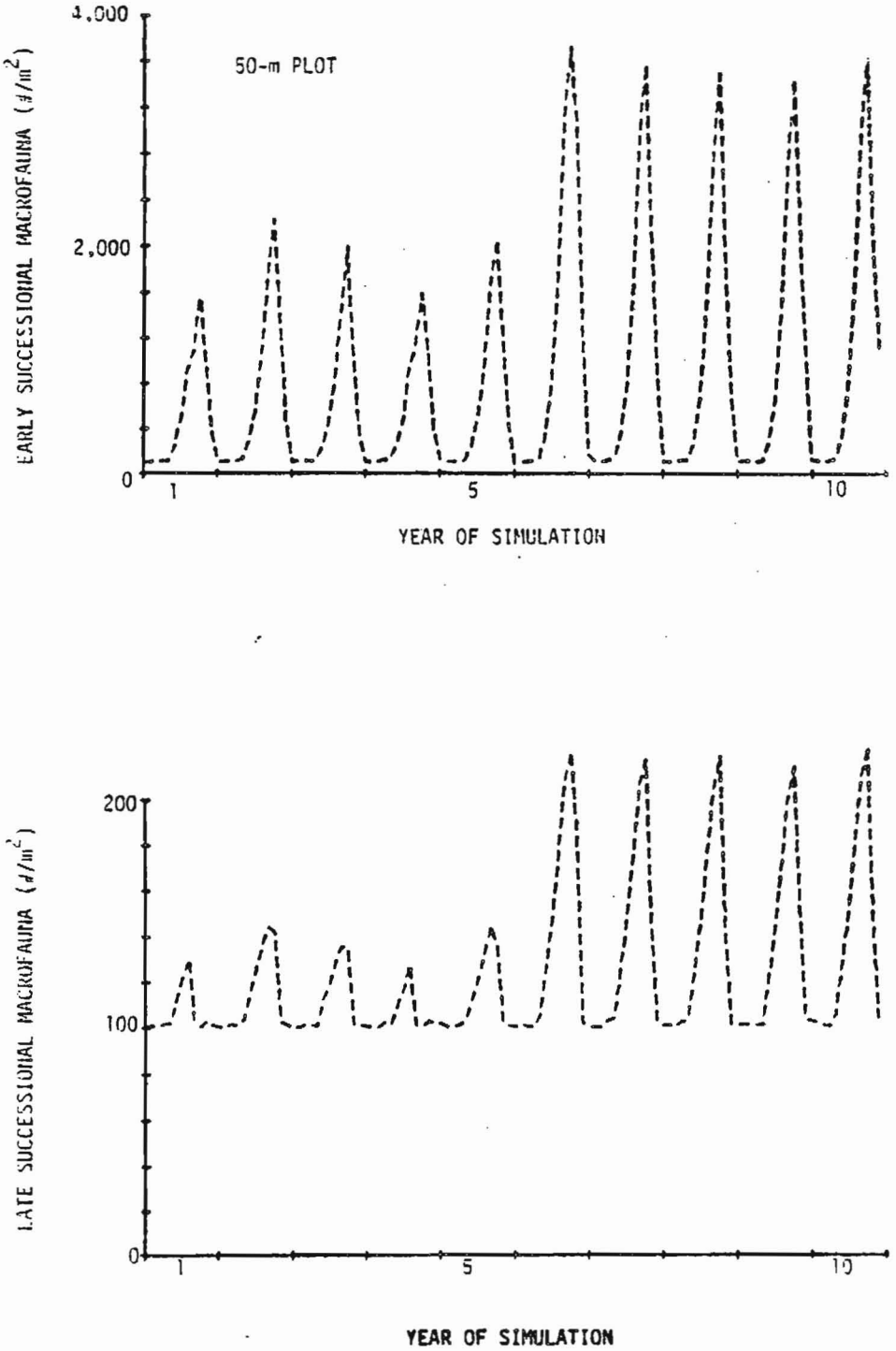

Figure 56. Scenario 3: macrofaunal assemblages at 50-m plot, 10-yr run.

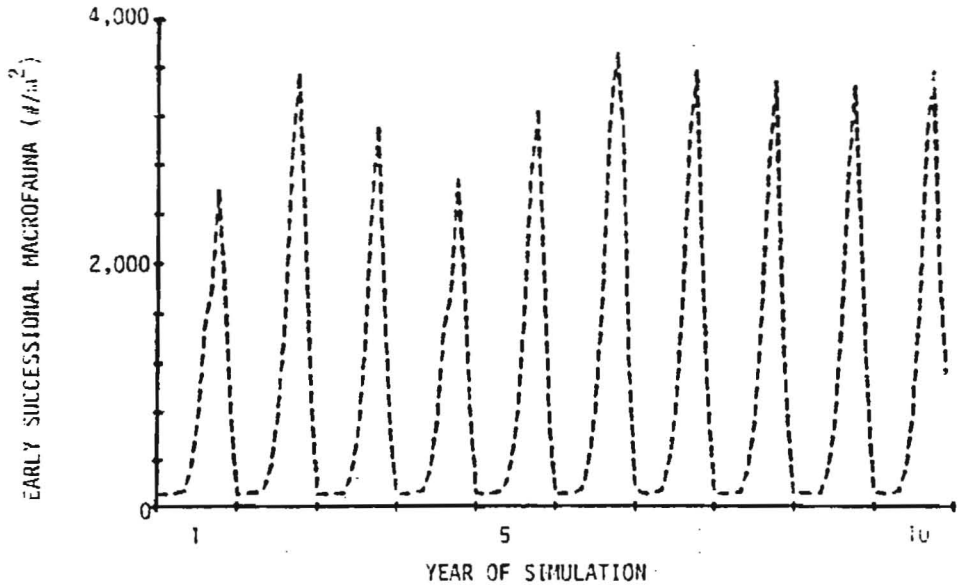

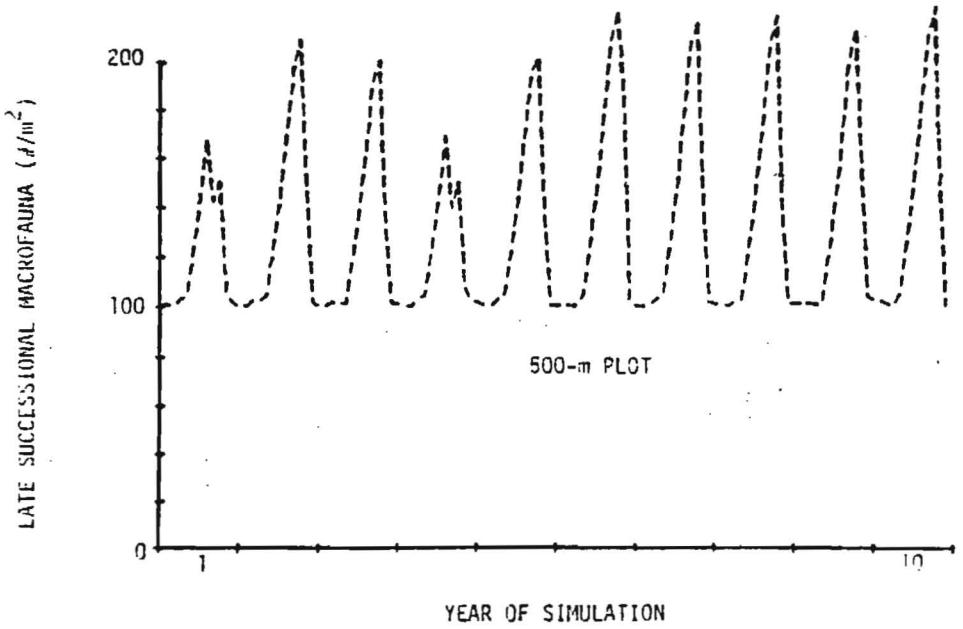

Figure 57. Scenario 3: macrofaunal assemblages at 500-m plot, 10-yr run.

Scenario 4

This scenario represents a very deep environment, such as might be encountered on the Atlantic slope. Conditions and parameter settings are summarized in Table 4; complete specifications are contained in the appended submodel descriptions. In this scenario, deposition of material from the bulk mud discharge is calculated according to Case 2, in which dynamic collapse of the mud plume occurs at a trap depth above the bottom.

Twenty-year run. Drilling and discharge begin on day 10 and continue for 5 years. There are no natural sediment disturbance events in this scenario. Thus, any material deposited remains as net accumulation. This results in final net accumulations of approximately: 1,300 cm at 5 m; 44 cm at 50 m; 0.5 mm at 500 m; 0.2 mm at 1,500 m; and less than 0.1 mm at 3,000 and 4,000 m (Figure 58). All of this material is from the cuttings discharges. Material from the bulk mud discharges is carried downcurrent beyond the 4,000-m plot before settling in this 1,000-m water depth. The assumptions of the plume fate calculations begin to break down severely at great distances and settling times. Thus, the model cannot reliably calculate where and what the deposition of this material will be, except to say that it is beyond the spatial bounds of the model and will likely be highly dispersed.

In this scenario, the initial conditions for macrofauna are set to steady state levels rather the minimum values used for the scenarios containing winter disturbance events. Initial conditions are 1,000/m^2 for the late successional macrofauna and 10/m^2 for the early successional macrofauna, which are suppressed by the late successional assemblage under steady state conditions. Behavior at the control plot (not depicted) consists of a constant 1,000/m^2 for late successional macrofauna and a constant 10/m^2 for early successional macrofauna. At the 5 and 50-m plots, both assemblages are quickly suppressed to minimum values by the physical impacts of deposited material and remain at those levels while drilling and discharge continue (depicted for 50-m plot in Figure 59). Following the end of discharge operations, the early

Table 4. Summary of Scenario 4 conditions.

DISCHARGE	
# wells	20
time per well	90 days
start of drilling	day 10
end of drilling	day 1,810
frequency of mud discharge	daily
volume of mud discharge	200 bbl
rate of mud discharge	1,000 bbl/hr
discharge depth	15 m
PHYSICAL	
water depth	1,000 m
average surface current	10 cm/sec
average bottom current	1 cm/sec
% of time current is in direction of transect	40%
mean amplitude of largest disturbance event	None
mean amplitute of largest disturbance event occurring at least once per year	None
BIOLOGICAL	
doubling time	
early successional macrofauna	60 days
late successional macrofauna	260 days
carrying capacity	
early successional macrofauna	1,000/m²
late successional macrofauna	1,000/m²
96-hr LC_{50} of material from bulk mud discharge	
early successional macrofauna	~ 50,000 ppm
late successional macrofauna	~ 130,000 ppm

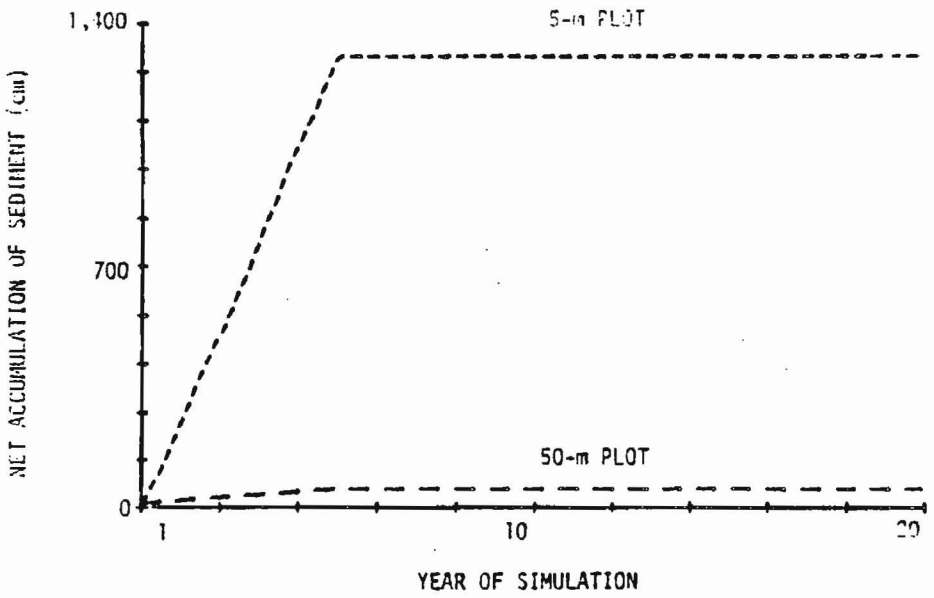

Figure 58. Scenario 4: net accumulation of sediment at 5 and 50-m plots, 20-yr run.

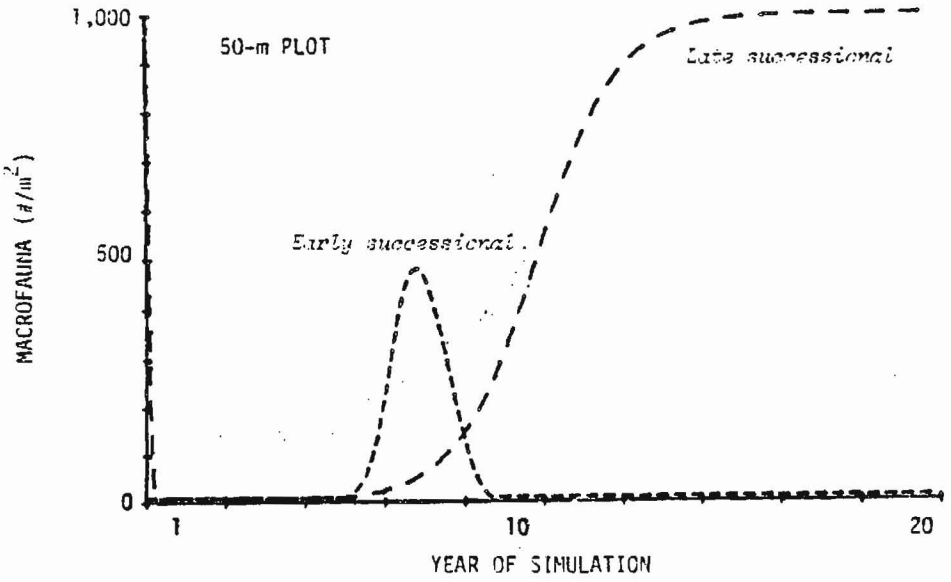

Figure 59. Scenario 4: macrofaunal assemblages at 50-m plot, 20-yr run.

successional macrofaunal assemblage responds most rapidly, reaches a peak, and then declines to the steady state level as a result of suppression by the more slowly growing late successional macrofauna. The asymptotic recovery of the late successional assemblage to near steady state conditions takes approximately 10 years. At the 500-m plot and beyond, the physical impacts are much smaller and produce only a slight depression of the late successional assemblage (Figure 60). This reduction in the late successional macrofaunal assemblage is not sufficient to allow significant increases of the early successional assemblage above its steady state, minimum level.

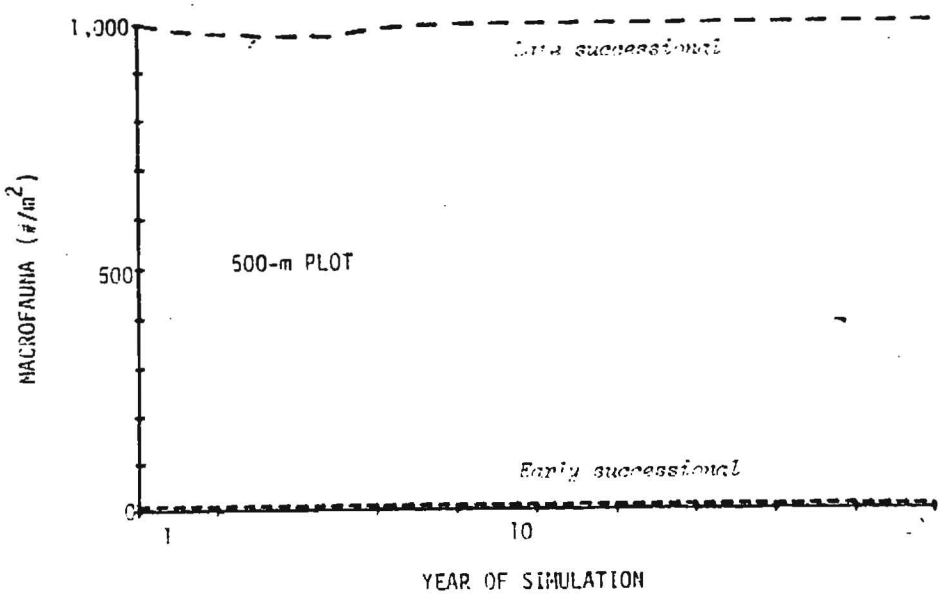

Figure 60. Scenario 4: macrofaunal assemblages at 500-m plot, 20-yr run.

SENSITIVITY

The behavior of the model as a whole is the result of a large number of complex interactions and parameter values. In this section, the effects of changing two important parameter values are examined as examples of how the model can be used to provide information on the importance of various processes or parameters. All conditions and parameters, except the one being varied, are identical to those of Scenario 2.

Mortality due to resuspension disturbance. The model represents mortality associated with resuspension events. These events are very important in determining the rate of replacement of discharged material with natural sediment, in addition to their role in determining population response through the direct mortality function. The effect of the direct mortality from resuspension events is examined by comparing the behavior of the macrofaunal assemblages in a 6-yr run of Scenario 2 under nominal conditions (as previously described) with a 6-yr run in which the direct mortality from resuspension is deactivated. There are no other differences between the runs (e.g., resuspension events alter sediment composition in the same way).

At the control plot, removal of the resuspension mortality function produces a strikingly different pattern of behavior (Figure 61 versus Figure 41). Annual cycles are eliminated as fall and winter storms no longer reduce the populations to low levels. Early successional macrofauna rapidly increase from the initial condition, approach the carrying capacity of 10,000, and then gradually decline due to suppression from the more slowly growing, late successional macrofauna. Under nominal conditions (Figure 41), both macrofaunal assemblages are reduced to minimum values by resuspension mortality in the fall and winter.

At the 5-m plot, impacts of discharged material keep both populations suppressed while drilling occurs (Figure 62). Following the cessation of discharge, a single complete succession occurs in the absence of resuspension mortality (Figure 62), rather than the annual cycle observed in the nominal run of Scenario 2 (Figure 42).

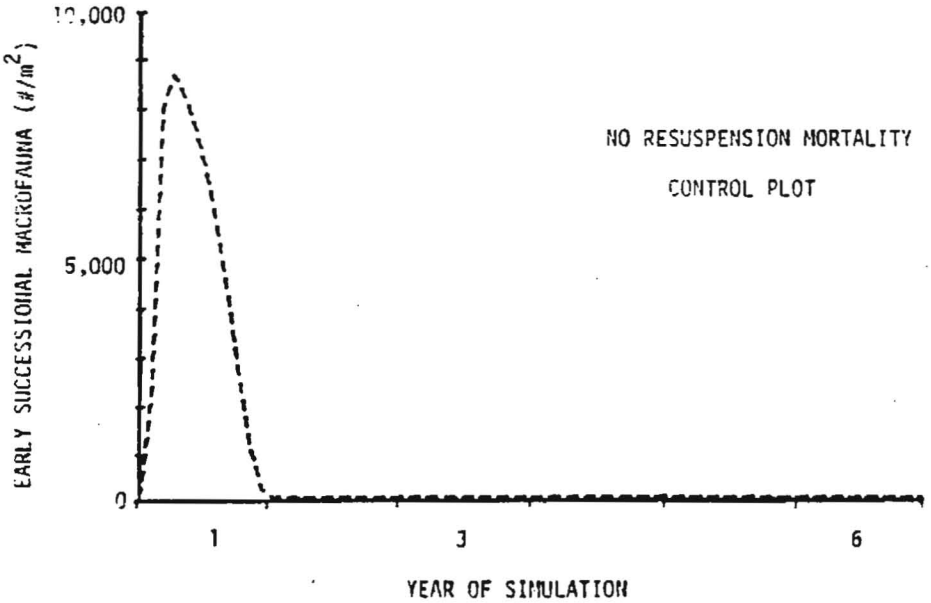

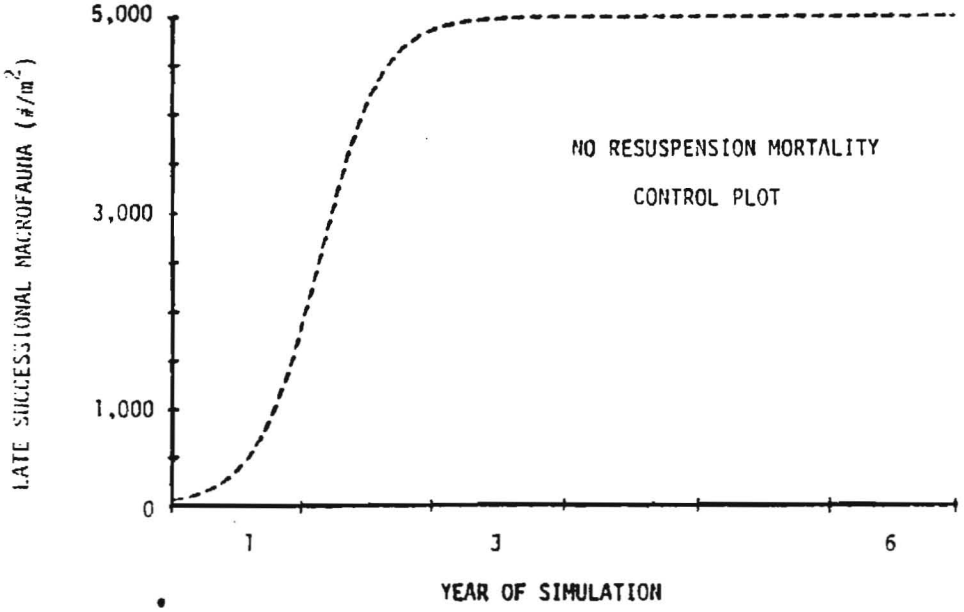

Figure 61. Effect of eliminating resuspension mortality on macrofaunal assemblages at control plot, 6-yr run of Scenario 2.

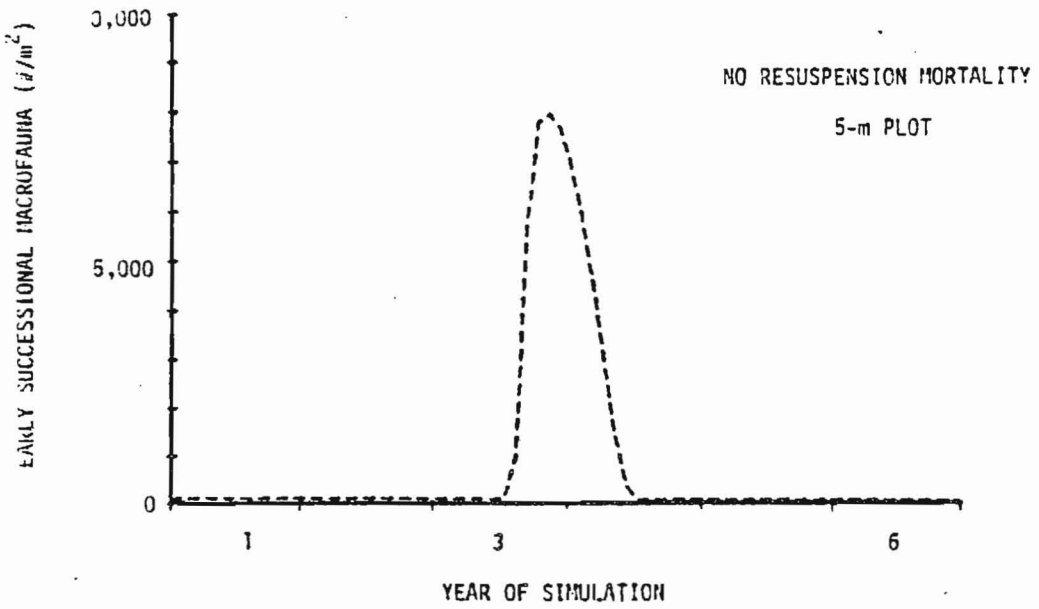

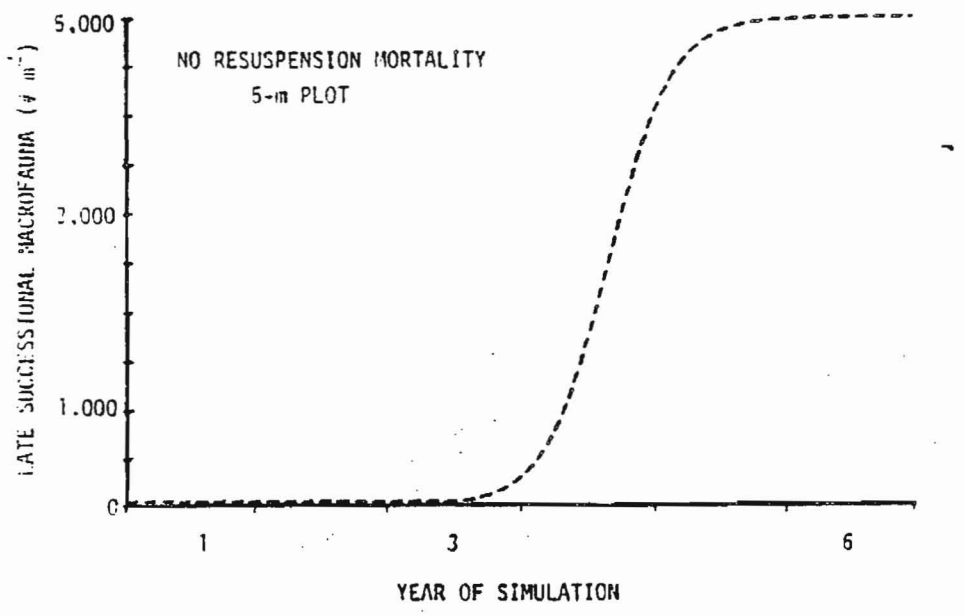

Figure 62. Effect of eliminating resuspension mortality on macrofaunal assemblages at 5-m plot, 6-yr run of Scenario 2.

At the 3,000-m plot, the absence of resuspension mortality allows successional growth and replacement (Figure 63). Succession is not delayed until after drilling and discharge cease, as it is at the more heavily impacted 5-m plot (Figure 62). However, growth is considerably slower than at the control plot with no resuspension mortality (Figure 61) because of the impacts of discharged material at the 3,000-m plot.

Oil Content of Mud

Considerable variation has been observed in the toxicities of discharged material. In the model, the relative toxicity of material from the bulk mud discharge is a function of the hydrocarbon concentration of that material as it is discharged. The toxicity is based on a regression of 96-hr LC_{50} values on hydrocarbon concentration (see MODEL DESCRIPTION and APPENDIX D). The nominal runs of the model described in preceding sections use an oil concentration of 0.0678 ppt, which corresponds to a 96-hr LC_{50} of approximately 130,000 ppm of whole mud for late successional macrofauna and approximately 50,000 ppm for early successional macrofauna. Additional runs of Scenario 2 were made with hydrocarbon concentrations set to 0.011 ppt (producing a 96-hr LC_{50} of approximately 500,000 ppm of whole mud for early successional macrofauna and no toxicity for late successional macrofauna) and 2.58 ppt (producing a 96-hr LC_{50} of approximately 500 ppm of whole mud for early successional macrofauna and approximately 1,300 ppm of whole mud for late successional macrofauna.

At distances close to the discharge point, physical impacts of discharged material keep the populations suppressed, and changing the toxicity does not result in much difference in the behavior of the populations while drilling is taking place. Following the cessation of discharge, concentrations drop relatively quickly and, thus, toxicity of discharged material does not substantially influence recovery times. This might not be the case in situations where the disturbance regime did not produce relatively rapid declines in sediment concentrations.

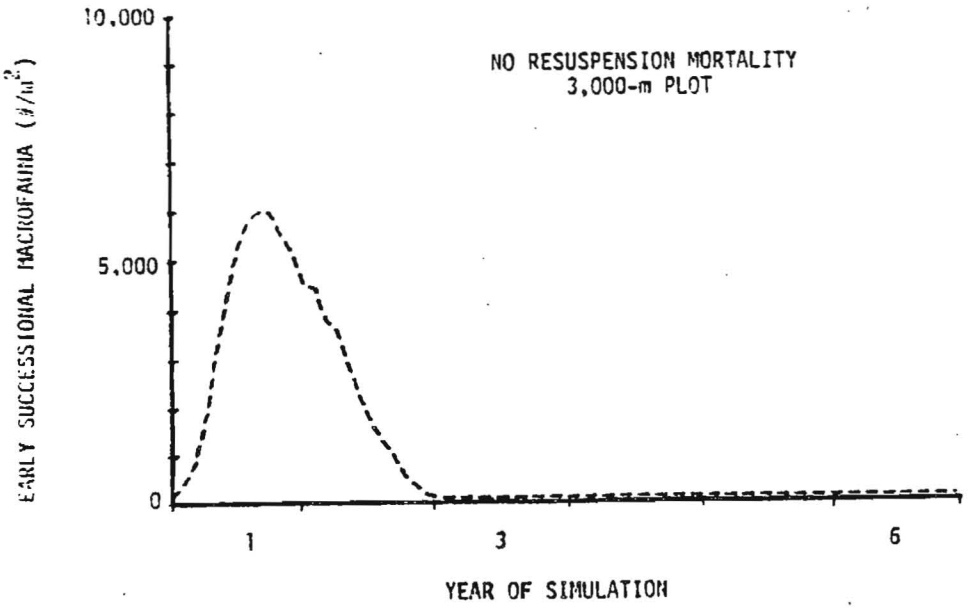

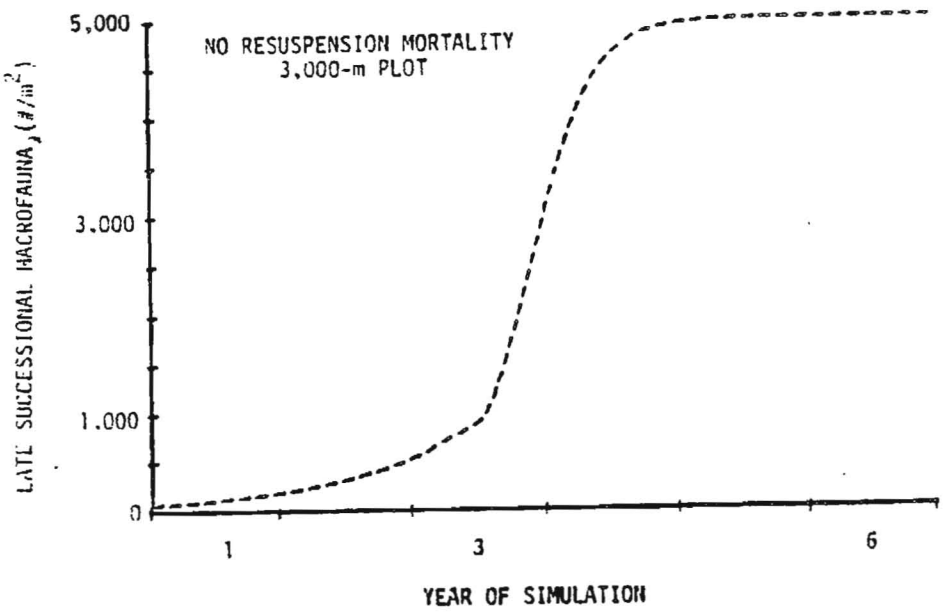

Figure 63. Effect of eliminating resuspension mortality on macrofaunal assemblages at 3,000-m plot, 6-yr run of Scenario 2.

At the 1,500-m plot of Scenario 2, deposition is small enough that the nominal oil concentration (and, hence, toxicity) allows some growth even during the period when discharges are occurring (Figure 64). Increasing the oil content (greater toxicity, lower 96-hr LC_{50}) eliminates this growth by increasing the mortality and increases the recovery time following the cessation of drilling and discharge (Figure 65). Decreasing the oil content (less toxicity, higher 96-hr LC_{50}) results in less mortality and somewhat greater growth (Figure 65), although not nearly to the levels at the control plot because the physical impacts of deposition still produce substantial mortality (Figure 41).

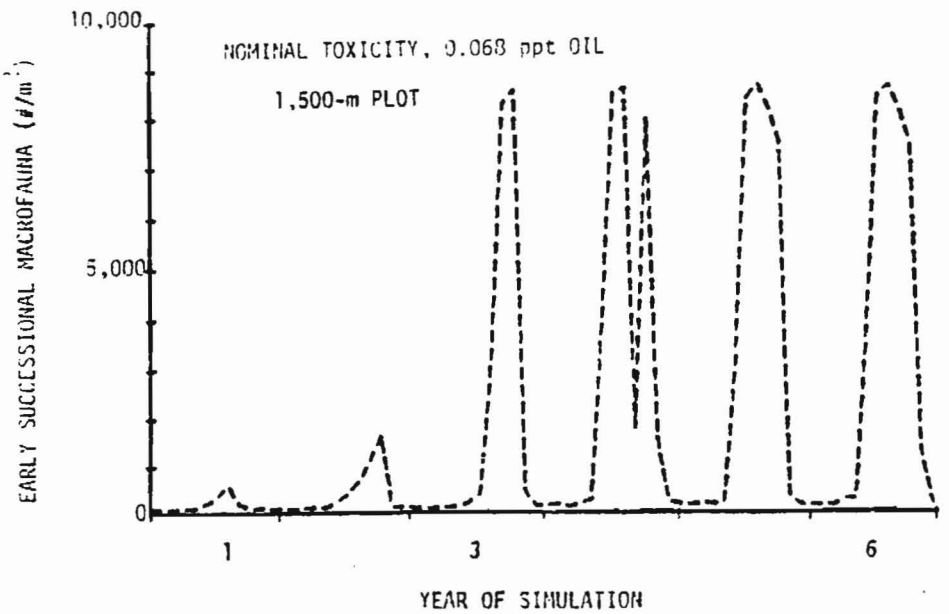

Figure 64. Scenario 2: early successional macrofaunal assemblage at 1,500-m plot, 6-yr run.

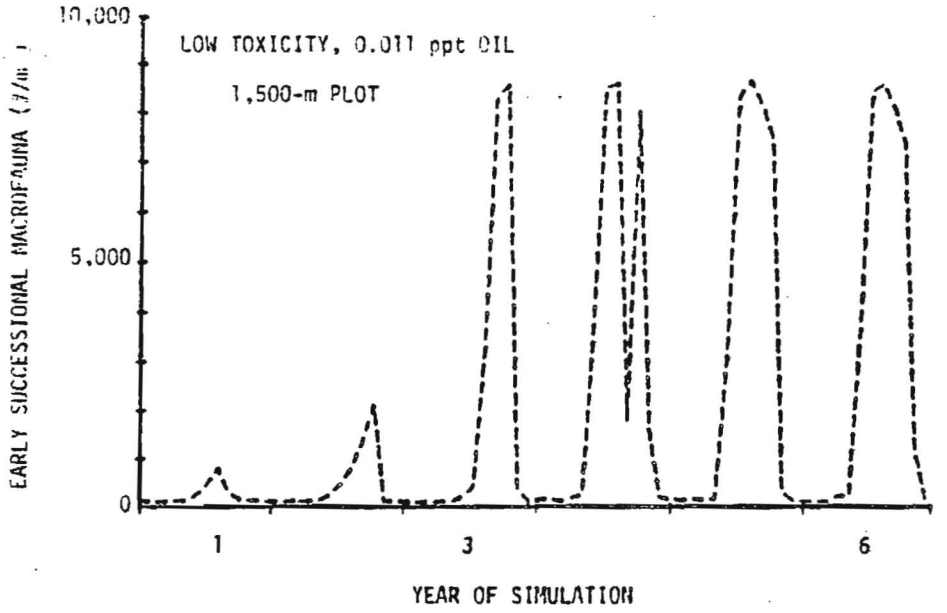

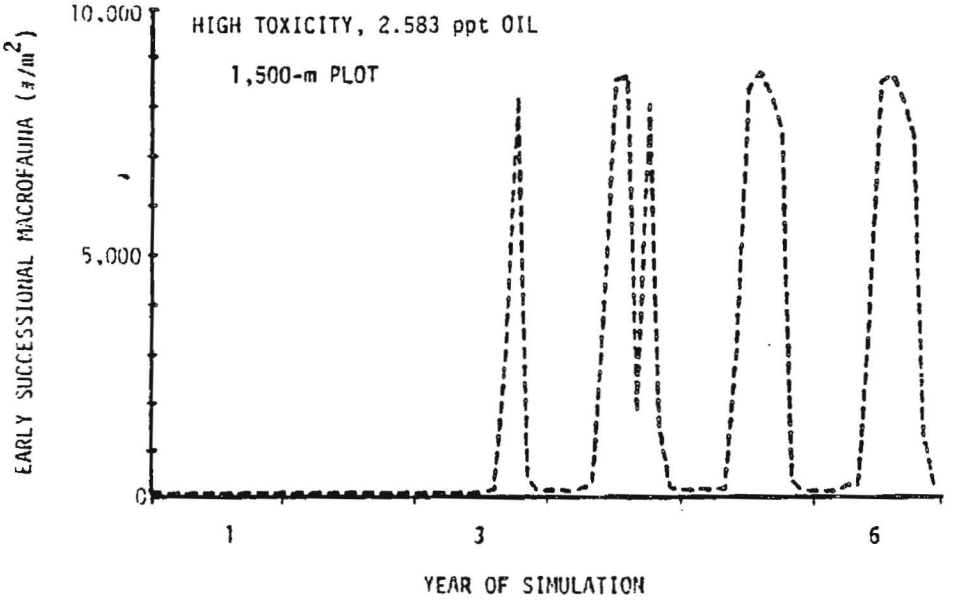

Figure 65. Effect of different hydrocarbon contents and toxicities of drilling mud on early successional macrofaunal assemblage at 1,500-m plot, 6-yr run of Scenario 2.

SUMMARY

The behavior of the model in the four scenarios presented in the preceding sections is summarized in Table 5. Differences in model behavior between scenarios are a result of the complex interaction of multiple differences in the parameter values characterizing the four scenarios. Among the important parameter differences are the duration of drilling and discharge operations, the depth of the water column, the current regime, the sediment disturbance regime, and the sensitivity and growth rates of the biota.

Rarely can a particular aspect of model behavior be isolated and explained on the basis of a single parameter. Several other qualifying points need to be kept in mind in interpreting the model output summarized in Table 5. The first is that only half a dozen distances along one transect away from the discharge point (in the direction of the dominant current) are being simulated. This is not a spatially integrated assessment. In particular, model behavior at distances along transects with other relationships to the currents would be different. A second point is that the simulations assume particular toxicity characteristics of the discharged material. In fact, toxicity characteristics can vary widely across different types of discharges. As a result, simulated effects can vary as a function of different toxicity characteristics within the range of observed toxicities (see SENSITIVITY section). A final general qualification is that the behavior should always be interpreted with an understanding of the formulations that produce it. Although the model is reasonably complex, it contains a number of simplifying, and to varying degrees, unrealistic assumptions. These include the constancy of current direction and velocity within a single discharge event, the relationship of sediment disturbance to alterations in the bottom topography, and the calculation of toxic effects as a function of simulated sediment concentrations of "whole mud".

Table 5. Summary of scenario behavior (values are approximate).

Variable	Scenario 1		Scenario 2	Scenario 3	Scenario 4
Period of drilling and discharge	5 years		2.5 years	5 years	5 years
Water depth	5 m		20 m	80 m	1000 m
% of mud discharges in transect direction	40%		40%	70%	40%
Range of deposition from discharge point, by size class diameters	Summer	Winter			
Bulk mud discharge, 10 µm	0-600 m	0-1.9 km	0-6 km	10-15 km	>50 km
Bulk mud discharge, 15 µm	0-300 m	0-850 m	0-2.7 km	4.6-6.6 km	>50 km
Bulk mud discharge, 30 µm	0-60 m	0-212 m	0-600 m	1.2-1.7 km	>50 km
Cuttings discharge, 30 µm	0-600 m	0-2 km	0-11 km	0-29 km	0- >50 km
Cuttings discharge, 100 µm	0-60 m	0-180 m	0-1 km	0-2.6 km	0-17 km
Cuttings discharge, 1,000 µm	0-30 m	0-30 m	0-30 m	0-30 m	0-170 m
Cumulative total deposition of discharged material at transect plots[a]					
5-m plot	109 m		45 m	89 m	13 m
50-m plot	169 cm		14 cm	3 cm	44 cm
500-m plot	2 cm		2 cm	5 mm	0.5 mm
1,500-m plot	0.4 mm		3 mm	0.9 mm	0.2 mm
3,000-m plot	0		0.3 mm	0.9 mm	0.09 mm
4,000-m plot	0		0.1 mm	0.9 mm	0.04 mm
Sediment disturbance regime	High energy		Moderate-high energy	Moderate-low energy	None

Table 5. (concluded).

Variable	Scenario 1	Scenario 2	Scenario 3	Scenario 4
Impacts on macrofaunal assemblages during drilling and discharge operations				
Heavily impacted plots	5, 50, 500-m	5, 50, 500-m	5 m	5, 50 m
Moderately impacted plots	1,500-m	1,500, 3,000, 4,000-m	50 m	--
Slightly impacted plots	-	-	500 m	500, 1,500 m
Recovery of macrofaunal assemblages following termination of drilling and discharge operations				
Heavily impacted plots	Up to 2 years	Within 1 year	2-3 years	8-10 years
Moderately impacted plots	Next growing season	3-6 months	3-6 months	-
Slightly impacted plots	-	-	3-6 months	1 year

[a]Cumulative deposition is not in general equal to net accumulation.

The pattern of deposition is strongly determined by three factors:

(1) Particle size or diameter. Smaller particles settle more slowly and, thus, are displaced farther downcurrent by a given current velocity. This results in the differences in ranges of deposition across particle size classes evident in Table 5 and also the differences between the bulk mud discharges and the cuttings discharges due to their different size class composition.

(2) Water depth. The deeper the water, the longer it takes for a particle of a given size to settle and, thus, the farther that particle will be displaced downcurrent by a given current velocity. This effect is evident in both the ranges of deposition and the patterns of cumulative deposition in Table 5.

(3) Current velocity. Higher current velocity moves particles farther downcurrent. Variation in current velocity produces the seasonal differences in ranges of deposition in Scenario 1, as well as the variation in the range of deposition among discharge events within seasons.

In deep water, the model simulates very large movements downcurrent for small particles. The assumption of unidirectional currents within a discharge event starts to break down in these conditions. The best interpretation of this output is that, under such conditions, the material stays in the water column so long that it is displaced and dispersed beyond the resolution of the model.

The factors determining the pattern of deposition, in combination with the amount of discharged material and the frequency with which currents are in the direction of the simulated transect, explain the cumulative thickness of material deposited at each plot (Table 5). Large particles from the cuttings discharges are deposited close to the discharge point and result in large cumulative depositions on these plots. In general, these cumulative depositions are not equivalent to the net accumulation at the plots. The sediment

disturbance regime interacts with the altered bottom topography, resulting from deposition, to limit the net accumulation, except in Scenario 4, which has no sediment disturbance events.

The natural sediment disturbance regime and the deposition of discharged materials interact with the characteristics of the biota in a given scenario to determine biological effects at different distances from the discharge point. Impacts can be conveniently separated into behavior during the period of discharge operations and recovery following the termination of discharge operations. There is a general correspondence between the amount of deposition at a plot and the severity of impacts during discharge operations, with heavily impacted plots generally receiving a cm or more of deposition per year. Several factors can modify this correspondence. These include the sediment disturbance regime, the sensitivity of the biota, and the toxicity of deposited material. In these model runs, physical impacts are important relative to toxicity because of the assumed toxicity characteristics. An assumption of highly toxic muds could result in very small depositions of material from the bulk mud discharge having as large or larger effect than much greater depositions of material from the cuttings discharges.

Recovery is a function of the magnitude of displacement or perturbation, the resiliency of the biota, the residual physical and chemical characteristics of the sediment, and the speed with which those characteristics return, if ever, to nominal conditions. In Scenario 4, with negligible sediment disturbances, the slowly growing biota takes years to recover at a severely impacted plot. In higher energy environments, the physical and chemical characteristics of the sediment return to near nominal conditions more quickly and the more resilient biota of these environments recovers more quickly. The specific dynamics of recovery can be strongly determined by the timing of low frequency, high intensity sediment disturbance events relative to the termination of discharge operations. These events basically "reset" the sediment conditions and, if they occur shortly after the termination of discharge, they can result in near minimal recovery times for a given level of impact.

DISCUSSION

The model achieves a relatively comprehensive linkage of the processes of deposition, sediment redistribution, mortality, and growth in the context of natural variation. The somewhat simplified representations linked together in the model consist, in large part, of explicit functional relationships that determine daily rates of change, as opposed to more implicit estimates of total effect (e.g., multiple regressions). Nonetheless, the model cannot be considered to produce reliable quantitative predictions of the dynamic impacts on biological populations that would occur as a result of the discharge of drilling muds and cuttings at a specific site.

LIMITS TO PREDICTIVE CAPABILITY

Limitations of the model in predicting integrated fate and effects with any high degree of confidence in the detailed, quantitative output can be traced to three general areas.

Model Refinement

The focus of the modeling effort was on the connection of a reasonable representation of physical fate to the biological responses of populations, rather than on highly detailed representations of individual processes. A number of simplifying assumptions were made that could be improved on by the development and incorporation of more refined algorithms in the model. These are discussed in some detail in the LIMITATIONS sections of the appended

submodel descriptions. More complex and realistic algorithms have been developed for several of the relevant processes, including plume fate (Brandsma et al. 1983) and aspects of sediment dynamics (Glenn 1983). Continued refinement of certain parts of the overall model can, however, reach the point of diminishing returns if other critical linkages and processes are not improved.

Lack of Understanding

There are several areas in which present understanding is not sufficient to support a truely reliable predictive algorithm. Probably the most critical and intractable of these concerns the nature of the concentration sequence that constitutes the effective exposure of organisms to toxic, discharged material. There are voluminous laboratory data on the toxicity of various drilling fluids to various marine organisms, based primarily on fixed-length, fixed-concentration, survivorship experiments (reviewed in Neff 1982 and Petrazzuolo 1981). Nonetheless, it is very difficult to extrapolate this information to effects on populations in the field by incorporation into an algorithm expressing daily mortality as a function of daily varying sediment concentrations of some fraction of the discharged material.

Data Requirements

The model described in this report has substantial data requirements. Possible refinements, such as more variable current directions and velocities within a single discharge event, could vastly increase those data requirements. The reliability of specific output can easily become limited by the reliability of the various parameter values used in a particular model run. These limitations are of two general types, depending on the nature of the parameters. Some parameters, such as the intrinsic growth rate or a particular toxicity mortality rate, are, at least in principle, measurable and can be assumed to remain reasonably constant. In practice, they can be very difficult to estimate accurately, and error in their specification can produce error in the model output. The model also requires information about future events that can be characterized only in terms of general probability distributions (e.g.,

when certain current velocities and storms will occur). Variation in these model inputs results in variation in potential model outputs. Any particular model run, thus, represents only one of a set of possible behaviors.

QUALITATIVE RESULTS

Despite the above-mentioned limitations concerning predictive capability, the modeling effort was very successful in facilitating a formal dialogue among managers and experts in the variety of processes operating when drilling muds and cuttings are discharged in the marine environment. Several qualitative conclusions, concerning both potential impacts and remaining data gaps, can be drawn from the efforts of this group to construct an explicit simulation model. These conclusions include the following:

(1) Simple, unequivocal conclusions about fate and effects across geographical regions and drilling operations are difficult, if not misleading, due to the large amount of variability in the characteristics of discharged material (e.g., oil content and toxicity), discharge conditions (e.g., duration of drilling operations), the physical environment (e.g., water depth, current direction, and sediment disturbance regime), and biological communities (e.g., intrinsic growth rates). Different combinations of these characteristics can result in substantial differences in simulated environmental fate and biological effects. For example, simulated recovery in some high-energy environments occurs within months after the cessation of discharge operations, even at heavily impacted sites, whereas simulated recovery in some low-energy environments takes years at heavily impacted sites.

(2) Considerable difficulties remain in the reliable extrapolation of results from laboratory toxicity experiments to predictions of population effects in the field.

(3) The volume of material discharged and the duration of production drilling operations simulated by the model are sufficient to produce substantial, simulated biological effects at some plots, both in terms of differences from a control plot during the period of discharge operations and in terms of recovery following the perturbations.

(4) Evaluation of the significance of potential effects involves the following factors:

- Definition of a specific spatial and temporal reference frame (e.g., What is the natural variation? Is 1 year to be considered a "long" or "short" time? Is 50 m to be considered a "large" or "trivial" distance?).

- Consideration of rare or unique resources and particularly sensitive biotic assemblages.

- Consideration of the potential for long term, cumulative effects.

Some of these aspects are clearly beyond the scope of this modeling effort (e.g., the model does not simulate the long term fate of resuspended material). The model does, however, contain an internal "reference frame" by comparison to simulated behavior at a control plot. The model, in general, simulates substantial "natural" variation at the reference or control plots, both over time due to sediment disturbance events in medium to high energy environments and over space due to geographically varying conditions, such as water depth and current regime).

REFERENCES

Auble, G. T., A. K. Andrews, R. A. Ellison, D. B. Hamilton, R. L. Johnson, and J. E. Roelle. 1982. Results of an adaptive environmental assessment modeling workshop concerning potential impacts of drilling muds and cuttings on the marine environment. U.S. Fish Wildl. Serv., Western Energy and Land Use Team, Ft. Collins, CO. 64 pp. Available as NTIS PB-83-114165.

Brandsma, M. G., L. R. Davis, R. C. Ayers, and T. C. Sauer, Jr. 1980. A computer model to predict the short-term fate of drilling discharges in the marine environment. Pages 588-610 in Research on environmental fate and effects of drilling fluids and cuttings. Lake Buena Vista, FL, January, 1980.

Brandsma, M. G., T. C. Sauer, Jr., and R. C. Ayers, Jr. 1983. Mud discharge model: report and user's guide. Exxon Production Res. Co., Houston, TX. v.p.

Fischer, H. B., E. J. List, R. C. Y. Koh, J. Imberger, and N. Brooks. 1979. Mixing in inland and coastal waters. Academic Press, New York. 364 pp.

Glenn, S. 1983. A continental shelf bottom boundary layer model: the effects of waves, currents, and a moveable bed. Ph.D. Diss., Massachusetts Inst. of Tech. and Woods Hole Oceanographic Inst. Woods Hole, MA. 237 pp.

Hastings, C. 1955. Approximations for digital computers. Princeton Univ. Press, Princeton, NJ. 201 pp.

Houghton, J. P., R. P. Britch, R. C. Miller, A. K. Runchal, and C. P. Falls. 1980. Drilling fluid dispersion studies at the lower Cook Inlet C.O.S.T. well. Pages 285-308 in Research on environmental fate and effects of drilling fluids and cuttings. Lake Buena Vista, FL, January, 1980.

Koh, R. C. Y., and Y. C. Chang. 1973. Mathematical model for barged ocean disposal wastes. EPA Grant 16070 FBY, EPA Pacific Northwest Environ. Res. Lab., EPA-660/2-73-029.

Koh, R. C. Y., and L. N. Fan. 1969. Further studies on the prediction of the radioactive debris distribution subsequent to a deep underwater nuclear explosion. Tetra Tech Rep., TC154.

Maurer, D. 1983. Background paper on burial effects of drilling fluids and cuttings (estimates of direct impacts; dredge spoil data). Unpubl. Rep.

Maurer, D., R. Keck, J. Tinsman, W. Leathem, C. Wethe, M. Huntzinger, C. Lord, and T. M. Church. 1978. Vertical migration of benthos in simulated dredged material overburdens. Vol. 1: Marine benthos. U.S. Army Corps of Eng., Waterways Exp. Stn., Tech. Rep. D-78-35:1-97.

Maurer, D., R. T. Keck, J. C. Tinsman, and W. A. Leathem. 1981. Vertical migration and mortality of benthos in dredged material. Part I: Mollusca. Mar. Environ. Res. 4:299-319.

_____. 1982a. Vertical migration and mortality of benthos in dredged material. Part II: Crustacea. Mar. Environ. Res. 5:301-317.

_____. 1982b. Vertical migration and mortality of benthos in dredged material. Part III: Polychaeta. Mar. Environ. Res. 6:49-68.

Maurer, D., R. T. Keck, J. C. Tinsman, W. A. Leathem, C. Wethe, C. Lord, and T. M. Church. In press. Vertical migration and mortality of marine benthos in dredged material: a synthesis. Int. Rev. Ges. Hydrobiol.

Neff, J. M. 1982. Fate and biological effects on oil well drilling fluids in the marine environment: A literature review. EPA-600/3-82-064, Environ. Res. Lab., Gulf Breeze, FL. 150 pp.

Petrazzuolo, G. 1981. Preliminary report on environmental assessment of drilling fluids and cuttings released onto the Outer Continental Shelf. Vol. I: technical assessment; Vol. 2: tables, figures, and appendix A. Draft report prepared for Industrial Permits Branch, Office of Water Enforcement and Ocean Programs Branch, Office of Water and Waste Management. U.S. Environ. Protection Agency. Washington, DC. v.p.

_____. 1983. Environmental assessment: drilling fluids and cuttings released onto the OCS. Submitted to the U.S. Environ. Protection Agency, Off. of Water Enforcement and Permits. Washington, DC.

Pielou, E. C. 1977. Mathematical ecology. J. Wiley, New York. 385 pp.

Rao, K. Personal communication. (see ACKNOWLEDGMENTS)

Sohio Alaska Petroleum Company. 1981. Beaufort Sea drilling effluent disposal study. Prepared for Reindeer Island stratigraphic test well participants. Prepared by Northern Tech. Serv. (Cited by Petrazzuolo 1983.)

Teeter, A. M., and D. J. Baumgartner. 1979. Prediction of initial mixing for municipal ocean discharges. U.S. Environ. Protection Agency, Corvallis Environ. Res. Lab. CERL Publ. 043.

U.S. Department of the Interior. 1976a. Environmental studies, south Texas Outer Continental Shelf, biology, and chemistry. Prepared by the Univ. of Texas Mar. Sci. Inst. for Rice Univ., Texas A&M Univ., and the Univ. of Texas. Contract AA550-CT6-17, U.S. Bur. Land Manage. (Cited by Petrazzuolo 1983.)

_____. 1976b. Baseline monitoring studies. Mississippi, Alabama, Florida Outer Continental Shelf 1975-1976. Volume VI, Rig Monitoring. Assessment of the environmental impact of exploratory oil drilling. Prepared by the State Univ. System of Florida, Inst. of Oceanography. Contract 08550-CTS-30, U.S. Bur. Land Manage. (Cited by Petrazzuolo 1983.)

Yudelson, J. M. 1967. A survey of ocean diffusion studies and data. W. M. Keck Lab. of Hydraulics and Water Resour., California Inst. Technol. Tech. Memo. 67-2.

APPENDIX A. MODEL STRUCTURE

The model consists of a very large loop of calculations, with each iteration representing 1 day. Thus, the iteration counter, ITIME, is the sequential day of simulation. Modulus (remainder) functions are used to calculate the following secondary counters: the year of simulation, IYEAR; the month within a year, IMONTH; and the Julian date, IDAY. In each day of simulation, sections of computer code corresponding to the three submodels are executed in the following order: Discharge and Plume Fate, followed by Sediment Redistribution, and, finally, Benthic Community Effects.

Mathematical notation for equations used in the model closely follows FORTRAN computer coding conventions:

(1) Multiplication is represented by *;

(2) Division is represented by /;

(3) Exponentiation is represented by ** or, where clearer, by a superscript (e.g., y^x = y**x);

(4) The logarithm, base e, of x is denoted by LOG(X);

(5) EXP(X) denotes e to the x power or e^x;

(6) AMIN1(X,Y) indicates the minimum of X and Y;

(7) AMAX1(X,Y) indicates the maximum of X and Y; and

(8) ABS(X) indicates the absolute value of X.

APPENDIX B. FORMULATION OF DISCHARGE AND PLUME FATE SUBMODEL

CALCULATIONS

Quantitative prediction of the fate of ocean discharged drilling materials generally requires extremely complex mathematical models. This complexity arises from temporal and spatial variation in current velocity and density stratification, the highly variable composition of drilling muds and formation solids, and the chemical and physical interactions of mud components following discharge. A number of complex mathematical models of ocean discharge have been developed over the last 10 years (e.g., Koh and Chang 1973; Teeter and Baumgartner 1979; Brandsma et al. 1980; Houghton et al. 1980). This submodel represents an attempt to incorporate many of the key factors influencing the fate of discharged drilling materials, while maintaining relative computational simplicity.

The submodel can be parameterized to represent different geographical areas (e.g., water depth, distribution of current velocity and direction, density stratification, well depth, and total solids discharged), different drilling muds (e.g., density and chromium and hydrocarbon concentrations), and different discharge procedures (e.g., amount, frequency, rate, and predilution). The complete sets of parameters in the Discharge and Plume Fate submodel that are used to specify drilling operations in the four scenarios of the MODEL BEHAVIOR section are presented in Tables B-1, B-2, and B-3.

Table B-1. Water column, drilling, and discharge parameters. Units and computer variable names are given in parentheses.

Parameter	Scenario 1	2	3	4
Water column characteristics				
water depth (m) (WDEPTH)	5	20	80	1,000
average surface current (cm/sec) (ASCURR)	13	25	15	10
average bottom current (cm/sec) (ABCURR)	13	10	5	1
standard deviation of current velocity (cm/sec) (VSTD)	6	10	6	5
proportion of time current is in direction of sample transect (from current rosette) (CFREQ)	0.40	0.40	0.70	0.40
ambient density in surface layer (g/cm^3) (PO)	1.025	1.025	1.025	1.025
density gradient ($g/cm^3/m$) (PA)	0.0001	0.0004	0.0004	0.0002
Drilling mud characteristics				
density (lb/gal) (DENSM)	13	13	13	13
% liquid (PWAT)	79.5	79.5	79.5	79.5
[BA] (mg/l) (BACONC)	141,000	141,000	141,000	141,000
[Cr] (mg/l) (CRCONC)	400	400	400	400
[#2 fuel oil] (g/l) (HYCONC)	0.0678	0.0678	0.0678	0.0678

Table B-1. (concluded)

Parameter	Scenario 1	2	3	4
Drilling and discharge characteristics				
# wells (NWELLS)	60	20	40	20
time per well (days) (TWELL)	30	45	45	90
discharge volume (bbl) (DISVOL)	200	200	200	200
discharge rate (bbl/hr) (DRATE)	1,000	1,000	1,000	1,000
diameter of discharge pipe (m) (PDIAM)	0.3048	0.3048	0.3048	0.3048
frequency of discharge (days) (DFREQ)	1	1	1	1
discharge depth (m) (DDEPTH)	surface	surface	5	15
total solids per well (mt) (TSOLID)	1,000	1,500	1,500	2,000
proportion of Ba associated with settleable solids (BASOL)	0.9	0.9	0.9	0.9
proportion of Cr associated with settleable solids (PCRSOL)	0.9	0.9	0.9	0.9
proportion of hydrocarbons associated with settleable solids (PHYSOL)	0.5	0.5	0.5	0.5
Gaussian diffusion coefficient (m^2/sec)				
surface plume (DCOEF4)	1.0	1.0	1.0	1.0
mud plume - case 1 (DCOEF1)	0.1	0.1	0.1	0.1
mud plume - case 2 (DCOEF2)	0.1	0.1	0.1	0.1
mud plume - case 3 (DCOEF3)	0.5	0.5	0.5	0.5

Table B-2. Source of discharged drilling material.

Discharge	Source	Percent of total solids discharged
Cuttings	formation solids: desilter	18.0
	formation solids: desander	6.0
	formation solids: shale-shaker	18.0
Bulk mud	mud additives	40.0
	formation solids	18.0

Table B-3. Average density and particle size distribution of discharged material. Computer variable names are given in parentheses.

Discharge	Average particle density (g/cm^3) (DENS)	Average particle diameter (μm) (SIZEC,SIZEM)	Percent of total solids discharged (PCUT,PMUD)
Cuttings	2.6	30	18.0
		100	6.0
		1,000	18.0
Bulk mud	3.9	10	8.7
		15	26.1
		30	23.2

Characteristics of Discharged Material

Drilling operations typically have continuous discharges of solids, designated here as cuttings discharges, at low rates (1-10 bbl/hr) while actually drilling and periodic bulk discharges, designated here as mud discharges, at higher rates (100-1,000 bbl/hr). The continuous discharges contain primarily cuttings from the solids control equipment; the bulk mud discharges contain some cuttings but are primarily spent muds that have lost their efficiency. For the scenario runs described in this report, it was assumed that the total amount of solids discharged may vary with geographical location but that characteristics of the discharged materials (Tables B-2 and B-3) remain the same. However, these characteristics are represented as parameters in the submodel and can be altered if site-specific data are available. Although discharged materials represent a continuum of particle sizes, they are aggregated into three size classes of cuttings and three size classes of drilling mud (Table B-2) for deposition calculations.

Deposition from Cuttings Discharge

Discharged cuttings are assumed to be distributed on the bottom according to the circular normal probability density function:

$$p = \frac{1}{2\pi\sigma^2} * \mathrm{EXP}\left\{ - \frac{(x - x_0)^2 + (y - y_0)^2}{2\sigma^2} \right\} \qquad (4)$$

where p = the probability density function

σ = the standard deviation

x_0, y_0 = the location of the discharge point (and center of distribution)

EXP = function producing e^x

The thickness of cuttings of a particle size class deposited within a 1-m² area on the bottom is:

$$\text{CUTDEP(I,ID)} = \text{DCUT(I)} \int_{x = x_1}^{x = x_2} \int_{y = y_1}^{y = y_2} p \, dxdy \qquad (5)$$

where CUTDEP(I,ID) = depth of cuttings of size class I deposited at distance ID (cm)

DCUT(I) = total cuttings of size class I discharged on current simulation day (mt)

p = the probability density function

x_1, x_2, y_1, y_2 = coordinates defining boundaries of 1-m² area

Because x and y are independent, the integrals can be evaluated separately and the depth of deposition approximated as the product of two error function differences:

$$\text{CUTDEP(I,ID)} = \text{DCUT(I)} * \left\{\text{erf} \frac{x_2 - x_0}{\sigma} - \text{erf} \frac{x_1 - x_0}{\sigma}\right\} \qquad (6)$$

$$* \left\{\text{erf} \frac{y_2 - y_0}{\sigma} - \text{erf} \frac{y_1 - y_0}{\sigma}\right\}$$

$$* ([10^6 / \text{DENS(3)}] / 10^4) / [1.0 - \text{PSPACE(3)}]$$

where CUTDEP(I,ID) = depth of cuttings of size class I deposited at distance DIST(ID) (cm)

DCUT(I) = total cuttings of size class I discharged (mt)

x_0, y_0 = coordinates of discharge point (m)

x_1, x_2, y_1, y_2 = coordinates defining boundaries of 1-m² area at plot ID (m)

$$\mathrm{erf}(z) = 1-[(a_1 t + a_2 t^2 + a_3 t^3) * \mathrm{EXP}(-z^2)] + e(z)$$

$$t = \frac{1}{1 + cz}$$

$$c = 0.47047$$

$$a_1 = 0.3480242$$

$$a_2 = -0.0958798$$

$$a_3 = 0.7478556$$

$$|e(z)| \leq 2.5 * 10^{-5}$$

DENS(3) = particle density of cuttings (g/cm^3)

PSPACE(3) = proportion of cuttings deposition that is pore space

The error function is from Hastings (1955). The standard deviation used in these calculations is a function of the distance the discharged material falls, the current velocity, the particle settling rate, and an angle of repose constraint on the resulting deposition. The initial calculation of the interval from the discharge point over which cuttings of a certain size are deposited is:

DDISTC(I) = [(WDEPTH - DDEPTH) / (SRATEC(I) / 100.0)] * AVGCUR (7)

where DDISTC(I) = distance from the discharge point over which cuttings of size class I are deposited (m)

WDEPTH = water depth (m)

DDEPTH = discharge depth (m)

SRATEC(I) = settling rate (cm/sec) of particle size I cuttings

AVGCUR = average current velocity (m/sec) in water column

It is initially assumed that the distance of deposition (DDISTC) represents two standard deviations for the circular normal distribution; that is, it is a radial distance within which 95% of the material is deposited. If, however, the slope of cuttings deposition between 1 and 2 standard deviations is greater than a specified angle of repose (ANGLER), then the number of standard deviations which DDISTC represents (SDFAC) is iteratively reduced until the angle of repose constraint is satisfied. The maximum angle of repose (ANGLER) is estimated as 18°. The actual distance of cuttings deposition (99.7% of material or 3 standard deviations) on a given day is calculated in meters:

$$CMET(I) = DDISTC(I) / (SDFAC / 3.0) \tag{8}$$

where CMET(I) = distance from discharge point corresponding to 3 standard deviations of cuttings deposition of size class I (m)

DDISTC(I) = distance away from discharge point over which cuttings of size class I are deposited (m)

SDFAC = the number of standard deviations represented by DDISTC(I)

The average current velocity (AVGCUR) is calculated as a simple average of the surface current (SCURR) and the bottom current (BCURR). The surface (or bottom) current velocity for any day in the simulation is randomly chosen from a normal distribution with a mean of ASCURR (or BSCURR) and a standard deviation of VSTD. The means and standard deviation are specified as input to the model, based on data for the geographical area represented.

To represent geographic areas where an ice cover is present during part of the year and discharge occurs below the ice, the effective water depth (WDEPTH) is decreased by 2 m and the average current velocity (AVGCUR) is multiplied by a current reduction factor. The settling rate for cuttings particles of size class I is calculated from Stoke's law:

$$SRATEC(I) = (1.0 / 18.0) * [DENS(3) - 1.025] * 980.0 * ([SIZEC(I) * 1.0 * 10^{-4}] ** 2.0) / 0.01 \quad (9)$$

where SRATEC(I) = settling rate of particle size class I (cm/sec)

DENS(3) = density of cuttings (g/cm^3)

980.0 = gravitational constant (cm/sec^2)

SIZEC(I) = particle diameter (μm)

Deposition from Bulk Mud Discharge

Deposition of material from the bulk mud discharge is dependent on the behavior of the plume between the discharge point and the bottom. Two general cases are considered in the current model: (1) the mud plume impacts the bottom and collapses; and (2) dynamic collapse of the mud plume occurs at a trap depth above the bottom. A special case (3) is considered for shallow water areas where the mud plume impacts the bottom but the water is so shallow that the mud plume and surface plume are mixed. The general sequence of calculations for determining deposition from the bulk mud discharge is to calculate a trap depth to determine which case is appropriate, compute the size of the mud cloud formed when the plume collapses, and calculate growth of the cloud and particle deposition as the cloud is carried down current.

Trap depth can be defined as the depth at which vertical descent of the mud plume is halted. It is also known as the depth of neutral buoyancy or the equilibrium depth. The calculations used in this model (Fischer et al. 1979) assume linear stratification in the water column and uniform crossflow. Trap depth is determined as a function of discharge momentum, discharge density difference, ambient crossflow velocity, and ambient density stratification. Required inputs include diameter of discharge pipe, discharge rate, bulk density of discharge, ambient density in surface layer, a representative density gradient, crossflow velocity, and depth of the discharge. Initial fluxes for trap depth calculations are determined as:

$$QT = DRATE * 0.159 * (1.0 / 60.0) * (1.0 / 60.0) \quad (10)$$

$$SMF = QT * (QT / [3.14159 * (PDIAM / 2.0) ** 2.0])$$

$$BT = 9.8 * [ABS (PO - PM) / PO] * QT$$

where QT = initial volume flux (m^3/sec)

DRATE = discharge rate (bbl/hr)

SMF = specific momentum flux (m^4/sec^2)

PDIAM = diameter of discharge pipe (m)

BT = specific buoyancy flux (m^4/sec^3)

ABS = absolute value function

PO = ambient density in surface layer (g/cm^3)

PM = bulk density of discharge (g/cm^3), including any predilution

The gravitational density anomaly is calculated as:

$$GE = 9.8 * (PA / PO) \quad (11)$$

where GE = gravitational density anomaly (1/sec^2)

PA = a representative density gradient (g/cm^3/m)

PO = ambient density in surface layer (g/cm^3)

9.8 = gravitation constant (m/sec^2)

Nondimensional parameters are determined by:

$$ST = [(SMF ** 2.0) * GE] / (BT ** 2.0) \quad (12)$$

$$PSI = (UT ** 2.0) / [(GE * SMF) ** 0.5]$$

where ST = stratification parameter

PSI = crossflow parameter

SMF = specific momentum flux (m^4/sec^2)

GE = gravitational density anomaly ($1/sec^2$)

BT = specific buoyancy flux (m^4/sec^3)

UT = average current velocity (m/sec)

Calculations for characteristic length scales are:

```
      ZB = BT / (UT ** 3.0)                                    (13)
      ZM = (SMF ** 0.5) / UT
  LAMBDA = UT / (GE ** 0.5)
```

where ZB = characteristic length scale for the buoyant plume (m)

ZM = characteristic length scale for the momentum jet (m)

LAMBDA = characteristic length scale for the jet in stratified crossflow (m)

UT = average crossflow velocity between surface and bottom (m/sec)

BT = specific buoyancy flux (m^4/sec^3)

SMF = specific momentum flux (m^4/sec^2)

GE = gravitational density anomaly ($1/sec^2$)

Depth penetrations to neutral bouyancy are calculated as:

```
      HB = 3.8 * (BT ** 0.25) / (GE ** 0.375)                  (14)
      HM = 3.8 * [(SMF / GE) ** 0.25]
```

where HB = depth penetration of buoyant plume (m)

HM = depth penetration of momentum jet (m)

BT = specific buoyancy flux (m^4/sec^3)

GE = gravitational density anomaly ($1/sec^2$)

SMF = specific momentum flux (m^4/sec^2)

A comparison is made between ZB and ZM to determine whether the stratification parameter, ST, or the crossflow parameter, PSI, is the most important. If the crossflow parameter is the important one (ZM > ZB), trap depth, ZT, is determined as:

$$ZT = HM \qquad \text{if } PSI < 1.0 \tag{15}$$

$$ZT = 3.8 * (ZM ** 0.667) * (LAMBDA ** 0.333) \qquad \text{if } 1.0 \leq PSI < (ZM / ZB)$$

$$ZT = 3.8 * (ZB ** 0.333) * (LAMBDA ** 0.667) \qquad \text{if } (ZM / ZB) \leq PSI$$

where ZT = trap depth (m)

HM = depth penetration of momentum jet (m)

PSI = crossflow parameter

ZM = characteristic length scale for momentum jet (m)

LAMBDA = characteristic length scale for jet in stratified crossflow (m)

ZB = characteristic length scale for the buoyant plume (m)

If the stratification parameter is more important (ZM < ZB), trap depth is determined as:

$$ZT = HM \qquad \text{if } [ST ** (-0.5)] < 1.0 \tag{16}$$

$$ZT = HB \qquad \text{if } 1.0 \leq [ST ** (-0.5)] < [(ZB / ZM) ** 2.0]$$

$$ZT = 3.8 * (ZB ** 0.333) * (LAMBDA ** 0.667) \qquad \text{if } [(ZB / ZM) ** 2.0] \leq [ST ** (-0.5)]$$

where ZT = trap depth (m)

HM = depth penetration of momentum jet (m)

ST = stratification parameter

HB = depth penetration of buoyant plume (m)

ZB = characteristic length scale for momentum jet (m)

LAMBDA = characteristic length scale for jet in stratified crossflow (m)

The final plume depth, TDEPTH, is determined by:

$$TDEPTH = AMIN1\ [(DDEPTH + ZT),\ WDEPTH] \tag{17}$$

where TDEPTH = final plume depth (m)

DDEPTH = discharge depth (m)

ZT = trap depth (m)

WDEPTH = water depth (m)

If the final plume depth is above the bottom, calculations proceed for case 2. If the final plume depth is at the bottom, case 1 calculations are used if water depth is greater than 5 m and case 3 calculations are used if the depth is less than or equal to 5 m.

Deposition of materials from the mud cloud at any distance from the discharge point is a function of the size of the mud cloud and the settling rates of the particles in the cloud. The cloud formed when the mud plume initially collapses is conceptualized as a box with a height of:

$$HCLOUD = [0.125 * (TDEPTH - DDEPTH - 1.0)] + 1.0 \tag{18}$$

and a width of

$$WCLOUD = [(DISVOL * DT * 0.159) / HCLOUD] ** 0.5 \tag{19}$$

where HCLOUD = height of mud cloud (m)

DDEPTH = discharge depth (m)

WCLOUD = width of mud cloud (m)

DISVOL = discharge volume (bbl)

DT = dilution of mud plume at final plume depth

TDEPTH = final plume depth (m)

The dilution of the mud plume at the final plume depth is calculated as:

$$DT = [0.15 * (BT ** 0.333) * (TDEPTH ** 1.667)] / QT \qquad (20)$$

where DT = dilution of the mud plume at the final plume depth

BT = specific bouyancy flux (m^4/sec^3)

TDEPTH = final plume depth (m)

QT = initial volume flux (m^3/sec)

The width of the mud cloud increases through entrainment of seawater as the cloud is carried downcurrent. Assuming Gaussian diffusion, the width of the cloud at any distance downcurrent is computed from the equation:

$$BPWIDE(ID) = 2.0 * ([2.0 * DCOEF2 * (TDIST + VT)] ** 0.5) \qquad (21)$$

where BPWIDE(ID) = cloud width at distance DIST(ID) (m)

DCOEF2 = horizontal diffusion coefficient (m^2/sec)

TDIST = time for the cloud to reach distance DIST(ID) (sec)

VT = virtual time it would have taken for cloud to reach its initial width, WCLOUD, assuming a point source discharge (sec)

The horizontal diffusion coefficient (DCOEF2) is used to account for all the forces (e.g., current shears and eddies) that are not represented mechanistically. Yudelson (1967) and Koh and Fan (1969) concluded that this diffusion coefficient could be estimated from a four-thirds power law:

$$DCOEF2 = (AL * [(BPW * 3.28) ** (4.0 / 3.0)]) * 0.0929 \qquad (22)$$

where DCOEF2 = the horizontal diffusion coefficient (m^2/sec)

AL = a dissipation parameter ($ft^{2/3}$/sec)

BPW = the horizontal length scale of the diffusing mud cloud (m)

In order to generate consistent estimates of DCOEF2 and, thus, BPWIDE(ID), regardless of the user-chosen distances for the 1-m^2 plots [DIST(ID)], a standard set of points for updating the horizontal length scale (BPW) and associated DCOEF2 is used. BPW and DCOEF2 are updated (using equations 21 and 22) at 5-m intervals for distances less than 50 m from the platform, at 50-m intervals for distances between 50 m and 500 m from the platform, at 100-m intervals for distances between 500 m and 5000 m from the platform, at 1,000-m intervals for distances from 5,000 m to 50,000 m, and at 10,000 m intervals for distances greater than 50,000 m from the platform.

The time to reach distance ID is determined as:

$$TDIST = DIST(ID) / AVGCUR \qquad (23)$$

and the virtual time it would have taken the cloud to reach its initial width is:

$$VT = [(WCLOUD / 2.0) ** 2.0] / (2.0 * DCOEF1) \quad (29)$$

where TDIST = time for the cloud to reach distance DIST(ID) (sec)

DIST(ID) = distance from the rig (m)

AVGCUR = average current from the surface to the bottom (m/sec)

VT = virtual time for cloud to reach width WCLOUD (sec)

WCLOUD = initial mud cloud width (m)

DCOEF1 = initial horizontal diffusion coefficient (m^2/sec)

The initial horizontal diffusion coefficient (DCOEF1) is calculated from:

$$DCOEF1 = (AL * [(WCLOUD * 3.28) ** (4.0 / 3.0)]) * 0.0929 \quad (25)$$

where DCOEF1 = initial horizontal diffusion coefficient (m^2/sec)

AL = a dissipation parameter ($ft^{2/3}$/sec)

WCLOUD = initial mud cloud width (m)

Particles of a given size class are assumed to start settling out of the mud cloud as soon as it is formed, at a rate determined from Stoke's law:

$$SRATEM(I) = (1.0 / 18.0) * ([DENS(2) - 1.025] * 980.0 * ([SIZEM(I) * 10^{-4}] ** 2.0) / 0.01 \quad (26)$$

where SRATEM(I) = settling rate of mud particle size I (cm/sec)

DENS(2) = particle density of settleable solids in bulk mud discharge (g/cm^3)

1.025 = density of seawater (g/cm^3)

980.0 = gravitational constant (cm/sec^2)

SIZEM(I) = diameter of particle size class I (μm)

For cases 1 and 3, this means that the first particles to settle out are deposited directly below the discharge point because the mud cloud forms on the bottom. For case 2, the first particles of a size class to settle out are carried downcurrent as they fall from the final plume depth to the bottom and deposition is, thus, offset from below the discharge point by a distance:

$$SDIST(I) = AVGCUR * (WDEPTH - TDEPTH) / [SRATEM(I) / 100.0] \quad (27)$$

where SDIST(I) = distance from discharge point to where particles of size class I are initially deposited (m)

AVGCUR = average current velocity in water column (m/sec)

WDEPTH = water depth (m)

TDEPTH = final plume depth (m)

SRATEM(I) = settling rate of particle size class I (cm/sec)

For all cases, deposition of particle size class I extends from the point of initial settling over the distance calculated as:

$$DDISTM(I) = (HCLOUD / [SRATEM(I) / 100.0]) * AVGCUR \quad (28)$$

where DDISTM(I) = distance of deposition of particle size class I from initial settling point (m)

HCLOUD = height of mud cloud (m)

SRATEM(I) = settling rate of particle size class I (cm/sec)

AVGCUR = average current velocity in water column (m/sec)

Within this region of deposition, it is assumed that the same amount of material of a given particle size class settles out in each 1-m strip that the cloud passes over as it is carried downcurrent. But, because the mud cloud is increasing in width through entrainment of seawater, the depth of material deposited decreases with distance from the discharge point. The average depth at any distance from the discharge point is calculated as:

$$\text{AMDEP(I,ID)} = [([\text{DMUD(I)} / \text{DDISTM(I)}] / \text{BPWIDE(ID)}) * ([10^6 / \text{DENS(2)}] / 10^4)] / [1.0 - \text{PSPACE(2)}] \quad (29)$$

where AMDEP(I,ID) = average depth of particle size class I deposited at distance DIST(ID) (cm)

DMUD(I) = total solids in bulk mud discharge of size class I (mt)

DDISTM(I) = distance of deposition of particle size class I from initial settling point (m)

BPWIDE(ID) = mud cloud width at distance DIST(ID) (m)

DENS(2) = particle density of settleable solids in bulk mud discharge (g/cm^3)

PSPACE(2) = proportion of pore space in mud deposition

Assuming a Gaussian distribution of deposition perpendicular to the current direction, because the mud cloud grows by entraining seawater from the edges, the depth of deposition at the center of a 1-m strip is:

$$\text{CMDEP(I,ID)} = \text{AMDEP(I,ID)} / 0.416 \quad (30)$$

where CMDEP(I,ID) = center depth of deposition of particle size class I at distance DIST(ID) (cm)

AMDEP(I,ID) = average depth of particle size class I deposited at distance DIST(ID) (cm)

Aggregate Deposition Variables

Calculations of muds and cuttings deposition are based on three particle size classes of muds and three somewhat different size classes of cuttings (Table B-2). The rest of the model, however, requires information in only two particle size classes, silt-clay (< 64 μm) and sand (≥ 64 μm). Workshop participants did not feel that these two size classes would adequately represent deposition behavior and, therefore, retained the size classes in Table B-2 for deposition calculations. Deposition variables are aggregated into the silt-clay and sand size classes for use by the rest of the model.

Chromium, Barium, and Hydrocarbon Concentrations

Concentrations of chromium, barium, and hydrocarbons in material from the bulk mud discharge are calculated by assuming they are partitioned among size classes in proportion to the amount of material in each particle size class. The model will, however, allow chromium, barium, and hydrocarbons to be selectively partitioned among size classes (e.g., proportionately more associated with small particles due to greater surface area) if such data are available.

The total amounts of chromium, barium, and hydrocarbons in a single bulk mud discharge are calculated as:

$$TBA = BACONC * DISVOL * (158.98 / 1000.0) * BASOL \quad (31)$$

$$TCR = CRCONC * DISVOL * (158.98 / 1000.0) * PCRSOL$$

$$THY = (HYCONC / 1000.0) * (DISVOL * 158.98 * 1000.0) * (PWAT * 1.025 + [(1.0 - PWAT) * DENS(2)]) * PHYSOL$$

where TBA = total barium in a bulk mud discharge (g)

DISVOL = discharge volume (bbl)

BACONC = barium concentration in the whole mud (mg/l)

BASOL = proportion of barium associated with the settleable solids in the mud plume (as opposed to the very fine-grained solids and the soluble phase in the surface-upper plume)

TCR = total chromium in a bulk mud discharge (g)

CRCONC = chromium concentration in the whole mud (mg/l)

PHYSOL = proportion of hydrocarbons associated with settleable solids in the mud plume

THY = total hydrocarbons in a bulk mud discharge (g)

HYCONC = concentration of hydrocarbons (No. 2 fuel oil) in the drill mud on a mass per mass whole mud basis (mg/g)

PWAT = proportion of discharge that is water

DENS(2) = density of solids in bulk mud discharge (g/cm^3)

PCRSOL = proportion of chromium associated with settleable solids in the mud plume

The amounts of chromium and hydrocarbons associated with each size class of materials in the bulk mud discharge are:

$$CRMUD(I) = TCR * PCR(I) \tag{32}$$

$$HYMUD(I) = THY * PHY(I)$$

where CRMUD(I) = chromium associated with material in particle size class I (g)

TCR = total chromium in a bulk mud discharge (g)

PCR(I) = proportion of chromium associated with size class I

HYMUD(I) = hydrocarbons associated with material in particle size class I (g)

THY = total hydrocarbons in a bulk mud discharge (g)

PHY(I) = proportion of hydrocarbons associated with size class I

The variables CRMUD(I) and HYMUD(I) are aggregated into the silt-clay and sand size classes, and concentrations in discharged material are calculated as:

$$CR(1,2) = CRSILT / TSILT \tag{33}$$

$$CR(2,2) = CRSAND / TSAND$$

$$HY(1,2) = HYSILT / TSILT$$

$$HY(2,2) = HYSAND / TSAND$$

where CR(ISC,2) = chromium concentration in deposited material (ppm)

HY(ISC,2) = hydrocarbon concentration in deposited material (ppm)

ISC = 1 denotes silt-clay, ISC = 2 denotes sand

CRSILT = total chromium associated with silt-clay size particles (g)

TSILT = total amount of silt size particles in bulk mud discharge (mt)

CRSAND = total chromium associated with sand size particles (g)

TSAND = total amount of sand size particles in bulk mud discharge (mt)

HYSILT = total hydrocarbons associated with silt-clay size particles (g)

HYSAND = total hydrocarbons associated with sand size particles (g)

Upper and Surface Plumes

When bulk mud discharges are made, an upper plume at the trap depth and a surface plume, both containing very fine-grained particles and some liquid fractions of the discharge, may shear off from the mud plume. Two indicators are calculated for these plumes: a solids dispersion ratio for the surface plume and a soluble fraction dilution ratio for the upper plume.

The upper plume has a thickness of the lesser of 20 m and the depth of the water column, and a width at distance DIST(ID) of:

$$UPWIDE(ID) = 2.0 * [(2.0 * DCOEF * TDIST) ** 0.5] \quad (34)$$

where UPWIDE(ID) = upper plume width at distance DIST(ID) (m)

DCOEF = diffusion coefficient (m/sec)

TDIST = time for upper plume to reach distance DIST(ID) (sec)

The volume of liquids discharged by the time the upper plume reaches distance DIST(ID) is:

$$DVOL(ID) = [(DRATE * 0.159) / (60.0 * 60.0)] * PWAT * PUPPER * [AMIN1(TDIST,DISP)] \quad (35)$$

where DVOL(ID) = volume of liquids discharged by the time the upper plume reaches distance DIST(ID) (m^3)

PWAT = proportion of liquid in the discharge

PUPPER = proportion of liquid fraction in upper plume

TDIST = time for upper plume to reach distance DIST(ID) (sec)

DRATE = rate of discharge (bbl/hr)

The soluble fraction dilution ratio is calculated as:

$$SBLDIL(ID) = PVOL(ID) / DVOL(ID) \quad (36)$$

where SBLDIL(ID) = soluble dilution ratio at distance DIST(ID)

PVOL(ID) = plume volume at distance DIST(ID) (m^3)

DVOL(ID) = volume of liquids discharged by the time the upper plume reaches distance DIST(ID) (m^3)

The solids dispersion ratio (suspended solids in discharge/suspended solids in surface plume) is calculated from a multiple regression using transport time and the inverse of discharge rate as independent variables:

$$DISPR(ID) = [10. ** C(1)] * [(1.0 / DRATE) ** C(2)] * [(TDIST / 60.0) ** C(3)] \quad (37)$$

where DISPR(ID) = solids dispersion ratio at distance DIST(ID)

DRATE = discharge rate (bbl/hr)

TDIST = time to reach distance DIST(ID) (sec)

C(1),C(2),C(3) = regression coefficients

This regression was derived from measured dispersion ratios from wells in the Gulf of Mexico, Tanner Bank, and the mid-Atlantic, summarized in Petrazzuolo (1981:Table 6-4). The squared correlation coefficient (R^2) for this regression is 0.74. For Case 3, where the surface plume, upper plume, and the mud cloud overlap, the dispersion ratio is computed for each class of mud particles from an entrainment factor and a settling factor. The settling factor is calculated as:

$$SF = 1.0 - [AMIN1 ([DIST(ID) / DDISTM(I)],1.0)] \quad (38)$$

where SF = settling factor

DIST(ID) = distance from the rig (m)

DDISTM(I) = distance of deposition of particle size class I from initial settling point (m)

The entrainment factor is:

$$EF = PVOL(ID) / (DVOL(ID) * [(1.0 - PWAT) / PWAT]) \quad (39)$$

where EF = entrainment factor

PVOL(ID) = plume volume at distance DIST(ID) (m^3)

DVOL(ID) = volume of liquids discharged when plume reaches distance DIST(ID) (m^3)

PWAT = proportion of liquid in discharge

The solids dispersion ratio for each particle size class is:

$$DISPR3(I,ID) = EF / SF \tag{40}$$

where DISPR3(I,ID) = dispersion ratio for particle size class I at distance DIST(ID)

EF = entrainment factor

SF = settling factor

Deposition on Sample Transect

The calculations described above define the characteristics of a single discharge event. These calculations are made for cuttings on any day a discharge occurs and for muds on days when a discharge occurs and the current is in the direction of the sample transect. A discharge event occurs if the current simulation day is within the time period of drilling specified as model input and if the current day is consistent with the specified frequency of discharge; that is, if:

$$IMOD = 0 \tag{41}$$

where IMOD = MOD [(ITIME - IBEG), IFREQ]

MOD = modulus function

ITIME = current simulation day

IBEG = day on which drilling begins

IFREQ = frequency of discharge (days)

Deposition of discharged materials on the sample transect is determined from current rosette data for the geographic area of interest. The proportion of time that the current flows in the direction of the sample transect (CFREQ) is input to the model. The model generates a uniformly distributed random number between 0 and 1. If this number is less than or equal to the input current frequency, the discharged material is assumed to fall on the transect. If this is the case on the current simulation day, deposition-related variables used by the rest of the model are set equal to the variables calculated above; otherwise, they are set equal to zero.

LIMITATIONS AND SENSITIVITIES

This submodel represents an attempt to incorporate many of the key factors influencing the fate of discharged drilling materials, while maintaining relative computational simplicity. A number of the more important simplifying assumptions are described below.

Deposition of cuttings is assumed to follow a circular normal probability density function. As such, it is independent of any seasonal variability in current direction. This may not be a bad assumption for larger cuttings particles with settling rates that are fast relative to current velocity, but it is less reasonable for predicting the exact location of deposition of the smaller cuttings particles, especially in deep water.

Diffusion coefficients that specify growth of the upper plume and the mud cloud as they are carried downcurrent are functions of the horizontal length scale of the cloud. These coefficients should more explicitly account for

effects of current velocity. These current velocity functional relationships are not now available, but investigators are examining the use of autocorrelation of current meter data to better estimate diffusion coefficients.

Although discharged materials represent a continuum of particle sizes, they are aggregated, for modeling purposes, into three size classes of cuttings and three size classes of drilling mud in order to reduce the number of calculations required. The settling rate of each size class is calculated as a function of its average particle size. This can result in a "bumpy" pattern of deposition moving away from the discharge point, with each bump representing a different particle size class. Increasing the number of size classes would bring the model results closer to a smooth pattern of deposition, decreasing in depth with increasing distance from the discharge point. The degree to which this simplified deposition behavior influences estimation of biological effects is unknown.

The frequency with which predominant currents cause discharged material to be deposited on the sample transect is determined from current rosette data for the geographic area of interest. However, the application of that frequency in the model is completely random throughout the year. As such, organisms on the sample transect may be subjected to burial events throughout the year in the model. In reality, these events might be restricted to certain seasons for a given transect. If this problem is significant, the model could be changed such that current direction and velocity are specified on a seasonal or monthly basis. A related issue, which proved too complex to be incorporated in this model, is the variation in current direction with depth. For example, surface currents in the western Gulf of Mexico may be predominantly in a southwesterly direction at 31 cm/sec in December, while bottom currents may be in a southerly direction 45% of the time at 8 cm/sec and in a northerly direction 36% of the time at 14 cm/sec due to tidal influence. The deposition of discharged materials under these conditions might be very different from that predicted by the model, which assumes a unidirectional current throughout the water column. The model does, however, incorporate daily variation in velocity

and makes an attempt to address some of the variation in current velocity with depth by using a surface and a bottom current velocity and assuming a linear change between these velocities with depth.

These limitations could be addressed by making the present model more complex. The Offshore Operators Committee model (Brandsma et al. 1980, 1983) is an example of a complex model that more explicitly represents many of these relationships. The objective of this project, however, was to build simple submodels that would still produce results that were reasonable enough to examine how discharge and fate dynamics were coupled to biological effects.

We have not undertaken a formal sensitivity analysis of this deposition model. However, analyses of other discharge models by some of the workshop participants suggest that the most sensitive parameters are likely to be: (1) bulk density of the discharge; (2) ambient density gradient; (3) current velocity; and (4) discharge velocity (volume rate/pipe area).

APPENDIX C. FORMULATION OF SEDIMENT REDISTRIBUTION SUBMODEL

The subgroup concerned with representing sediment dynamics began by classifying some of the spatial and temporal variability in conditions that might be encountered in the discharge of drilling muds and cuttings. This classification was developed along the dimensions of geographical regions, depth, sediment processes, and nature of substrate (Table C-1).

The submodel itself is based on an accounting of the net result of fluxes of sediment expressed as the thickness of sediment, SED(ID,IL,ISC,IT), as distinguished by distance from discharge point (ID), layer (IL), size class (ISC), and type (IT). The thickness of sediment includes a proportion of pore space represented by PSPACE(IT), assumed to be 0.5 for all sediment types. The submodel is capable of representing a large number of combinations of values of the variables in Table C-1; specific parameter estimates were developed only for four scenarios in order to explore model behavior.

CALCULATIONS

The first calculation is an initialization of the sediment composition of the top 5-cm layer to reflect the size distribution of natural sediment (Table C-2). This calculation is made only on the first day of simulation.

Table C-1. General factors influencing sediment dynamics.

Geographical regions	Depth of water (m)	Sediment process	Nature of substrate
High latitude (including ice processes) West Coast East Coast Western Gulf	0-5 5-30 30-80 80-180 > 180	<u>Ice</u> Ice rafting Ice scouring Sediment entrapment during ice formation <u>Water</u> Surface gravity waves Tides Inertial oscillations Shelf circulation Shelf waves Shelf-break phenomena Internal tides <u>Substrate</u> Bioturbation Auto-suspension	Size class distribution Origin of material and bedforms (biogenic, etc) Shear characteristics (including potential modification by biotic activity)

Table C-2. Size class distribution of natural sediment, SIZEN(ISC). Values are the fraction (volume/volume) of natural sediment in each size class.

Scenario	Size class	
	Silt-clay (ISC = 1)	Sand (ISC = 2)
1	0.45	0.55
2	0.2	0.8
3	1.0	0.0
4	0.9	0.1

Schedule of Disturbance Events

The disturbance environment of any site is represented in a particular scenario by the types of disturbance events (e.g., "Northern" storm, tide, and hurricane) associated with that area. The magnitude and timing of these events are variable. The model calculates the magnitude (in terms of cm of sediment disturbed) and timing (in terms of the beginning and ending days of the next occurrence of each type of event) from input data characterizing the distributions of magnitudes and intervals for each event type. The starting date, ISTART(IE); ending date, IEND(IE); and magnitude, AMP(IE), of the first occurrence of each event type are specified as initial conditions in the input data (Table C-3).

For each type of event, a check is made to determine if the current day of simulation, ITIME, is the day immediately following the last scheduled day of that event, IEND(IE). If this is the case, the next occurrence of that type of event is scheduled by updating ISTART(IE), IEND(IE), and AMP(IE). The new value of the starting day, ISTART(IE), is calculated by adding an interval, INT, to the old value of ISTART(IE). The value of the interval, INT, is determined by randomly sampling from normal distributions of the intervals between the first day of a given type of disturbance and the first day of the next occurrence. The means of these distributions, PMEAN(IE,IMONTH), vary by disturbance type and month (Table C-4), whereas the standard deviations, CHAR(IE,IVAR = 3), vary only by disturbance type (Table C-5). Some disturbance events (e.g., hurricanes) have mean intervals greater than or equal to a full year. For these events the mean interval, AMEAN(IE,IMONTH), and standard deviation of the interval, CHAR(IE,IVAR = 3), are specified in years rather than days. After rounding a randomly sampled value from these distributions to the nearest year, the value is multiplied by the number of days in a year to obtain the interval in days to the next occurrence. Thus, these low frequency events are assumed to always occur on the same day of the year if they occur at all in a given year. These events are distinguished by a switch, NYR(IE), that is set equal to one rather than to zero.

Table C-3. Initial conditions for sediment disturbance processes. Days represent days after start of simulation.

Scenario	IE	Disturbance type	Starting day ISTART(IE)	Ending day IEND(IE)	cm of sediment disturbed AMP(IE)
1	1	Storm (no ice entrapment of sediment)	255	257	5.0
	2	Storm (with ice entrapment of sediment)	308	309	3.0
	3	River discharge[a]	180	189	-0.5[a]
	4	Ice gouging	15	15	75.0
	5	Nominal surface gravity waves	1	1	0.3
2	1	"Northern" storm	1	2	7.0
	2	Tropical cyclone	271	272	4.7
	3	Tide	61	61	0.5
	4	Hurricane	241	241	17.5
	5	Nominal surface gravity waves	1	1	0.1
3	1	"Northern" storm	1	2	1.5
	2	Tropical cyclone	271	272	1.0
	3	Tide	61	61	0.2
	4	Hurricane	241	241	2.0
	5	Nominal surface gravity waves	1	1	0.04
4	0	None	---	---	---

[a]Represents net natural deposition rather, than disturbance.

Table C-4. Mean interval until next disturbance event for an event occurring in a given month, PMEAN(IE,IMONTH). Values are in days unless otherwise indicated. Values in parentheses are not actual events; i.e., they have no magnitude (AMEAN=0 cm) and are included only to facilitate generation of the actual event sequence.

Scenario	IE	Disturbance type	IMONTH(1 = JAN ...12 = DEC)											
			1	2	3	4	5	6	7	8	9	10	11	12
1	1	Storm (no ice entrapment of sediment)	(210)	(180)	(150)	(120)	(90)	(60)	(30)	(30)	30	300	(270)	(240)
	2	Storm (with ice entrapment of sediment)	(270)	(240)	(210)	(180)	(150)	(120)	(90)	(60)	(30)	(8)	8	6
	3	River discharge	(1)	(1)	(1)	(1)	(1)	1	1	(1)	(1)	(1)	(1)	(1)
	4	Ice gouging[a]	7	7	(7)	(7)	(7)	(7)	(7)	(7)	(7)	(7)	(7)	7
	5	Nominal surface gravity waves	1	1	1	1	1	1	1	1	1	1	1	1
2	1	"Northern" storm	6	6	8	10	(120)	(90)	(60)	(30)	(10)	10	8	6
	2	Tropical cyclone	(1)	(1)	(1)	(1)	(1)	(1)	(1)	(1)	1	1	(1)	(1)
	3	Tide	(30)	(1)	1	1	1	1	1	1	1	1	(90)	(60)
	4	Hurricane[a]	(5)	(5)	(5)	(5)	(5)	(5)	(5)	5	5	5	(5)	(5)
	5	Nominal surface gravity waves	1	1	1	1	1	1	1	1	1	1	1	1
3	1	"Northern" storm	6	6	8	10	(120)	(90)	(60)	(30)	(10)	10	8	6
	2	Tropical cyclone	(1)	(1)	(1)	(1)	(1)	(1)	(1)	(1)	1	1	(1)	(1)
	3	Tide	(30)	(1)	1	1	1	1	1	1	1	1	(90)	(60)
	4	Hurricane[a]	(5)	(5)	(5)	(5)	(5)	(5)	(5)	5	5	5	(5)	(5)
	5	Nominal surface gravity waves	1	1	1	1	1	1	1	1	1	1	1	1
4	0	None	--	--	--	--	--	--	--	--	--	--	--	--

[a]In years.

Table C-5. Other characteristics of disturbance events, CHAR(IE,IVAR).

Scenario	IE	Disturbance type	Variable, IVAR: 1-fraction of silt/clay size class affected	2-fraction of sand size class affected	3-standard deviation of interval between events	4-standard deviation of sediment disturbed (cm)	5-event length (day)
1	1	Storm (no ice entrapment of sediment)	1.0	1.0	3.0 day	2.0	3
	2	Storm (with ice entrapment of sediment)	1.0	1.0	0.5 day	1.0	2
	3	River discharge	1.0	1.0	0.0 yr	0.0	10
	4	Ice gouging	1.0	1.0	1.0 yr	10.0	1
	5	Nominal surface gravity waves	1.0	1.0	0.0 day	0.1	1
2	1	"Northern" storm	1.0	1.0	0.5 day	1.0	2
	2	Tropical cyclone	1.0	1.0	0.0 yr	1.0	2
	3	Tide	1.0	1.0	0.0 day	0.0	1
	4	Hurricane	1.0	1.0	2.5 yr	2.0	1
	5	Nominal surface gravity waves	1.0	1.0	0.0 day	0.1	1
3	1	"Northern" storm	1.0	1.0	0.5 day	0.1	2
	2	Tropical cyclone	1.0	1.0	0.0 yr	0.1	2
	3	Tide	1.0	1.0	0.0 day	0.0	1
	4	Hurricane	1.0	1.0	2.5 yr	2.0	1
	5	Nominal surface gravity waves	1.0	1.0	0.0 day	0.4	1
4	0	None	--	--	--	--	--

Some events do not occur at all during certain times of the year. However, sampling from truncated, normal populations (values less than 1.0 are set equal to 1.0) may inappropriately schedule an event in these periods. As described below, the magnitude of these events is always calculated as 0.0 during times of the year in which they are not expected to occur. In order to avoid unnecessary calls to the sampling subroutine, PMEAN(IE,IMONTH) is formulated to move ISTART(IE) quickly through months in which a particular event should not occur.

After determining the new starting day for the next occurrence of an event, the ending day, IEND(IE), is calculated by adding the length of that event, CHAR(IE,5), as given in Table C-5, to the starting day, ISTART(IE), and subtracting one. Thus, a 1-day event ends on the same day it starts.

The month of the year in which the next occurrence of the event will take place is calculated from the new value of ISTART(IE) in days. Next, the magnitude of the disturbance event, AMP(IE), in cm of sediment disturbed, is calculated by randomly sampling from truncated, normal distributions (values less than 0.0 are set equal to 0.0), defined by the mean magnitude of disturbance events occurring in particular months, AMEAN(IE,IMONTH), as given in Table C-6, and the standard deviation of the magnitude of each type of disturbance event, CHAR(IE,IVAR = 4), as given in Table C-5. In months when the event is not expected to occur [i.e., AMEAN(IE,IMONTH) = 0.0], the magnitude of the event, AMP(IE), is set equal to 0.0.

The sampling calculations described above are executed independently for the different types of disturbance events. The amount of disturbance on a given day, STR(ID), is assumed to equal the dominant event [with the largest value of AMP(IE) occurring on that day].

Table C-6. Mean magnitude of disturbance events, AMEAN(IE,IMONTH), in cm.

Scenario	IE	Disturbance type	IMONTH(1=JAN ...12=DEC) 1	2	3	4	5	6	7	8	9	10	11	12
1	1	Storm (no ice entrapment of sediment)	0.0	0.0	0.0	0.0	0.0	0.0	0.0	0.0	5.0	5.0	0.0	0.0
	2	Storm (with ice entrapment of sediment)	0.0	0.0	0.0	0.0	0.0	0.0	0.0	0.0	0.0	0.0	3.0	3.0
	3	River discharge[a]	0.0	0.0	0.0	0.0	0.0	-0.5	-0.5	0.0	0.0	0.0	0.0	0.0
	4	Ice gouging	75.0	75.0	0.0	0.0	0.0	0.0	0.0	0.0	0.0	0.0	0.0	75.0
	5	Nominal surface gravity waves	0.3	0.3	0.3	0.3	0.3	0.5	0.5	0.5	0.5	0.3	0.3	0.3
2	1	"Northern" storm	7.0	7.0	4.7	3.5	0.0	0.0	0.0	0.0	0.0	3.5	4.7	7.0
	2	Tropical cyclone	0.0	0.0	0.0	0.0	0.0	0.0	0.0	0.0	4.7	4.7	0.0	0.0
	3	Tide	0.0	0.0	0.5	0.5	0.5	0.5	0.5	0.5	0.5	0.5	0.0	0.0
	4	Hurricane	0.0	0.0	0.0	0.0	0.0	0.0	0.0	17.5	17.5	17.5	0.0	0.0
	5	Nominal surface gravity waves	0.1	0.1	0.1	0.1	0.1	0.1	0.1	0.1	0.1	0.1	0.1	0.1
3	1	"Northern" storm	1.5	1.5	1.0	0.75	0.0	0.0	0.0	0.0	0.0	0.75	1.0	1.5
	2	Tropical cyclone	0.0	0.0	0.0	0.0	0.0	0.0	0.0	0.0	1.0	1.0	0.0	0.0
	3	Tide	0.0	0.0	0.2	0.2	0.2	0.2	0.2	0.2	0.2	0.2	0.0	0.0
	4	Hurricane	0.0	0.0	0.0	0.0	0.0	0.0	0.0	2.0	2.0	2.0	0.0	0.0
	5	Nominal surface gravity waves	0.04	0.04	0.04	0.04	0.04	0.04	0.04	0.04	0.04	0.04	0.04	0.04
4	0	None	--	--	--	--	--	--	--	--	--	--	--	--

[a]Represents net natural deposition, rather than disturbance.

Resuspension and Replacement

If the topography of the bottom has not been altered, the resuspension caused by disturbance events is generally assumed to result in no net change in the total amount of sediment (measured as thickness in cm) at a given plot. Rather, the multiple, individual resuspensions associated with a disturbance event are conceptualized as removing a given thickness of sediment at the plot and replacing that thickness with natural sediment. In all the model runs described in the report, natural sediment is assumed to have constant properties (e.g., size class composition and chromium concentration). Some long term effects of discharge might be represented by altering the properties of "natural" or background sediment in an area over time.

There are several ways in which a change in total sediment height may result from a disturbance event: (1) when the topography of the bottom has been altered, the amounts of sediment removed and replaced are adjusted as a function of the altered topography (e.g., a thick pile erodes more quickly than a thin pile); (2) when the size class distribution of the plot differs from that of natural sediment and the disturbance event is specified as differentially affecting the two size classes; (3) during ice formation when some fraction of the resuspended material is entrapped or frozen in the ice; and (4) in a hurricane or ice scour event when leveling may occur. Leveling due to hurricane and ice scour events is calculated and described separately from the resuspension process.

After updating the schedule of events as described in the previous section, the main calculations are done for each of the 1-m^2 plots along the transect. First, the magnitude of the disturbance event, STR, is adjusted as a function of altered topography at a plot:

$$SOUT(ID) = STR * [1.0 / (1.0 - [TOTHT(ID) / BBLY])] \qquad (42)$$

where SOUT(ID) = adjusted magnitude of disturbance event (cm of sediment removed)

STR = magnitude of disturbance event (cm)

TOTHT(ID) = net accumulated thickness of sediment at a plot (cm)

BBLY = thickness of reference bottom boundary layer (cm)

Equation 42 increases the thickness of sediment removed as the thickness of the sediment "pile" at a plot, TOTHT(ID), becomes a larger fraction of a reference boundary layer, BBLY, which is assumed to be 200 cm. When the topography of the bottom is not altered from the initial conditions [i.e., TOTHT(ID) = 0.0], the adjusted thickness of sediment removed is the same as the nominal value of the disturbance event, STR. As the thickness of the sediment "pile" approaches the thickness of the reference layer, BBLY, the multiplicative adjustment approaches infinity. Thus, the value of SOUT(ID) is bounded at a maximum thickness of sediment removed, SMAX, which is assumed to be 100 cm. This adjustment in the thickness of sediment removed by a disturbance event (and the concomitant adjustment in replacement of sediment, described below) was developed as a simple approximation to the complex relationships through which alterations in bottom topography interact with waves and currents to determine sediment resuspension and transport.

The total sediment disturbed in each layer is calculated as follows:

$$FOUT(IL = 1) = AMIN1\ [SOUT(ID),\ HT(ID,1)] \tag{43}$$

$$FOUT(IL = 2) = AMIN1\ [SOUT(ID) - HT(ID,1),\ HT(ID,2)],\ \text{if}\ SOUT(ID) < HT(ID,1),$$

otherwise, FOUT(IL = 2) = 0.0

where FOUT(IL) = thickness of sediment removed by layer (cm)

SOUT(ID) = adjusted magnitude of disturbance event (cm of sediment removed)

HT(ID,IL) = total sediment by layer, always 5.0 for IL = 1 (cm)

The sediment removed from each sediment layer due to resuspension associated with a given disturbance event is calculated for each plot as follows:

$$SUBT(IL,ISC,IT) = FOUT(IL) * CHAR(IE,ISC) * [SED(ID,IL,ISC,IT) / HT(ID,IL)] \quad (44)$$

where SUBT(IL,ISC,IT) = loss of sediment of a particular type and size class (cm)

FOUT(IL) = thickness of sediment removed by layer (cm)

CHAR(IE,ISC) = fraction of sediment in a given size class affected by a given disturbance

SED(ID,IL,ISC,IT) = sediment present of a particular type and size class (cm)

HT(ID,IL) = total sediment present (cm)

The amount of sediment replacing the sediment removed in the resuspension process is adjusted from the nominal thickness of sediment disturbed as follows:

$$SIN(ID) = STR * (1.0 - [TOTHT(ID) / BBLY]) \quad (45)$$

where SIN(ID) = adjusted magnitude of disturbance event (cm of sediment replaced)

STR = magnitude of disturbance event (cm)

TOTHT(ID) = net accumulated thickness of sediment at a plot (cm)

BBLY = thickness of reference boundary layer (cm)

The sediment replaced to each sediment layer in the resuspension process is calculated as:

$$ADD(IL,ISC,1) = F(IL) * SIZEN(ISC) * CHAR(IE,ISC) \quad (46)$$

where ADD(IL,ISC,IT=1) = addition of sediment (cm, all natural type)

SIZEN(ISC) = fraction of natural sediment in each size class

When ice cover is forming (see Tables C-4 and C-6), the sediment replacement, ADD(IL,ISC,IT = 1), is reduced by a multiplicative factor, FGRAB, nominally set to 0.9.

Deposition from Drilling Operations

Each day, deposition from bulk mud discharges, DEPM(ID,ISC), and cuttings discharges, DEPC(ID,ISC), is provided in cm of sediment, including pore space, by plot and sediment size class, from the Discharge and Plume Fate submodel. These depositions are equated to the additions of the respective sediment types to the top layer of a given plot, ADD(IL = 1,ISC,IT = 2) and ADD(IL = 1,ISC,IT = 3).

Natural Deposition

Natural deposition is treated as a special type of event and designated by a value of NDEP equal to the index number, IE, of the event. The magnitude and scheduling of this type of event are handled as if it was a resuspension event, except that the mean magnitude, AMEAN(IE,IMONTH), is entered as a negative number. Thus, this event is never the dominant event in determining

the thickness of sediment disturbed, STR(ID). When a natural deposition event occurs, the sediment deposited [the absolute value of IAMP(IE = NDEP)] is multiplied by the size class fractions of natural sediment, SIZEN(ISC), and added to the sediment input of natural sediment to the top layer of a particular plot, ADD(IL = 1,ISC,IT = 1).

Natural deposition occurs only in Scenario 1 for 10 days in the late spring-early summer. It is intended to represent sediment deposition in shallow, near-coast areas during periods of high river discharge associated with snow and ice melting.

Leveling

Hurricanes are assumed to level the sediment to a slope not exceeding 10.0°. Ice scour events are assumed to reset sediment thickness and composition completely to natural conditions. Both of these are low frequency events; hurricanes occur, on the average, every 5 years and ice scour events occur, on the average, every 7-8 years.

Hurricanes (designated by a value of NHURR equal to the event index number) resuspend and replace a thickness of sediment, AMP(IE = NHURR), in the same manner as other disturbance events. In addition, sediment is removed from plots as necessary to bring the slope between adjacent plots to 10.0°. The calculation proceeds from the farthest plot (ID = 7) inward to the discharge point (ID = 1), assuming that sediment deposition is greater nearer the discharge point. The actual height difference between two plots is compared to the maximum allowable height difference calculated as the tangent of 10.0 times the distance between plots in cm. If the actual height difference is greater than the maximum allowable, sediment is removed from the innermost plot to bring the actual height difference down to the maximum allowable. The sediment to be removed is taken first from the top layer (IL = 1) and then from the bottom layer (IL = 2), if the amount to be removed exceeds the thickness of the top layer. The sediment to be removed is partitioned to size classes and added to the total loss of sediment at a plot as follows:

$$SUBT(IL,ISC,IT) = SUBT(IL,ISC,IT) + R(IL) * CHAR(IE=NHURR,ISC) * [SED(ID,IL,ISC,IT) / HT(ID,IL)] \quad (47)$$

where SUBT(IL,ISC,IT) = thickness of sediment lost (cm)

R(IL) = thickness of sediment loss required to reach slope of 10.0° (cm)

CHAR(IE=NHURR,ISC) = fraction of a size class affected by event

SED(ID,IL,ISC,IT) = thickness of sediment present (cm)

HT(ID,IL) = total thickness of sediment by layer (cm)

NHURR = index number (IE) of a hurricane event

The thickness of sediment removed, HLEV(ID), is calculated and saved to be used later to adjust the value of total sediment disturbed at each plot, as it will be passed to other submodels.

Ice scour events (designated by NSCOUR equal to the event index number) are assumed to reset the sediment to initial conditions (thickness of bottom layer equal to zero, composition of the top layer equal to that of natural sediment). Subsequent sections calculating net flux and re-establishing layers are skipped, and execution proceeds directly to the calculation of summary indicators. The total thickness of sediment removed in this resetting calculation is stored as the value SLEV(ID), to be used later in adjusting STIR(ID) as it is used by other submodels.

Net Flux

The net result of fluxes into and out of each sediment layer is used to update the sediment composition of each plot as follows:

$$SED(ID,IL,ISC,IT) = SED(ID,IL,ISC,IT) + ADD(IL,ISC,IT) - SUBT(IL,ISC,IT) \quad (48)$$

where SED(ID,IL,ISC,IT) = sediment present (cm)

ADD(IL,ISC,IT) = sediment added to a plot (cm)

SUBT(IL,ISC,IT) = sediment removed from a plot (cm)

A resulting thickness is calculated for each layer, HT(ID,IL), by summing over size classes and types of sediment.

Re-establishing Layers

Next, it is necessary to re-establish the thickness of the top layer at 5.0 cm. Three cases are distinguished:

(1) The top layer is greater than 5.0 cm, in which case sediment is moved down from the top layer to the bottom layer.

(2) The top layer is less than 5.0 cm and the deficit is available from the bottom layer, in which case sediment is moved up from the bottom layer to the top layer.

(3) The top layer is less than 5.0 cm and the deficit is not all available from the bottom layer, in which case all the sediment from the bottom layer and some underlying natural sediment are moved up to the top layer.

The case and total amount of sediment that needs to be moved are determined by comparing the thickness of the top layer, HT(ID,IL = 1), to 5.0 cm and by comparing the difference between HT(ID,IL = 1) and 5.0 cm to the bottom layer, HT(ID,IL = 2). Both layers are assumed to be well-mixed. Thus, the fractional composition of sediment moved is identical to that of the layer from which it is moved (underlying natural sediment all being of type IT = 1,

with the size class distribution specified in SIZEN(ISC). After establishing the amount and composition of sediment to be moved from each layer in a particular case, the donating layer of SED(ID,IL,ISC,IT) is decremented by size class and type and the receiving layer is incremented. If sediment is moved up from the underlying natural sediment, the thickness moved up is accumulated in HOLE(ID) in order to allow calculations of net changes in total thickness. The thickness of each layer, HT(ID,IL), is recalculated following the re-establishment of a 5.0-cm top layer by summing over size classes and types.

Summary Indicators

The cumulative, net change in sediment thickness, TOTHT(ID), is calculated as the sum of the thickness of the variable second layer less any thickness moved up from the underlying natural sediment, HOLE(ID). The proportion of sand in the current day's deposition, PSDEP(ID), is calculated as the sum of the thickness of the sand size class (ISC = 2) of natural, bulk mud discharge and cuttings discharge types, divided by the total thickness of the current day's deposition. A similar calculation is made for the proportion of sand in the top 5.0-cm sediment layer, PSSED(ID). If there is no deposition at a given plot, PSDEP(ID) is set equal to PSSED(ID). The actual thickness of sediment disturbed at each plot, STIR(ID), is calculated as the greater of the sediment disturbance associated with that day's event [i.e., the value of SOUT(ID)] and the thickness of sediment removed at a given plot by any leveling event occurring that day [i.e., HLEV(ID) or SLEV(ID)].

Concentrations of barium, chromium, and hydrocarbons in the top sediment layer at each plot [BASED(ID), CRSED(ID), and HYSED(ID), respectively] are calculated as weight/weight concentrations in parts per million (ppm). The calculation for chromium concentration is:

$$CRSED(ID) = \frac{\sum_{ISC} \sum_{IT} SED(ID,1,ISC,IT) * DENS(IT) * PSPACE(IT) * CR(ISC,IT)}{\sum_{ISC} \sum_{IT} SED(ID,1,ISC,IT) * DENS(IT) * PSPACE(IT)} \quad (49)$$

where CRSED(ID) = chromium concentration in top sediment layer (ppm, mg/kg)

SED(ID,IL=1,ISC,IT) = sediment thickness of top layer (cm)

DENS(IT) = sediment density (g/cm^3)

PSPACE(IT) = proportion of volume that is pore space, by sediment type

CR(ISC,IT) = sediment chromium concentrations (ppm, mg/kg)

The calculations for BASED(ID) and HYSED(ID) are similar, with the replacement of CR(ISC,IT) by BA(ISC,IT) and the replacement of CR(ISC,IT) by HY(ISC,IT). A similar calculation is made for the hydrocarbon concentration in the current day's deposition, based on the thicknesses of various types of deposition, rather than the thickness of the top layer.

The fraction whole mud (volume/volume) in the top sediment layer of each plot is calculated as follows:

$$BFWM(ID) = 10^6 * [SED(ID,1,1,2) + SED(ID,1,2,2)] / HT(ID,1) \quad (50)$$

where BFWM(ID) = fraction of mud-discharged sediment type (IT=2) in top sediment layer (ppm, volume/volume)

SED(ID,IL,ISC,IT=2) = sediment thickness (cm)

HT(ID,IL=1) = total thickness of top sediment layer (cm)

PARAMETER ESTIMATION

Parameters characterizing the disturbance regime and size distribution of natural sediment (Tables C-3 and C-4 through C-6) were initially estimated by workshop participants. Some adjustments were made in response to examination of preliminary model results and comments on a draft report. The parameterization was accomplished by reference to field observations of current velocities and sediment composition, especially for Gulf of Mexico sites; however, the parameter values should not be interpreted as representing a specific location.

Chromium concentrations (mg/kg) of both size classes of natural sediments are set to 5.0 ppm in Scenario 1 and to 40.0 ppm in Scenarios 2-4. Petrazzuolo (1983) summarized several field studies of the effects of discharged drilling materials on sediment composition. Background chromium concentrations in studies on the Mustang Island Lease Area of the South Texas Outer Continental Shelf ranged from 19.6 to 40.9 ppm at a site in Block 755 and had a mean value of 49.5 ppm at a site in Block 792 (U.S. Department of the Interior 1976a,b, as summarized in Petrazzuolo 1983). The value of 5.0 ppm for Scenario 1 was chosen, based on a predischarge chromium concentration of 5.2 ppm in the sediments at the Challenge Island #1 site in the Beaufort Sea (Sohio Alaska Petroleum Company 1981, as summarized in Petrazzuolo 1983). A background barium concentration of 300 ppm (mg/kg) is used for natural sediment in all scenarios. Concentrations of barium and chromium in the material from the cuttings discharge are assumed to be equal to natural sediment concentrations; concentrations in the material discharged in the bulk mud discharge are calculated in the Discharge and Plume Fate submodel. Concentrations of hydrocarbons (as might correspond to the No. 2 oil used to determine relative toxicity) were assumed to be zero in natural sediments. Hydrocarbon concentrations in discharged material are calculated by the Discharge and Plume Fate submodel.

LIMITATIONS

Compared to the Benthic Community Effects submodel, the Sediment Redistribution submodel executes a large number of calculations each day and has a large number of variables (distinguishing between sediments based on distance from discharge point, layer, size class, and type). However, the calculations are conceptually simple in that they basically consist of accounting for movements of the different kinds of sediment individually and keeping a running total.

Parameterization

Representing the disturbance regime in terms of distributions of intensity and timing of events characterized directly as a thickness of sediment resuspended is a compromise. A mechanistic formulation relating movement of sediment to current velocities and sediment characteristics was judged to be too complex in terms of functional form and data requirements. Nonetheless, the data requirements of the simpler approach are still large. Furthermore, the parameters that need to be estimated are quite synthetic in the sense that the net result of a large number of complicated processes is implicit in a single value. As a result, a considerable amount of experience and professional judgement is required to estimate the parameters accurately.

Leveling and Erosion

In the model, alterations in bottom topography (e.g., a mound or "pile") modify the thickness of sediment removed and replaced by a given disturbance event. The thickness of sediment removed increases and the thickness of sediment replaced decreases as nonlinear functions of the fraction of a fixed bottom boundary that is taken up by the thickness of the sediment mound. Although qualitatively reasonable, this formulation is a simple approximation of much more complex interactions.

Sediment removal during a hurricane is calculated to achieve a maximum slope of 10.0° between transect plots, starting with the plot farthest from the discharge point. This approach is a rough approximation if the distances between transect plots are different or if sediment deposition does not monotonically decrease with increasing distance from the discharge point.

Resolution

The sediment calculations are based on two, well-mixed layers (a top layer fixed at 5.0 cm and a variable thickness bottom layer). This is a strongly simplifying assumption about the complex layering and mixing phenomena that most likely occur in the real world. A larger number of thinner layers could be utilized. This would, however, result in very substantial increases in the complexity of the calculations and would necessitate some way of representing the exposure of benthic organism as integrated over those layers.

The model is currently programmed using "singe-precision" calculations. Numerical error, or "round-off", can result in an error of around 1 ppm when adding the various fractions of the top 5.0-cm layer. This error did not seem to justify the use of "double-precision" calculations in the context of the other uncertainties in the model formulation.

APPENDIX D. FORMULATION OF BENTHIC COMMUNITY EFFECTS SUBMODEL

BURIAL

Formulation

The approach developed for burial mortality was strongly influenced by a background paper prepared by Maurer (1983) for the workshop. In his review, Maurer found little direct research on the effects of burial of marine fauna by drilling muds and cuttings. He suggested, however, that the substantial body of research on the effects of dredge material be used to estimate effects caused by burial with drilling muds and cuttings. The consensus of the participants in this group was to base the submodel on dredge material disposal research, realizing that there may be important chemical and physical differences between drilling muds and cuttings and dredge materials. Thus, both the structure and the parameters used in the burial portion of the submodel represent working hypotheses.

The major difficulty in developing the Benthic Community Effects submodel was to adequately represent the extreme variability in the response of marine benthos to burial. While some organisms are unable to survive burial of even a few centimeters, others show a surprising ability to migrate vertically and escape burial of a meter or more. The experimental work of Maurer et al. (1978, 1981, 1982a,b, in press) and the review of Maurer (1983) suggested that burial response may be influenced by the following factors:

(1) Morphology of the organism;

(2) Life history and behavior of the organism;

(3) Depth of burial;

(4) Type of sediment deposited;

(5) Duration of burial;

(6) Water temperature or season; and

(7) Chemical conditions.

Some of these factors appear to act synergistically, and their interactions are poorly understood. Subgroup participants felt there was insufficient information currently available to quantitatively describe, and link, the effects of all of the factors in the submodel. The approach adopted was to structure the submodel to:

(1) Be flexible enough to be modified to reflect the morphological and behavioral adaptations characteristic of communities in widely different environments;

(2) Explicitly represent the general relationship that burial mortality increases with burial depth; and

(3) Explicitly account for the general relationship that burial mortality increases as the particle size distribution of deposited materials diverges from that of the animal's natural habitat.

The relationships between mortality and depth of burial and between mortality and sediment type were emphasized because they are both consistently observed in burial experiments and directly relevant to the assessment of drilling mud effects. During the workshop, the subgroup participants attempted

to represent the effects of burial duration by including time lags in burial-induced mortality. While there is experimental evidence to support this assertion, this approach was subsequently discarded and replaced with the assumption that all mortality is incurred on the day of burial. This assumption was made because of uncertainty about how the mortality would be distributed over future days, especially under variable conditions (e.g., additional burial events).

Calculations

In the model, both natural and drilling-related sediment deposits may bury benthic communities and result in the death of a proportion of the existing community. The number of animals killed is subtracted from the previous total to update current density estimates for each indicator community. Within the submodel, mortality rates are estimated for each community based on burial depth, whether the deposited material is "natural" or "exotic", and on an estimate of the relative sensitivity of the benthic community to burial. The relationship between burial depth and mortality is expressed as:

$$BMOR(IC,ID) = f[DDEP(ID)] \tag{51}$$

where BMOR(IC,ID) = the proportion of animals killed

DDEP(ID) = the depth of deposited sediment (cm)

f = piecewise linear functions depicted in Figures D-1 through D-3

These mortality curves (Figures D-1 through D-3) provide the key parameters for the burial calculations. Thus, their development is a crucial factor in determining the accuracy and reliability of any model application. The mortality curves are input by model users, highlighting the need to develop specific curves for individual model applications.

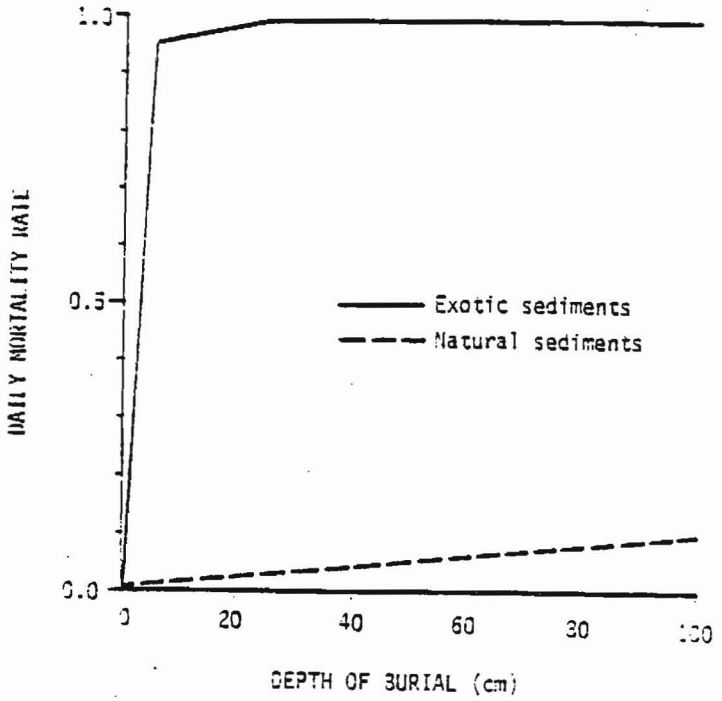

Figure D-1. Mortality rates for meiofaunal assemblage as a function of depth of burial

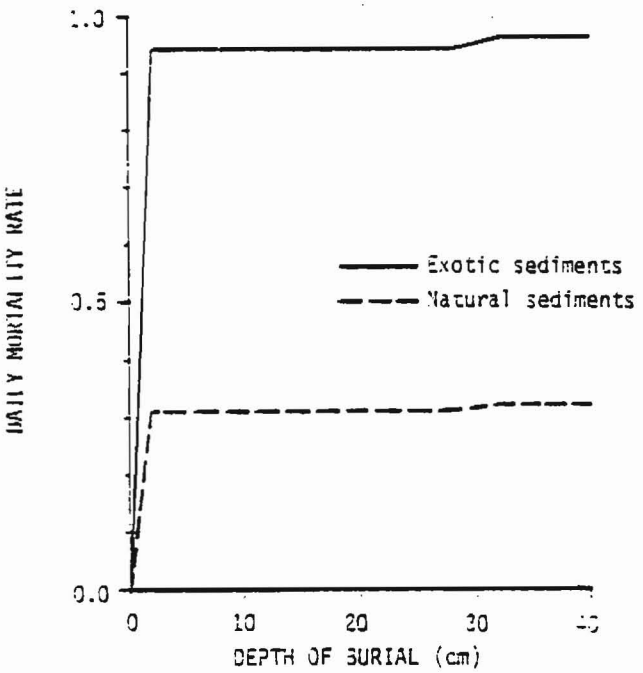

Figure D-2. Mortality rates for pioneer macrofaunal assemblage as a function of depth of burial.

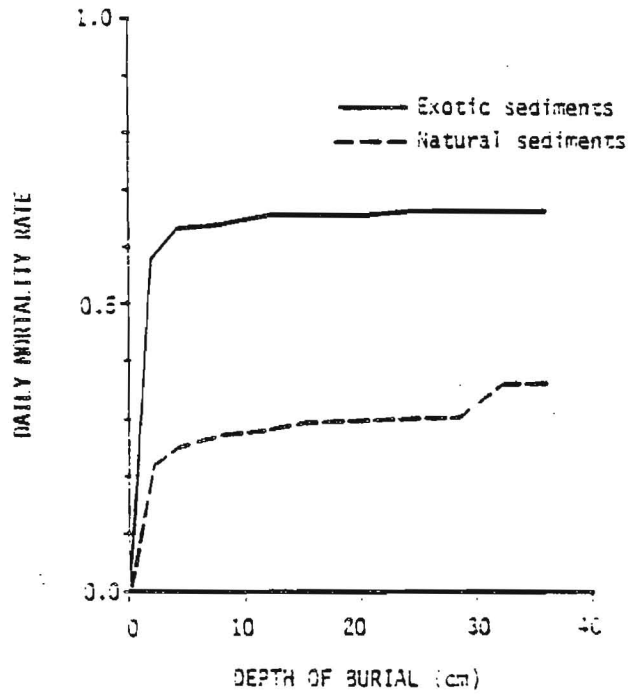

Figure D-3. Mortality rates for late successional macrofaunal assemblage as a function of depth of burial. Figure D-3 is identical to Figure 10.

The mortality relationships in Figures D-1 through D-3 were developed at the workshop as general cases for use in model testing. They were not intended to represent a specific site, but it was hoped they would provide reasonably general descriptions of the burial mortality relationships for the three indicator communities. Development of the curves required complicated sets of assumptions, which are important to understanding model results. Also, assumptions used by participants may provide guidance for future model users. The mortality curves for meiofauna (Figure D-1) were estimated by workshop participants. No applicable data sources were identified for use in constructing these curves.

Curves for the pioneer and late succession macrofauna were based on a series of assumptions, illustrated in Figures D-4 through D-7. First, the percentage of the total community represented by major taxonomic groups was

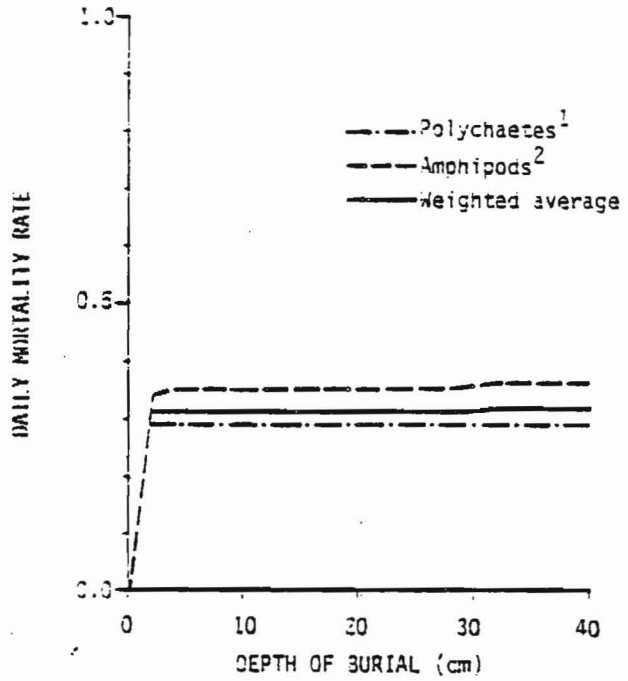

1. Community assumed to be 60% polychaetes. Data are from experiments on Scoloplos fragilis presented in Maurer et al. (1978:Table 21; 15-day tests in 100% sand).

2. Community assumed to be 40% amphipods. Data are from experiments on Parahaustorius longimerus presented in Maurer et al. (1978:Table 23; 15-day tests in 100% sand).

Figure D-4. Derivation of estimated mortality curve for pioneer macrofaunal assemblage buried by "natural" sediments.

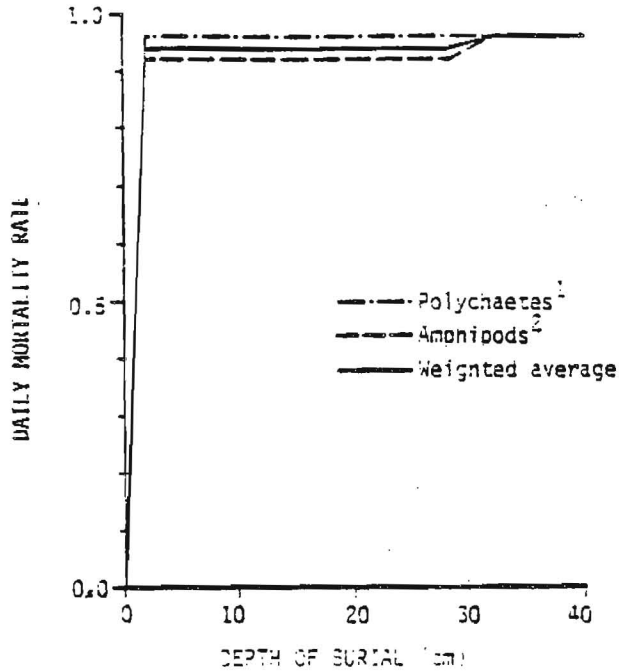

1. Community assumed to be 60% polychaetes. Data are from experiments on Scoloplos fragilis presented in Maurer et al. (1978:Table 21; 15-day tests in 92-99% silt-clay).

2. Community assumed to be 40% amphipods. Data are from experiments on Parahaustorius longimerus presented in Maurer et al. (1978:Table 23; 15-day tests in 79-83% sand).

Figure D-5. Derivation of estimated mortality curve for pioneer macrofaunal assemblage buried by "exotic" sediments.

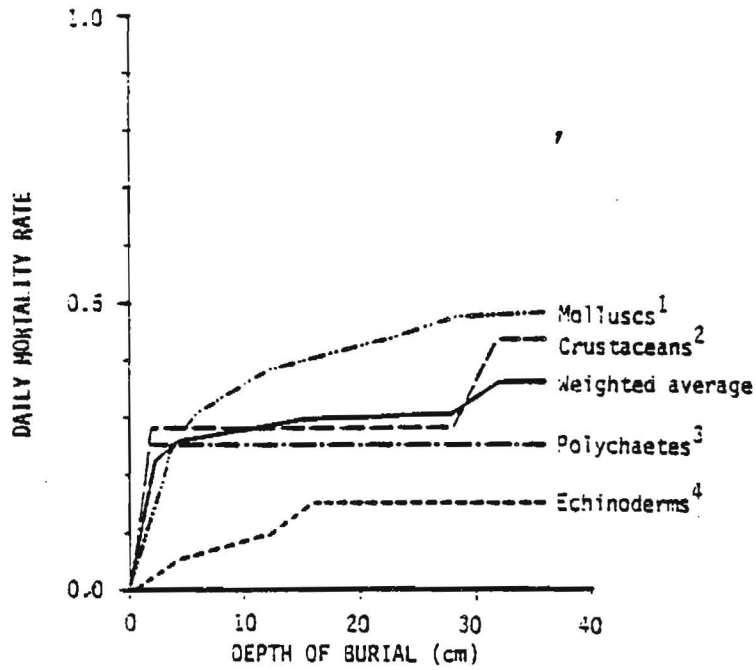

1. Community assumed to be 20% molluscs. Data are from experiments on Mercenaria mercenaria presented in Maurer et al. (1978:Table 20; 15-day tests in 92-99% silt-clay).

2. Community assumed to be 35% crustaceans. Data are from experiments on Neopanope sayi presented in Maurer et al. (1978:Table 18; 8-day tests in 54-55% silt-clay).

3. Community assumed to be 35% polychaetes. Data are from experiments on Nereis succinea presented in Maurer et al. (1978:Table 22; 15-day tests in 92-99% silt-clay).

4. Community assumed to be 10% echinoderms. Curve was estimated by workshop participants.

Figure D-6. Derivation of estimated mortality curve for late successional macrofaunal assemblage buried by "natural" sediments.

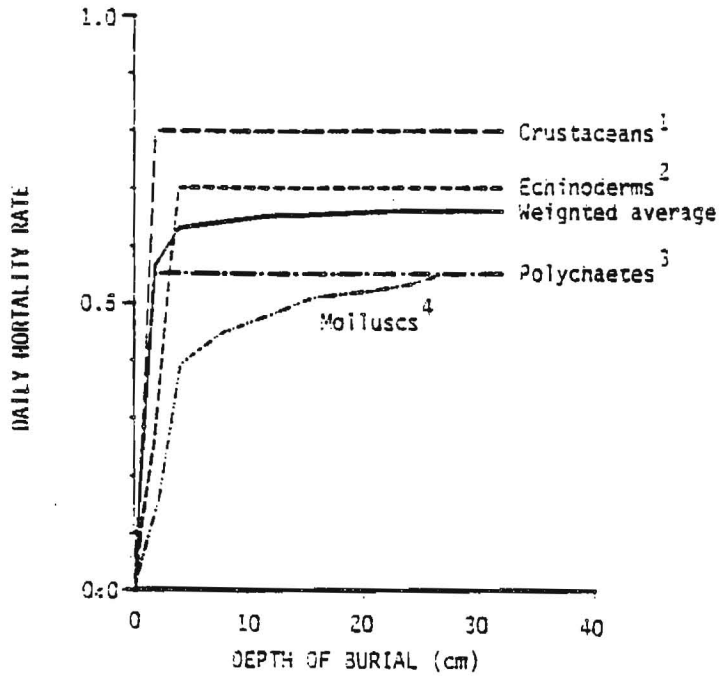

1. Community assumed to be 35% crustaceans. Data are from experiments on Neopanope sayi presented in Maurer et al. (1978:Table 18; 8-day tests in 100% sand).

2. Community assumed to be 10% echinoderms. Curve was estimated by workshop participants.

3. Community assumed to be 35% polychaetes. Data are from experiments on Nereis succinea presented in Maurer et al. (1978:Table 22; 15-day tests in 100% sand).

4. Community assumed to be 20% molluscs. Data are from experiments on Mercenaria mercenaria presented by Maurer et al. (1978:Table 20; 15-day tests in 100% sand).

Figure D-7. Derivation of estimated mortality curve for late successional macrofaunal assemblage buried by "exotic" sediments.

estimated. Indicator species for each taxonomic group were identified. Mortality curves for each species were then plotted, using experimental data presented by Maurer et al. (1978), based on work with dredge spoil material. Finally, a composite curve was derived, using a weighted average of the individual curves. All of the individual curves were based on 15-day burial experiments at summer water temperatures, except as noted in the footnotes to Figures D-4 through D-7. These 15-day experiments were considered the best indicator of the total mortality induced by a burial event, although the animals might persist for some time after burial.

As noted in Figures D-1 through D-3, separate mortality curves are used to depict each indicator community's response to "natural" or "exotic" sediments. This is required because sediment type is assumed to influence burial mortality nonlinearly. A user-specified threshold value is used to select the appropriate curve at each time step in the simulation. The threshold is defined as the difference in particle size distribution (expressed as proportion sand) required to distinguish between "natural" and "exotic" sediments. Exact values for the threshold are not known; however, experiments by Maurer et al. (1978, 1981, 1982a,b) suggested that a change in particle size distribution of about 25.0% (i.e., increase or decrease in proportion sand content of 0.25) is sufficient to cause the dramatic increase in burial mortality. A value of 0.25 is used in the model runs presented here.

Mortality rates interpolated from the depth-mortality curves are adjusted by multiplying the resulting mortality rate by a user-specified estimate of relative community sensitivity (Table D-1). This factor, which essentially shifts the mortality curves upward or downward along the y axis, was included for possible use in the submodel because data may not be available to estimate mortality curves for all environments. The community sensitivity coefficients in Table D-1 represent participants' estimates of the greater sensitivity of continental shelf and slope communities relative to the shallow water responses depicted in Figures D-1 through D-3.

Table D-1. "Community sensitivity" coefficients estimated by subgroup participants. Coefficients describe the relative sensitivity of shelf and slope communities in comparison to the shallow water communities described in Figures D-1 through D-3.

Community type/ sediment type	Community location		
	Shallow water	Shelf	Slope
Pioneer communities			
Natural sediment	1.0	4.0	6.0
Exotic sediment	1.0	8.0	12.0
Late successional communities			
Natural sediment	1.0	3.0	4.5
Exotic sediment	1.0	6.0	9.0

TOXICITY

Formulation

Following removal of animals due to burial, the Benthic Community Effects submodel computes additional mortality associated with the toxicity of deposited materials. This involves four primary steps:

(1) For each species assemblage, an acute toxicity relationship between daily survival and concentration of deposited materials is developed for a reference mud and provided as input to the model.

(2) The acute toxicity relationships are adjusted if the mud simulated in the model is other than the reference mud.

(3) The acute toxicity relationships are adjusted if the model communities are subjected to an exposure long enough to be considered chronic.

(4) Daily survival rates for the assemblages are determined from the adjusted toxicity relationships and the exposure concentration (provided by the Sediment Redistribution submodel) and are multiplied by the number of individuals present in each assemblage.

Calculations

Development of relationships between exposure and daily survival involves two very important choices. First, because composite toxicity data are not available for the three species assemblages considered in the model, a single species for which data are available is chosen to represent each assemblage. The model presently uses data for *Mysidopsis* sp. (an opossum shrimp) to represent the early successional macrofaunal assemblage and *Palaemonetes* sp. (a grass shrimp) to represent the late successional macrofaunal assemblage. Suitable data for a representative of the meiofaunal assemblage are not presently available. No output for the meiofaunal assemblage is presented here; however, the model can be used to examine the results of hypothetical toxicity relationships for meiofauna.

Second, toxicities vary considerably with both the type of mud and the part of the mud (e.g., whole mud, solids fraction, suspended particulate fraction, aqueous fraction) used in the exposure. The model presently uses data developed from whole mud exposures. While solids fraction data might approximate the kind of exposure being simulated in the model more closely, such data were not available for *Palaemonetes*. In order to facilitate comparisons between scenarios, a whole mud with an oil content of 0.0678 ppt is used in the scenarios described in this report. All of these data can be easily changed, however, to represent different geographic locations or to incorporate new information as it becomes available.

Although the model operates on a daily time step, laboratory toxicity tests for spent drilling muds do not typically include 24-hr exposures. Relationships between exposure concentrations and daily survival for a reference mud (in this case, P-1) were, therefore, derived in the following way. Table D-2 shows the results of probit analysis of laboratory data on the exposure of Mysidopsis to whole P-1 mud (Rao, pers. comm.). Table D-3 illustrates the conversion of the survival rates and exposures in Table D-2 to daily survival rates, assuming that survival is constant over the duration of the exposure. For example, a survival rate of 0.7 for a 96-hr exposure yields a daily survival rate of 0.915 (i.e., $0.915^4 = 0.7$).

Table D-2. Concentrations (ppm) of whole P-1 mud resulting in various survival rates of juvenile Mysidopsis for exposures of different length.

Duration of exposure	Survival rate				
	0.9	0.7	0.5	0.3	0.1
48 hr	6	60	100	140	190
72 hr	8	35	54	72	100
96 hr	7	32	49	66	91

Table D-3. Constant daily survival rates corresponding to the combinations of survival rate and exposure duration shown in Table D-2.

Duration of exposure	Survival rate				
	0.9	0.7	0.5	0.3	0.1
48 hr	0.949	0.837	0.707	0.548	0.316
72 hr	0.965	0.888	0.794	0.669	0.464
96 hr	0.974	0.915	0.841	0.740	0.562

Concentrations from Table D-2 and daily survival rates from Table D-3 were plotted in Figure D-8. These data tended to separate into two patterns that indicate that the full toxicity effects of the P-1 mud are not manifested in an exposure as short as 48 hr. The 48-hr data were, therefore, omitted from Figure D-9, which shows the results of regression analysis of the daily survival rate as a function of the square of the concentration. The solid line represents the least-squares fit of the data points. Note, however, that the y-intercept of this line is less than 1.0, implying some mortality even when the exposure concentration is 0. Because mortality in the absence of drilling mud is accounted for elsewhere in the model, the regression represented by the dashed line, where the intercept is forced to be 1.0, was chosen for use in the model.

A similar analysis of data for Palaemonetes larvae is presented in Table D-4 and Figures D-10 and D-11 (Rao, pers. comm.). Daily survival rates are, of course, the same as those shown in Table D-2, because the survival rates and exposure durations in Table D-3 are the same as those in Table D-1. The data for Palaemonetes differ from those for Mysidopsis in two respects. First, there is no obvious difference in daily survival rates for exposures of different lengths (Figure D-10). Data from all exposures were, therefore, used in developing the toxicity relationship. Second, the regression illustrated in Figure D-11 has a y-intercept greater than 1.0. Therefore, it was not necessary to force a regression line through y = 1.0. The regression is used as shown in Figure D-10, with a limit set in the model such that the resulting survival rate cannot exceed 1.0.

The basic toxicity relationships shown in Figures D-10 and D-11 are input to the model in the form of the slopes and intercepts of the regression lines. Given the availability of appropriate laboratory toxicity data, similar relationships could be developed for any drilling mud. However, because laboratory data are unavailable for many muds, it is desirable to have some means of relating the toxicity relationships described above to those that might result

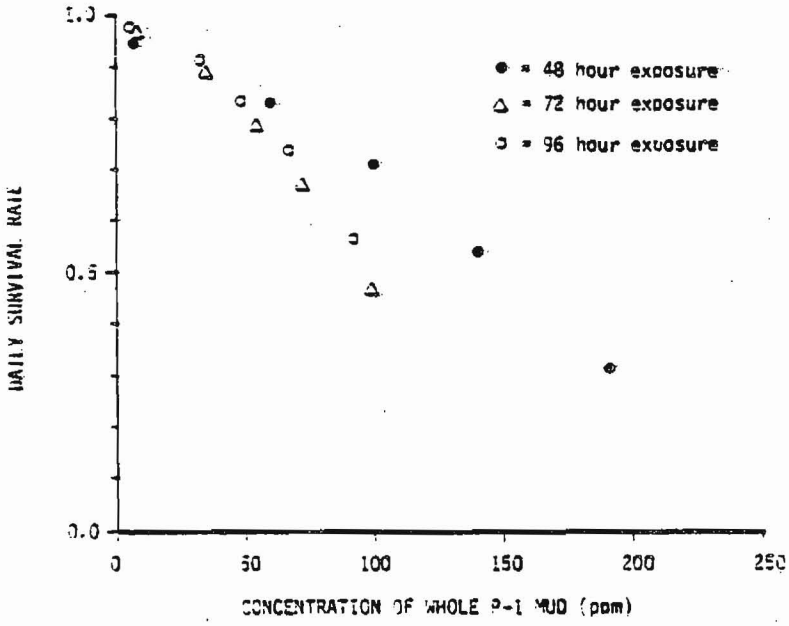

Figure D-8. Daily survival rate of juvenile Mysidopsis as a function of concentration of whole P-1 drilling mud.

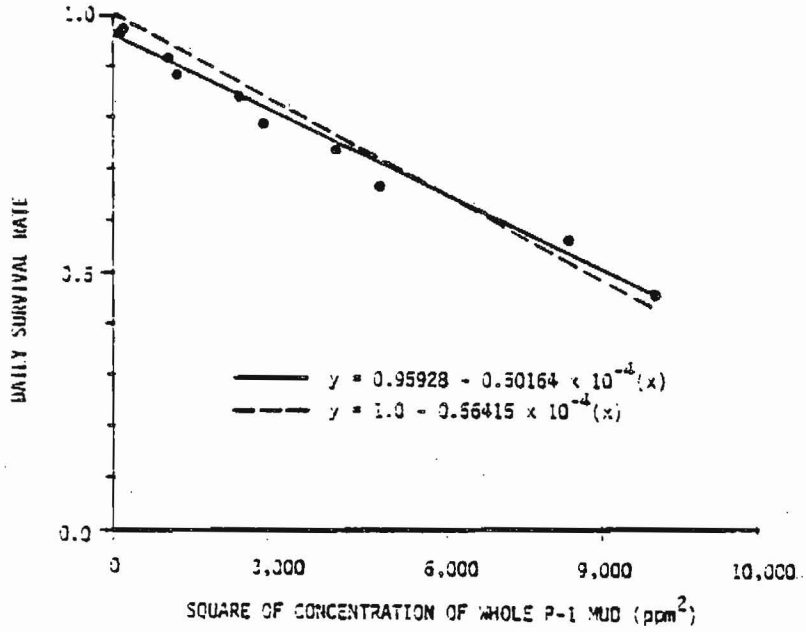

Figure D-9. Daily survival rate of juvenile Mysidopsis as a function of the square of concentration of whole P-1 drilling mud. Data from 48-hr exposure were omitted.

Table D-4. Concentrations (ppm) of whole P-1 mud resulting in various survival rates of Palaemonetes larvae for exposures of different length.

Duration of exposure	Survival rate				
	0.9	0.7	0.5	0.3	0.1
48 hr	105	140	170	195	235
72 hr	102	132	158	179	215
96 hr	97	124	142	161	185

from other muds. This is done through a comparison of hydrocarbon contents for a series of muds and their relative 96-hr LC_{50} toxicities to Palaemonetes larvae (Table D-5) (Rao, pers. comm.). In Figure D-12, the natural logarithm of the ratio in Table D-5 is shown as a function of the natural logarithm of the oil concentration. The regression illustrated in Figure D-12 is used in the equations:

$$HYFAC = HYINT - HYSLP * [ALOG (HYCONC)] \quad (52)$$

$$HYFAC = EXP (HYFAC)$$

where HYFAC = adjustment factor for hydrocarbon concentration (used below)

HYINT = intercept of regression in Figure D-12

HYSLP = slope of regression in Figure D-12

HYCONC = oil concentration provided by the Discharge and Plume Fate submodel (ppt)

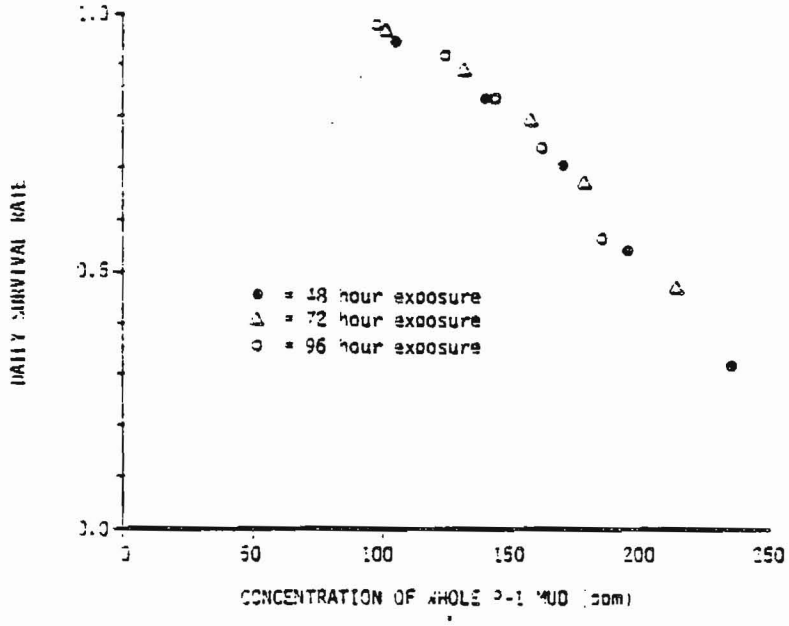

Figure D-10. Daily survival rate of Palaemonetes larvae as a function of concentration of whole P-1 drilling mud.

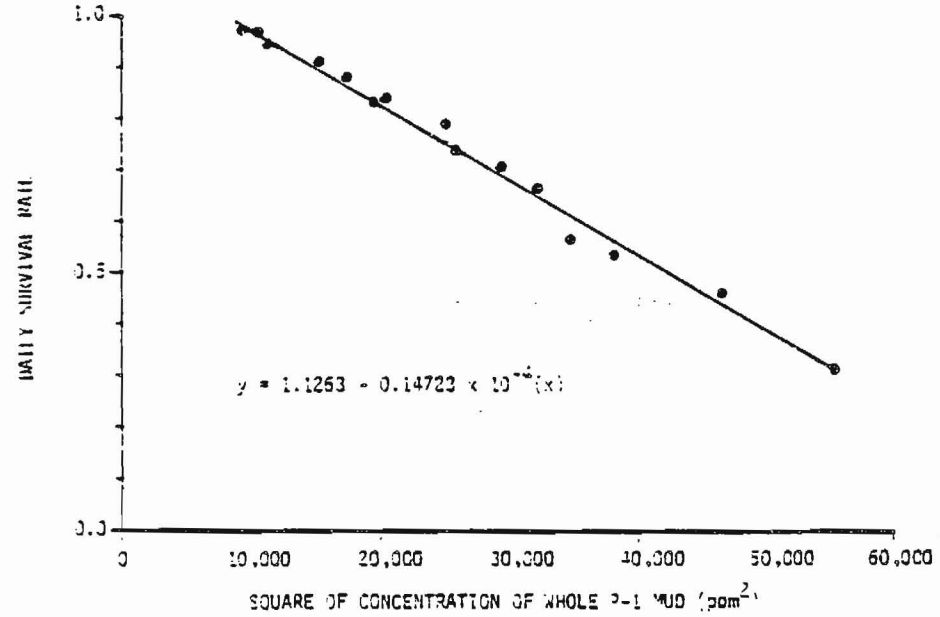

Figure D-11. Daily survival rate of Palaemonetes larvae as a function of the square of concentration of whole P-1 drilling mud.

Table D-5. Oil concentrations of various drilling muds and their toxicity to Palaemonetes larvae (Rao, pers. comm.).

Mud	No. 2 oil concentration (ppt)	96-hr LC_{50} (ppm)	Ratio of 96-hr LC_{50} to 96-hr LC_{50} for P-1 mud
P-1	9.43	142	1.0
P-3	3.98	658	4.63
SV76	3.59	1,706	12.01
AN31	1.18	2,390	16.83
P-8	0.56	2,557	18.00
P-5	1.41	3,570	25.14
P-2	2.14	4,276	30.11
P-4	0.67	4,509	31.75
MI	0.19	28,750	202.46
P-7	0.50	35,420	249.44
P-6	0.10	> 100,000	> 704.23

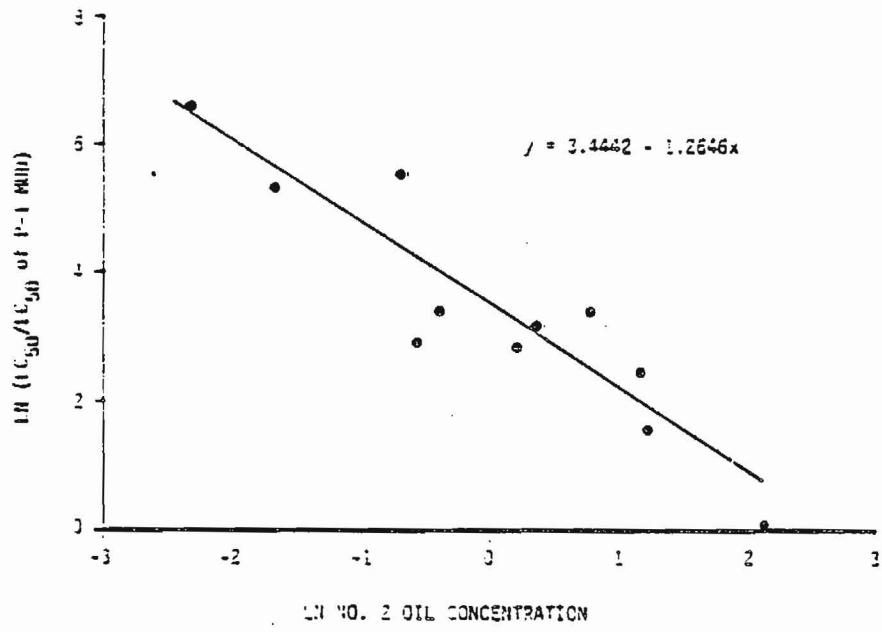

Figure D-12. Relative toxicity of various muds compared to P-1 mud as a function of No. 2 oil concentration.

Following this calculation, the submodel enters a loop to perform a series of computations for each distance from the discharge point. If no drilling mud is present in the sediment at a given distance (BFWM(ID) = 0), the counter that determines when a chronic exposure occurs (LDAY(ID)) is reset to 0 and the remainder of the calculations are skipped for that distance.

If drilling mud is present in the sediments, then the effective concentration for that distance is determined from the equations:

$$EFCONC(ID) = BFWM(ID) \;/\; HYFAC \qquad (53)$$

$$\text{if } [LDAY(ID) \geq LCHR]\; EFCONC(ID) = EFCONC(ID) \;/\; CHRFAC$$

where EFCONC(ID) = the effective concentration of drilling mud in the sediment to be used in determining daily survival rates (ppm)

BFWM(ID) = the exposure concentration produced by the Sediment Redistribution submodel (ppm)

HYFAC = adjustment factor for oil content (see above)

LDAY(ID) = number of consecutive days of exposure to drilling mud

LCHR = number of consecutive days required before an exposure is considered chronic

CHRFAC = adjustment factor for chronic toxicity

Recall that HYFAC represents the ratio of the toxicity (96-hr LC_{50} for Palaemonetes) of the mud being simulated to that of the reference P-1 mud used to establish the basic toxicity curves (Figure D-12). Thus, if the exposure concentration is 10 ppm, but HYFAC is 2, the effective concentration for the mud being simulated is only 5 ppm when the basic toxicity curve is used to estimate survival. Note that this is exactly equivalent to dividing the slope of the basic toxicity curve by 2 and using the exposure concentration produced by the Sediment Redistribution submodel to estimate survival.

The effective concentration is adjusted in a similar manner (equation 62) if the number of days of continuous exposure to drilling muds is large enough for the exposure to be considered chronic. Participants indicated that a useful rule-of-thumb is that an acute exposure to a given concentration results in about the same survival rate as a chronic exposure to one-tenth of that concentration. For the current model runs, a chronic exposure is defined as continuous exposure for 28 days or more (LCHR = 28). If the exposure is chronic [LDAY(ID) $\geq$ 28], the effective concentration is divided by 0.1 and the resulting value is used to calculate survival rate from the basic toxicity curve. This is equivalent to dividing the slope of the toxicity curve by 0.1 and using the adjusted exposure concentration [BFWM(ID)] to compute survival.

Following calculation of the effective concentration for each distance, the submodel calculates the survival rate for each community from the equation:

$$TSURV(IC,ID) = TXINT(IC) - TXSLP(IC) * [EFCONC(ID) ** 2.0] \quad (54)$$

where TSURV(IC,ID) = the daily survival rate

TXINT(IC) = the y-intercept of the basic toxicity curve (Figures D-9 and D-11)

TXSLP(IC) = the slope of the basic toxicity curve (Figures D-9 and D-11)

EFCONC(ID) = the effective concentration of drilling muds (ppm)

TSURV(ID,ID) is limited so that it can never be greater than 1.0 nor less than 0.01 and multiplied by the number of individuals present in the assemblage. Finally, the chronic exposure counter [LDAY(ID)] is incremented by 1 at each distance where drilling mud is present.

RESUSPENSION MORTALITY

Following mortality associated with burial and toxicity, the number of individuals per m^2 in each species assemblage may be further reduced due to resuspension or movement of sediments by events such as storms, tides, and ice action. Mortality associated with such events is calculated as a function of the depth of sediment disturbance on the current day of simulation (calculated by the Sediment Redistribution submodel) according to the equation:

$$DSURV(IC,ID) = f[STIR(ID)] \quad (55)$$

where DSURV(IC,ID) = survival rate due to sediment disturbance

STIR(ID) = depth of sediment disturbance (cm)

f = the piecewise linear functions illustrated in Figure D-13

Parameter values defining the relationships in Figure D-13 were estimated by workshop participants from general experience with marine benthic communities.

POPULATION GROWTH

Formulation

After removal of individuals due to the three mortality factors described above, the model calculates increases in the number of individuals per m^2 of each species assemblage as a result of the combination of reproduction and larval recruitment. Growth of the meiofaunal and late successional species assemblages is represented with simple logistic equations (Pielou 1977) of the form:

$$dN_i/dt = N_i(r_i - s_iN_i) \quad (56)$$

where i = 1 for the meiofaunal assemblage and 3 for the late successional macrofaunal assemblage

N_i = the number of individuals per m^2

r_i = the potential per capita growth rate in the absence of competition

s_i = the reduction in the potential per capita growth rate per individual present (a measure of the degree of intraspecific competition)

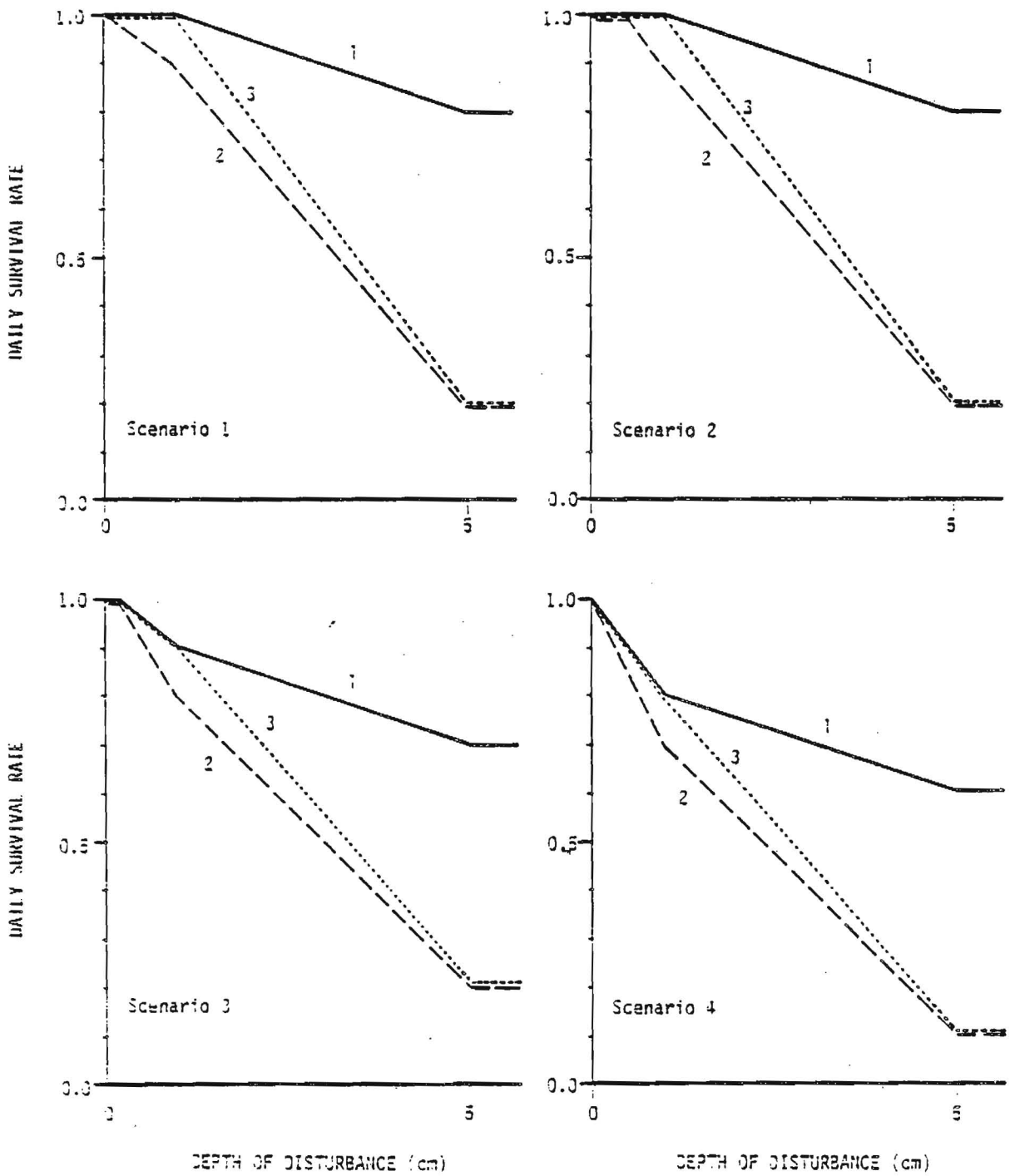

Figure D-13. Benthic community survival rates as a function of depth of sediment disturbance (1 = meiofauna, 2 = early successional macrofauna, 3 = late successional macrofauna).

For the early successional or pioneer macrofaunal assemblage, the growth equation is modified slightly to represent the competitive effect of individuals in the late successional macrofaunal assemblage:

$$dN_i/dt = N_i\ (r_i - s_iN_i - k_iN_3) \tag{57}$$

where $i = 2$ for the early successional macrofaunal assemblage

N_i = the number of individuals per m^2

r_i = the potential per capita growth rate in the absence of competition

s_i = the reduction in the potential per capita growth rate per individual present (a measure of the degree of intraspecific competition)

k_i = the reduction in the potential per capita growth rate of the pioneer assemblage per individual of the late successional assemblage present (a measure of the degree of interspecific competition)

Because, in general, the simultaneous differential equations (56) and (57) cannot be solved explicitly, a discrete time formulation is used to perform the computations. The discrete time version of equation (56) is (Pielou 1977):

$$N_{i,t+1} = \frac{a_iN_{i,t}}{1 + b_iN_{i,t}} \tag{58}$$

where $a_i = e^{ri}$

$b_i = s_i(a_i - 1)/r_i$

r_i = the potential per capita growth rate in the absence of competition

s_i = the reduction in the potential per capita growth rate per individual present (a measure of the degree of intraspecific competition)

i = 1 for the meiofaunal assemblage and 3 for the late successional macrofaunal assemblage

N_i = the number of individuals per m^2

This formulation is applied to the meiofaunal and late successional macrofaunal assemblages, because neither are affected by interspecific competition.

The discrete time version of equation (57) is:

$$N_{i,t+1} = \frac{a_i N_{i,t}}{1 + b_i N_{i,t} + c_i N_{3,t}} \tag{59}$$

where i = 2 for the early successional macrofaunal assemblage

N_i = number of individuals per m^2

$a_i = e^{ri}$

$b_i = s_i(a_i - 1)/r_i$

$c_i = k_i(a_i - 1)/r_i$

r_i = the potential per capita growth rate in the absence of competition

s_i = the reduction in the potential per capita growth rate per individual present (a measure of intraspecific competition)

k_i = the reduction in the potential per capita growth rate of the pioneer assemblage per individual of the late successional assemblage present (a measure of the degree of interspecific competition)

This equation is applied to the early successional macrofaunal assemblage, because it is affected by competition from the late successional assemblage (N_3).

Parameter Estimation

Parameter values for these equations were estimated by workshop participants in the following manner. At very low population densities, there is little reduction of the potential per capita growth rates due to competition. Under such conditions, equations (56) and (57) can be approximated by:

$$dN_i/dt = r_i N_i$$

This equation can be integrated to yield the familiar exponential growth model:

$$N_{i,t} = N_{i,0}\, e^{r_i t} \tag{61}$$

where $N_{i,t}$ = the number of individuals per m^2 in assemblage i at time t

$N_{i,0}$ = the number of individuals per m^2 in assemblage i at time zero

t = the number of time intervals over which growth occurs

r_i = the potential per capita growth rate in the absence of competition

If the time required for a population to double (i.e., $N_{i,t}/N_{i,0} = 2$) is considered, then:

$$2 = e^{r_i d_i}$$

where d_i = an estimate of the time required for assemblage i to double in the absence of competition (days)

Rearranging terms:

$$r_i = [\mathrm{LOG}\ (2.0)]\ /\ d_i \tag{62}$$

Potential growth rates (r_i) for each assemblage were calculated from equation (62) using doubling times estimated by workshop participants on the basis of general experience with marine benthic communities (Table D-6).

A new term, K_i, is defined as the maximum number of individuals of a species assemblage that can be supported per m^2. When $N_i = K_i$, dN_i/dt must be zero, because no further population growth can occur. In this case, equation (56) can be rewritten as:

$$0 = K_i(r_i - s_i K_i) \tag{63}$$

Rearranging terms:

$$s_i K_i^2 = r_i K_i$$

$$s_i = r_i / K_i$$

The intraspecific competition coefficients, s_i, can, thus, be calculated from the potential growth rates, r_i (equation 63), and estimates of the carrying capacities, K_i, for each species assemblage. Values for K_i (Table D-6) were estimated by workshop participants on the basis of general knowledge of marine benthic communities.

Interspecific competition coefficients (k_i) are harder to estimate due to the difficulty of obtaining information from experiments in which numbers of each competitor are carefully monitored. Workshop participants, therefore, arbitrarily assumed that the reduction in the early successional assemblage growth rate (k_2) due to the presence of an individual in the late successional assemblage should be about 10 times greater than the reduction (s_2) due to the presence of an individual in the early successional assemblage.

Table D-6. Basic parameters for the population growth model.

Parameter	Scenario 1	Scenario 2	Scenario 3	Scenario 4
Meiofaunal assemblage				
Doubling time (d_1)	6 days	6 days	20 days	60 days
Potential growth rate (r_1)	0.116	0.116	0.035	0.012
Carrying capacity (K_1)	$5 * 10^6$	$5 * 10^6$	$1 * 10^6$	$1 * 10^5$
Intraspecific competition coefficient (s_1)	$2.31 * 10^{-8}$	$2.31 * 10^{-8}$	$3.47 * 10^{-8}$	$1.16 * 10^{-7}$
Early successional macrofaunal assemblage				
Doubling time (d_2)	6 days	6 days	20 days	60 days
Potential growth rate (r_2)	0.116	0.116	0.035	0.012
Carrying capacity (K_2)	$1 * 10^4$	$1 * 10^4$	$1 * 10^4$	$1 * 10^3$
Intraspecfic competition coefficient (s_2)	$1.16 * 10^{-5}$	$1.16 * 10^{-5}$	$3.47 * 10^{-6}$	$1.16 * 10^{-5}$
Interspecific competition coefficient (k_2)	$1.16 * 10^{-4}$	$1.16 * 10^{-4}$	$3.47 * 10^{-5}$	$1.16 * 10^{-4}$
Late successional macrofaunal assemblage				
Doubling time (d_3)	60 days	60 days	120 days	260 days
Potential growth rate (r_3)	0.012	0.012	$5.78 * 10^{-3}$	$2.67 * 10^{-3}$
Carrying capacity (K_3)	$5 * 10^3$	$5 * 10^3$	$1 * 10^4$	$1 * 10^3$
Intraspecific competition coefficient (s_3)	$2.31 * 10^{-6}$	$2.31 * 10^{-6}$	$5.78 * 10^{-7}$	$2.67 * 10^{-6}$

Calculations

The computer code for the growth portion of the Benthic Community Effects submodel operates in the following way. First, the Julian date of the current simulation iteration (IDAY) is compared to two user-specified Julian dates representing the beginning (NBEG) and end (NEND) of the period during which population growth can occur. If the current Julian date is not within this window, the remainder of the growth portion of the model is bypassed. Currently, this occurs only in the data set for Scenario 1, where growth is assumed to occur only between June 1 (NBEG = 151) and September 30 (NEND = 270).

Minimum doubling times for each species assemblage (Table D-6) can be increased either due to the presence of hydrocarbons in the sediment or due to changes in the particle size distribution in the sediment. This mechanism largely reflects the preference of larvae to settle on uncontaminated sediments with particle size distributions similar to those occurring naturally. First, the potential increase in doubling time due to hydrocarbon contamination is determined as:

$$RDBHY(ID) = f[HYSED(ID) \text{ or } HYDEP(ID)] \tag{64}$$

where RDBHY(ID) = potential increase in doubling time due to hydrocarbon contamination

HYSED(ID) = concentration of hydrocarbons in the mixed 5-cm layer (ppm)

HYDEP(ID) = concentration of hydrocarbons in the layer deposited on current day (ppm)

f = the piecewise linear function shown in Figure D-14

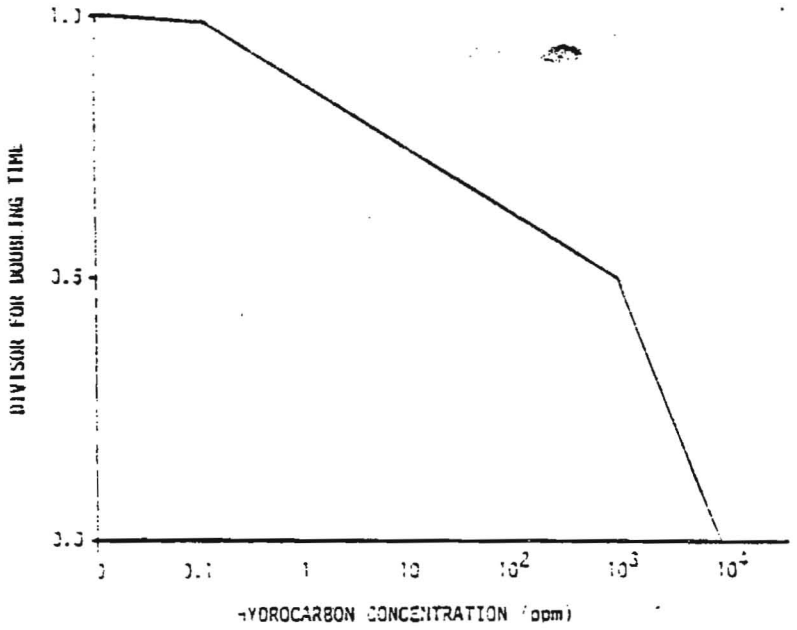

Figure D-14. Division in doubling time as a function of sediment hydrocarbon concentration.

If deposition occurs on the current day of the simulation, the concentration of hydrocarbons in the layer deposited [HYDEP(ID)] is used to determine the potential increase in doubling time. Otherwise, the concentration of hydrocarbons in the mixed 5-cm layer [HYSED(ID)] is used.

Next, the potential increase in doubling time due to changes in sediment particle size distribution is determined as:

$$RDBPS(ID) = f[PSSED(ID) \text{ or } PSDEP(ID)] \tag{65}$$

where RDBPS(ID) = potential increase in doubling time due to changes in sediment particle size distribution

PSSED(ID) = proportion sand in the mixed 5-cm layer

PSDEP(ID) = proportion sand in the layer deposited on the current day

f = the piecewise linear functions illustrated in Figure D-14

If deposition occurs on the current day of the simulation, the proportion sand in the layer deposited [PSDEP(ID)] is used to determine the potential increase in doubling time. Otherwise, the proportion sand in the mixed 5-cm layer [PSSED(ID)] is used.

The minimum of RDBHY(ID) and RDBPS(ID) is chosen [RDB(ID)] and divided into the minimum doubling times [DBIN(IC) or d_i in Table D-6] to provide the actual doubling times to be used in calculating the current day's growth for each species assemblage:

$$DB(IC,ID) = DBIN(IC) / RDB(ID) \tag{66}$$

where DB(IC,ID) = actual doubling time (days)

DBIN(IC) = minimum doubling time (d_i from Table D-6) (days)

RDB(ID) = minimum of values determined from Figures D-14 and D-15

The continuous and discrete time per capita growth rates in the absence of competition are computed from the equations:

$$AC(IC,ID) = 0.6931472 / DB(IC,ID) \tag{67}$$

$$AD(IC,ID) = EXP\ [AC(IC,ID)]$$

where AC(IC,ID) = the potential per capita growth rate in the absence of competition (equivalent to r_i)

DB(IC,ID) = actual doubling time (days)

AD(IC,ID) = the discrete time equivalent of the potential per capita growth rate (equivalent to a_i)

EXP = function producing e^x

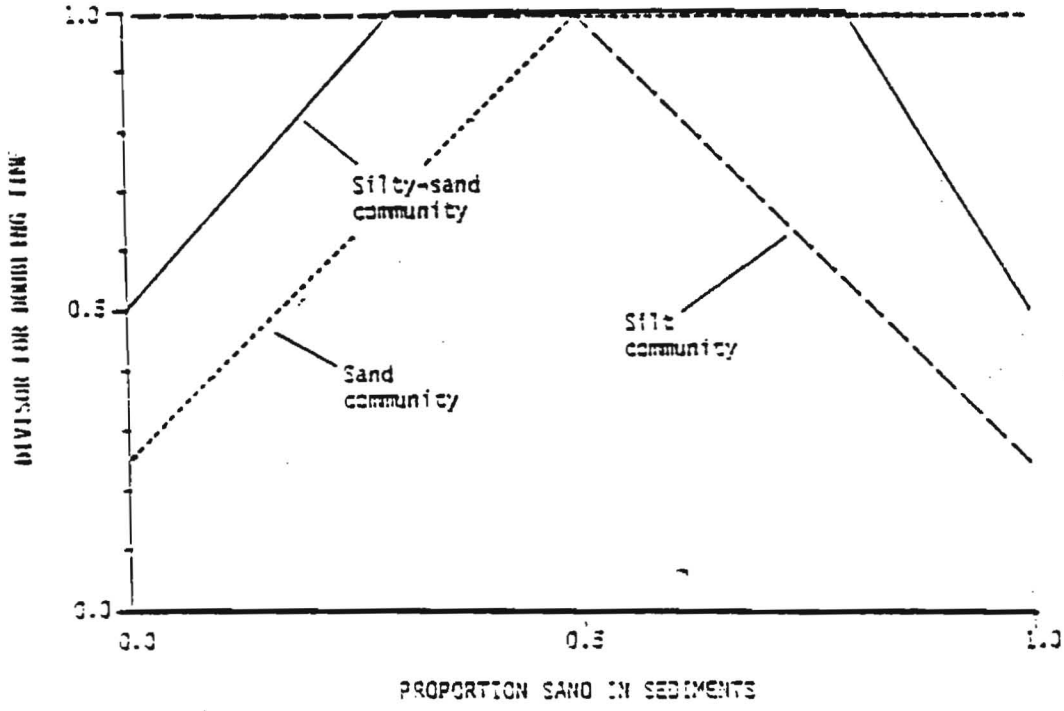

Figure D-15. Division in doubling time as a function of proportion sand in the sediment. The solid line is used if the natural sediment is a silty sand (Scenario 1); the short-dashed line is used if the natural sediment is mainly sand (Scenario 2); the long-dashed line is used if the natural sediment is mainly silt (Scenarios 3 and 4).

Equation 67 is, thus, equivalent to equations 57 and 58 with no competition (i.e., $s_i = 0$).

The continuous and discrete time intraspecific competition coefficients are calculated from the equations:

$$BC(IC) = AC(IC,ID) / CAR(IC) \tag{68}$$

$$BD(IC,ID) = BC(IC) * [AD(IC,ID) - 1.0] / AC(IC,ID)$$

where BC(ID) = the reduction in the potential per capita growth rate per individual present (equivalent to s_i)

AC(IC,ID) = the potential per capita growth rate in the absence of competition (equivalent to r_i)

CAR(IC) = carrying capacity (K_i from Table D-6) (number of individuals per m^2)

BD(IC,ID) = the discrete time equivalent of the reduction in the potential per capita growth rate per individual present (equivalent to b_i)

AD(IC,ID) = the discrete time equivalent of the potential per capita growth rate (equivalent to a_i)

The discrete time version of the interspecific competition coefficient is calculated as:

$$CD(IC,ID) = (CC(IC) * [AD(IC,ID) - 1.0]) / AC(IC,ID) \tag{69}$$

where CD(IC,ID) = the discrete time equivalent of the reduction in the potential per capita growth rate per individual present in the competing assemblage (equivalent to c_i)

CC(IC) = the reduction in the potential per capita growth rate per individual present in the competing assemblage (k_i from Table D-6)

AC(IC,ID) = the potential per capita growth rate in the absence of competition (equivalent to r_i)

AD(IC,ID) = the discrete time equivalent of the potential per capita growth rate in the absence of competition (equivalent to a_i)

The variable CC(IC) is given a non-zero value only for the early successional macrofaunal assemblage, because it is the only component of the benthic community that experiences interspecific competition (i.e., from the late successional macrofaunal assemblage).

Finally, changes in population sizes are computed from the equations:

POP(IC,ID) = [AD(IC,ID) * POP(IC,ID)] / [1.0 + BD(IC,ID) * POP(IC,ID)], for IC = 1 and 3 (70)

POP(IC,ID) = [AD(IC,ID) * POP(IC,ID)] / [1.0 + BD(IC,ID) * POP(IC,ID) + CD(IC,ID) * POP(3,ID)], for IC = 2

where POP(IC,ID) = number of individuals per m^2

AD(IC,ID) = the discrete time equivalent of the potential per capita growth rate in the absence of competition (equivalent to a_i)

BD(IC,ID) = the discrete time equivalent of the reduction in the potential per capita growth rate per individual present (equivalent to b_i)

CD(IC,ID) = the discrete time equivalent of the reduction in the potential per capita growth rate per individual present in the competing assemblage (equivalent to c_i)

Note that only the early successional macrofaunal assemblage (IC = 2) has a non-zero term for reduction in growth rate due to competition.

LIMITATIONS

While the present formulation of the Benthic Community Effects submodel represents a considerable improvement over the version that resulted from the first workshop, it still has several limitations that should be kept in mind when interpreting output. Perhaps the most important of these limitations is the fact that the data that are available are generally for particular species, rather than for species assemblages or communities. At best, this implies the need for considerable judgement concerning the relevance of species-specific data to multispecies assemblages when estimating parameters for the model. At worst, it can lead to a set of data developed with inconsistent assumptions. For example, the burial data currently used in the model were estimated by averaging species-specific values weighted by expected species composition. Toxicity data, on the other hand, were chosen for single species thought to be representative of each assemblage. In yet another approach, growth parameters were simply estimated on a community basis, without reference to particular indicator organisms or specific weighting procedures. Each of these approaches seemed appropriate because each was consistent with available information and understanding. The net result, however, may be a data set that is not really representative of any community at any geographic location.

A second general limitation is that available data tend to represent variable time periods (e.g., 15-day burial experiments and 48-hr to 96-hr toxicity tests), usually larger than the daily time step chosen for the model. Furthermore, experimental results from multiple exposures, either with or without intervening depuration periods, are almost nonexistent. Simplifying assumptions (e.g., constant daily survival over the period of exposure in laboratory toxicity tests) must, therefore, be made in order to utilize the available information. Some of these assumptions are undoubtedly reasonable; some are probably not. The net result in terms of model behavior is not easy to determine.

In addition, there are several limitations specific to particular parts of the Benthic Community Effects submodel.

Burial

Data available for estimating burial effects are largely the result of experiments with dredge material. The extent to which responses to drilling muds and cuttings, which have different physical and chemical properties, would differ is not known at this time. In addition, even dredge material data are available only for a limited number of species.

Toxicity

The principal limitation of the toxicity portion of the model is that there may be little correspondence between the kinds of exposures from which laboratory data are reported, the kinds of exposures that the model simulates, and the kinds of exposures that an organism experiences in the real world. Laboratory data used in the current parameter set are from static tests with whole mud. In these tests, sufficient whole mud (solids fraction, suspended particulate fraction, and aqueous fraction) is added to sea water to produce a desired exposure concentration. These experiments differ from the exposure concentrations simulated in the model in two important aspects. First, the model uses only settleable solids, a combination of the solids fraction and suspended particulate fraction (where the contribution of each depends on the distance from the discharge point) in determining the exposure concentration. Second, the model computes the exposure concentration by assuming that these materials are mixed in a 5-cm layer of sediment, rather than in the surrounding seawater. Real-world exposures may often be somewhere in between these two extremes, especially in the case of discharges in shallow water. Because whole muds are usually more toxic than either the solids fraction or the suspended particulate fraction, it is likely that the present data set overestimates mortality. This could be corrected to some extent if more toxicity data were available for the solids fraction. However, using solids fraction data would still not account for the difference between exposure to a seawater mixture and exposure to a sediment mixture.

A second limitation of the toxicity section of the model is in the use of the mud oil content to predict toxicity (Figure D-2). Three factors are important here. First, data relating oil content to toxicity were available only for a single species (Palaemonetes). How this relationship might differ for other species is not known.

Second, while the regression fits the data points fairly well, its use can lead to survival rates that are quite different than those reported for any single mud. For example, a (P-1) mud with an oil content of 9.43 ppt should, by definition, have a toxicity ratio (Table D-5) of 1.0. With this value, a concentration of 142 ppm would yield a daily survival rate for Palaemonetes of 0.83 (Figure D-11) and a 96-hr survival rate of 0.47 ($0.83^4 = 0.47$). This value compares favorably to the survival rate of 0.5 reported for Palaemonetes exposed to 142 ppm whole P-1 mud for 96 hr (Table D-4). However, the oil content regression actually produces a ratio of 1.83 for an oil content of 9.43 ppt. With this value, the effective concentration is 142.0/1.83 = 77.6 and the predicted 96-hr survival rate is 1.0. The only solution to this problem presently available is to develop separate toxicity curves for each combination of species and mud to be tested in the model.

The third factor is the assumption that the oil content of a discharged whole mud at the discharge point is an accurate reflection of its toxicity over time. There are a lot of reasons to suspect that the oil content (especially of the more volatile fractions) will change as settleable solids separate from the liquid phase of the mud, pass through the water column, and remain in the sediments over time. The model assumes that the relative toxicity of a given volume of whole mud remains constant, as determined by its initial oil content. This is most likely a very conservative assumption (i.e., toxicity is overestimated). The magnitude of the error is difficult to estimate, in part because many of the same processes also operate to change oil concentrations of various fractions in laboratory experiments.

Finally, there was considerable discussion at the workshop concerning bioaccumulation and depuration of chromium and the ways in which these processes might be simulated. While considerable work has been done in this area (Petrazzoulo 1983), the reported results do not generally lend themselves to a simulation treatment. The most consistent patterns are discernible in results reported in "enrichment units", which are ratios between chromium concentrations in exposed animals and those in control animals. There is no obvious way in which these enrichment units can be added and subtracted, or partitioned between short-term and long-term body storage sites, as the model communities are subjected to a series of exposures on consecutive days of simulation. However, while not presented in the MODEL BEHAVIOR section of this report, the model does calculate chromium concentrations in the sediment, and these results can at least be compared qualitatively with laboratory information.

Resuspension mortality

The most important limitation of the resuspension mortality section is in the difficulty of adequately estimating parameters. The model output depicted in the body of this report illustrates that assumptions concerning the relationship between sediment resuspension and mortality can have important consequences for population behavior. Experimental data for establishing these relationships are very scarce. Parameter values presently used are simply estimates made by workshop participants based on general experience with marine benthic communities.

Growth

The most important limitations of the growth section of the model also are in the area of parameter estimation. Interspecific competition coefficients and increases in doubling time due to particle size distribution and oil content of the sediments are particularly troublesome. In addition, switching between particle size distribution and oil content of the deposited layer (on days when deposition occurs) and the mixed 5-cm layer (on days when

no deposition occurs) may represent a conceptual flaw. As presently formulated, any deposition, no matter how thin (e.g., 10^{-6} cm), causes this switch to be made. A more reasonable formulation would perhaps be to place a lower limit on the thickness of the deposited layer required to activate this switch.